MOMENT CONNECTIONS FOR VIERENDEEL TRUSSES OF SQUARE HOLLOW STRUCTURAL SECTIONS

MOMENT CONNECTIONS FOR VIERENDEEL TRUSSES OF SQUARE HOLLOW STRUCTURAL SECTIONS

By

YONG KING LOO, B.Sc. (Eng.)

A Project Thesis

Submitted to the School of Graduate Studies

in Partial Fulfilment of the Requirements

for the Degree

Master of Engineering

McMaster University

1973

MASTER OF ENGINEERING (1973) McMASTER UNIVERSITY
(Civil Engineering) Hamilton, Ontario.

TITLE : Moment Connections for Vierendeel Trusses of Square Hollow Structural Sections

AUTHOR : Yong King Loo, B.Sc.(Eng.)
(National Chung-Hsing University)

SUPERVISOR : Dr. R. M. Korol

NUMBER OF PAGES : ix , 120

SCOPE AND CONTENTS :

A research programme is presented for the analytical evaluation of the deflections of Vierendeel trusses comprised of semi-rigid connections under panel point loadings. The semi-rigid connections are made of two unequal width square HSS members welded at right angles. As the flexibility of the joints increases when the width ratio is less than 1.0, the joints are unable to develop the moment capacity of the web member and excessive deflections limit functional capability of the truss. Hence, several types of joint reinforcement are recommended. A yield line method is attempted to estimate the strength capacity of the joint with and without reinforcements. In addition, a plate analysis forms the basis for estimating elastic joint stiffness for evaluating anticipated deflections at mid span.

ACKNOWLEDGEMENTS

I wish to express my sincere gratitude to my research supervisor Dr. R. M. Korol for his guidance and encouragement during the course of this research programme.

Financial assistance given by the Civil Engineering Department of McMaster University in the form of a teaching assistantship is thankfully appreciated.

Also, I am grateful to the Computing Center of the University for allowing me to use its excellent computing facilities.

This research was sponsored by CIDECT (Comite International pour le Developpment et l'etude de la Construction Tubulaire) with direct motivation of the Steel Company of Canada, to whom I extend my sincere thanks.

TABLE OF CONTENTS

ILLUSTRATIONS

CHAPTER I

INTRODUCTION

1.1 HOLLOW STRUCTURAL SECTIONS

The new structural shape of Hollow Structural Sections (HSS) have gained wide popularity during the last few years. This is mainly because of a number of advantages namely:

(i) HSS provide outstanding strength in proportion to their weight, especially under compressive and torsional loading. This advantage is much better than those of conventional steel shapes.

(ii) The flat and smooth surfaces of rectangular and square sections provide easy attachment for a branch HSS member, such as beam to column and web member to chord member in trusses.

(iii) The smooth and clean appearance of the sections is aesthetically pleasing.

(iv) The ease of painting is also a benefit. Besides that, it gives protection to the interior surface from corrosion if both ends of a member are completely sealed.

(v) In multi-storey buildings these sections can be used in conjunction with a circulating fluid to

provide fire resistance.

In order to use these sections properly, the behaviour of welded connections made from HSS members must be known. Unfortunately, the literature on HSS connections has not yet been adequately available. In this volume attention is focused on the connections of unequal width square. HSS members welded at right angles and subsequent behaviour on truss deflection and strength for design purposes. It is hoped that some light will be cast on this interesting problem.

1.2 CLASSIFICATION OF CONNECTIONS

On the basis of structural behaviour, the HSS connections can be divided into two categories, namely the equal-width connections ($d/b = 1$) and the unequal-width connections ($d/b < 1$), where d and b are the widths of the web and chord members respectively.

These two categories are shown in Fig. 1.1 .

For the equal-width connections, most of the load applied on the branch member (or web member) is directly transferred from the web plates of the branch to the web plates of the main member (chord member) as they are in the same plane joined together by weld material. Also, the load on the flange plates of the branch will not be applied to the flange plate of the main member. Instead, most of the load is transmitted through the corners of the connection as the flange plate of the main member has a low stiffness in comparison with the web plate of the main member.

When the widths of the sections are unequal ($d/b < 1$), the behaviour of the joint becomes the plate problem with loading mainly resisted by flexure of the connected plate. The strength and stiffness of this type of connection are drastically reduced.

As joint flexibility increases rapidly with d/b, the joint can no longer develop the yield moment or the plastic moment of the cross-section as it does when $d = b$.

A graph, shown in Fig. 1.2, is plotted with relative rotation ϕ versus width ratio (constant applied moment) to show the change of flexibility of the unequal-width connection with respect to width ratio.

Both types of connections are basically semirigid (AISC type III connection). The former type, however, will have a larger rigidity in most practical situations and would be, more or less, expected to behave as AISC type I connection (i.e., rigid connections) [1]

1.3 OBJECTIVE OF STUDY

A constant-height Vierendeel truss composed of square hollow structural sections with unequal width of joints will be referred to in the investigation of semi-rigid connections made of HSS.

This research work was motivated by Stelco (Steel Company of Canada) which fabricates HSS Vierendeel trusses. While sufficient information exists for designers for equal-width connections, [2] the same is not the case for unequal-

width connections. For this reason, design information is required if the aesthetic and economical advantages, together with many others, of these HSS trusses are to be exploited.

A prime objective of this research is to assess the flexibility of a typical Vierendeel truss composed of square HSS under working loads to determine whether excessive deflections might pose a problem. Hence, while a companion research study also conducted at McMaster is to assess experimentally the ultimate moment capacity and flexibility of various types of connections in HSS, this study will be confined to an analytical evaluation of

(1) The deflections of a Vierendeel truss comprised of semi-rigid connections under panel point loading.

(2) Strength capacity and behaviour of HSS connections, and,

(3) The effectiveness of joint stiffeners.

It should be emphasized that Vierendeel trusses have in general strength properties and aesthetic qualities that are attractive to the designer. There are cases, however, when deflection limitations may rule out such a structural alternative. The case of a deep truss of limited span, i.e. floor to floor depth and exterior wall to wall length in office buildings is a possible application. Two examples will be used to provide continuity of the various chapters of this volume. Both examples illustrate the need for considering deflection and strength in the design process.

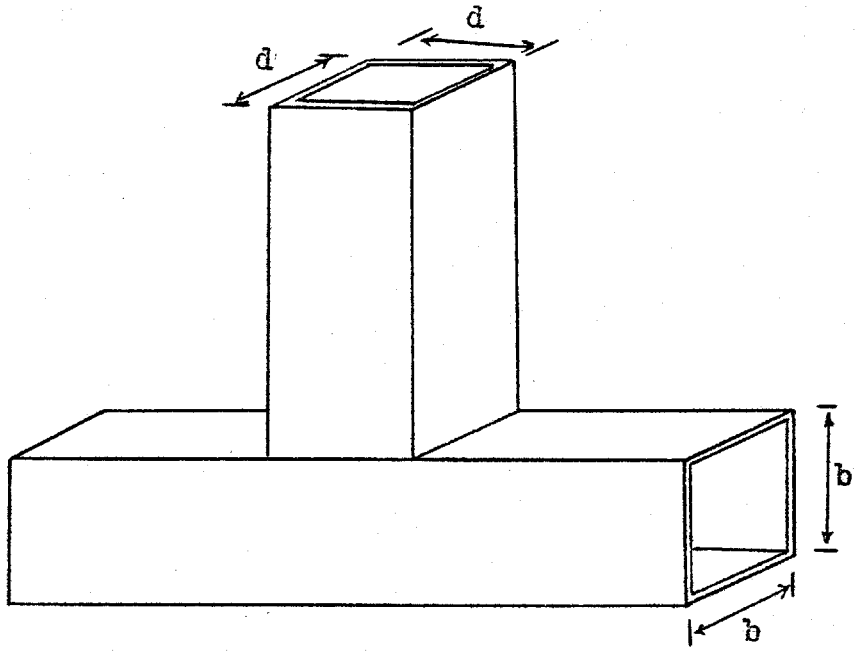

Equal Width HSS Connection d = b

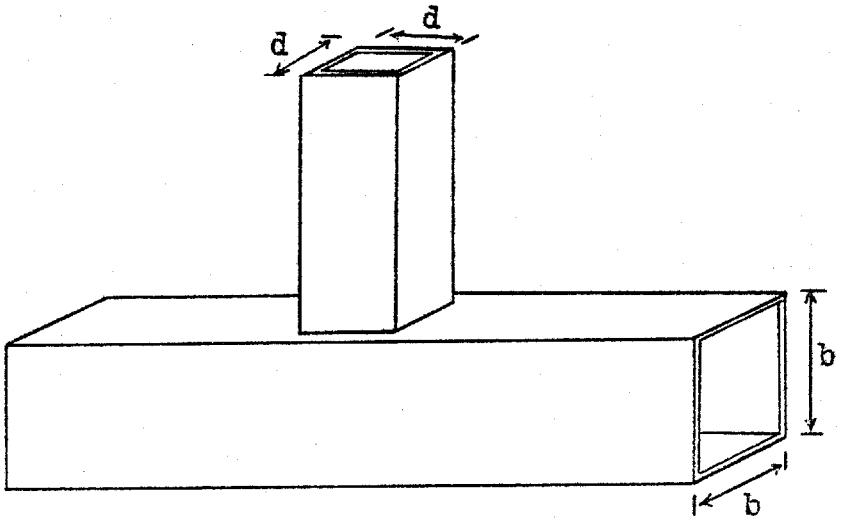

Unequal Width HSS Connection d < b

Fig. 1.1 Classification of HSS Connections

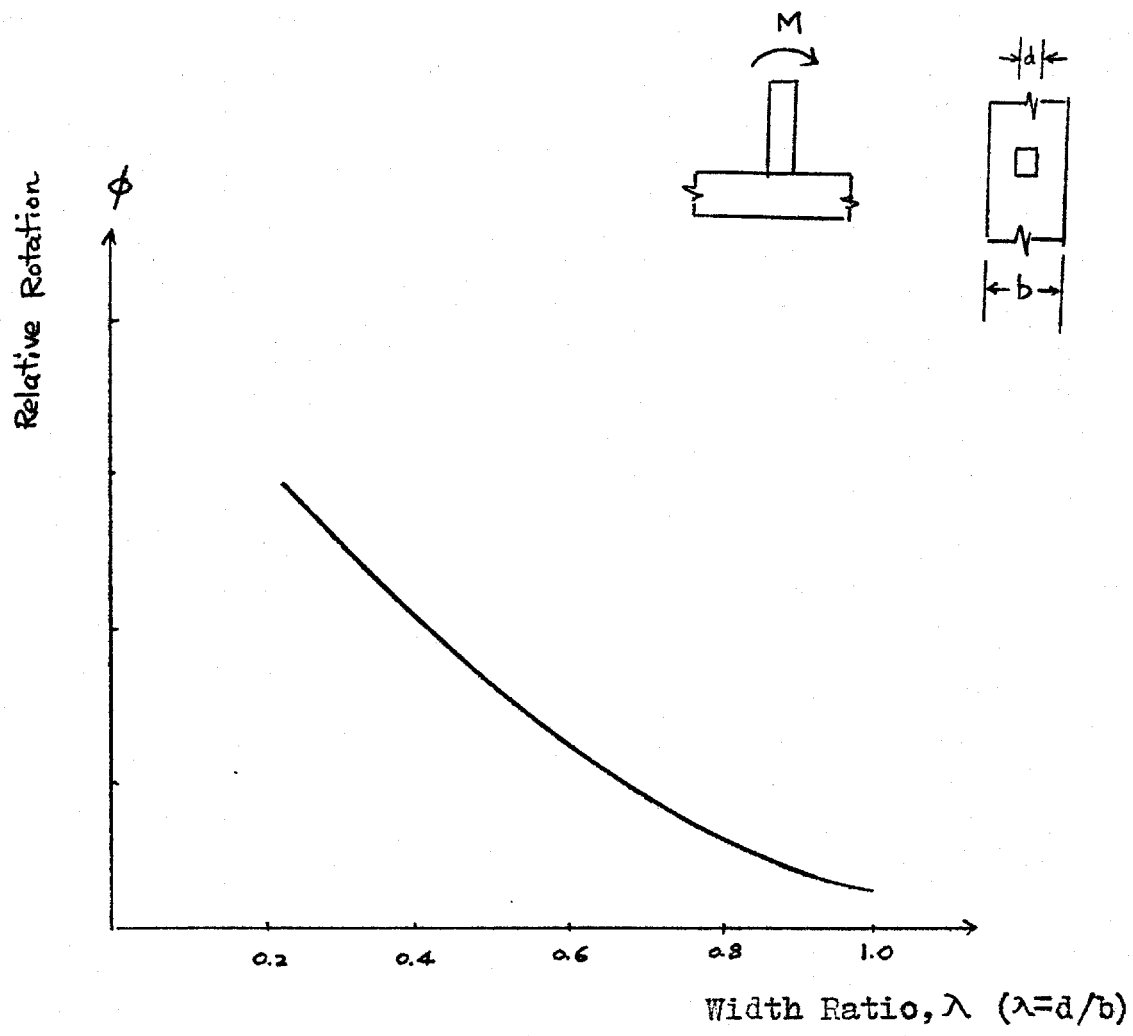

Fig. 1.2 Relative Rotation Versus Width Ratio λ
Under elastic Condition

CHAPTER II

METHOD OF ANALYSIS FOR VIERENDEEL TRUSS WITH SEMI-RIGID CONNECTIONS

2.1 VIERENDEEL TRUSS

A Vierendeel truss is a hyperstatic frame composed of a series of rectangular or trapezoidal panels without diagonal members. The truss was first proposed by Professor Vierendeel in 1896. The main function of the truss at that time was for bridges. In recent years, Vierendeel trusses have been used as roof trusses in low-rise buildings such as schools and gymnasiums. It is also a commonly used structure for overhead pedestrian bridges. The Vierendeel truss to be studied in this volume is the one with rectangular panels as shown in Fig. 2.1.

2.2 METHOD OF ANALYSIS FOR VIERENDEEL TRUSS

The method consists of putting the slope-deflection equations in matric form in a simple and systematic way. [3]

The explanation of the method is probably best given by illustrating an example as follows:

Consider a Vierendeel truss with concentrated loads acting at panel points as shown in Fig. 2.1

The eight-panel Vierendeel truss is externally determinate,

but is internally indeterminate to the 24th degree. The total degree of indeterminacy could easily be determined by experience or by the formula

$$n = 3m + r - 3j \qquad (2.1)$$

where n = the degree of indeterminacy

m = total number of members in the structure

r = numbers of reactions

j = numbers of joints

Consider the Vierendeel truss in Fig. 2.2. As there are 18 joints (including the supports) in the truss, there are 18 possible unbalanced moments acting at these joints. And also, there are 8* possible unbalanced linear forces acting at certain joints as shown in Fig. 2.2 The unbalanced moments are assumed to be in clockwise direction and the unbalanced linear forces are assumed either in vertical or horizontal directions. These unbalanced forces (moments and linear forces), denoted as P with subscripts indicating their individual locations, are due to the applied loads acting on the truss.

---

* The number of possible unbalanced linear forces in a structure can be determined by considering the number of degrees of freedom in joint translation in the structure. According to the formula [4], the total number of joints in translation in a structure is

$$S = 2j - (2f + 2h + r + m)$$

where S = degree of freedom in joint translation or sways
j = number of joints including supports
f = number of fixed supports
h = number of hinged supports
r = number of roller supports
m = number of members in the structure

As a result of these possible unbalanced forces due to the external loads, the truss responds with joint rotations and joint translations which are accordingly in the same directions as the unbalanced forces as shown in Fig. 2.2

Fig. 2.3 shows the end moments, denoted as M with subscripts, acting on the ends of all members. They are all assumed in a clockwise direction. (The end moments can also be regarded as 'distributed moments' from the point of view of the Moment Distribution Method).

2.2.1 STATIC MATRIX A

Every joint or part of the truss can be isolated as a free-body-diagram so long as the internal forces are in equilibrium with the external forces. Consider every same pair of joints in Figs (2.2) and (2.3). By using the conditions that $\sum$ Moments = 0, the following equations can be written as,

$$\begin{aligned} P_1 &= M_1 + M_{34} \\ P_2 &= M_2 + M_3 + M_{36} \\ P_3 &= M_4 + M_5 + M_{38} \\ &\vdots \qquad\quad \vdots \\ P_{18} &= M_{32} + M_{49} \end{aligned} \tag{2.2}$$

The expression for P_{19} can be found by considering the free-body diagram of the top chord continuous member as shown in Fig (2.4.b). Using the condition that the sum of all horizontal forces must be equal to zero, i.e. $\sum F_x = 0$, we get

$$P_{19} = -1/H\ (M_{33} + M_{34} + M_{35} \ \ldots\ M_{49} + M_{50})$$

Similarly, the expressions for P_{20}, P_{21} ... P_{26} can be obtained by considering the equilibrium condition of the vertical forces of the free-body diagram of the individual web member separately as shown in Fig. (2.4.C).

Let $\{P\}$ be a column matrix showing values of unbalanced moments at the joints and unbalanced linear forces. Let $\{M\}$ be a column matrix showing values of end moments.

Re-writing the expressions for P_1, P_2, P_3 ... P_{26} into matric form, we get,

$$\underset{(26\times1)}{\{P\}} = \underset{(26\times50)}{[A]} \; \underset{(50\times1)}{\{M\}} \qquad (2.3)$$

[A] is denoted as the static matrix which is defined as a matrix expressing the balancing moments at the joints and balancing lateral forces in terms of the end moments.

The static matrix [A] is tabulated in Table (2.1)

2.2.2 DEFORMATION MATRIX [B]

Deformation matrix [B] is defined as a matrix which expresses the elastic rotations, θ, at the ends of all members, as caused by the end moments M in terms of joint rotations or translations, X.

$$\{\theta\} = [B]\{X\} \qquad (2.4)$$

[B] may be established columnwise by considering the effects of each joint rotation and translation X on all the elastic end rotations θ . [B] is called the deformation

matrix because it is solely based on the effects of the disturbing external joint rotations or translations on the flexural deformation at the ends of the members.

Consider, for instance, the effect of X_1 (keeping X_2, X_3, X_4, ... X_{26} all equal to zero) will be

$$\theta_1 = X_1 \qquad \text{and} \qquad \theta_{34} = X_1$$

Similarly, the effect of X_2 (keeping all other X's zero) will be

$$\theta_2 = X_2 , \quad \theta_3 = X_2 \quad \text{and} \quad \theta_{36} = X_2$$

Turning to the effect of horizontal joint translation, X_{19} , as shown in Fig. (2.5a). From which

$$\theta_{33} = \theta_{34} = \theta_{35} = \theta_{36} = \cdots$$
$$= \theta_{48} = \theta_{49} = \theta_{50} = -\frac{1.0}{H} X_{19}$$

where H is the height of the truss.

The effect of each vertical joint displacement, for instance, X_{20} , as shown in Fig. (2.5b) , is

$$\theta_1 = \theta_2 = \theta_{17} = \theta_{18} = -\frac{1.0}{L} X_{20}$$

$$\theta_3 = \theta_4 = \theta_{19} = \theta_{20} = +\frac{1.0}{L} X_{20}$$

where L is panel length.

By considering the effects of each joint rotation or translation in this way, the deformation matrix [B] can be

established columnwise.

Table(2.2) shows the established matrix [B] for the Vierendeel truss.

A comparison between Tables (2.1) and (2.2) shows that the deformation matrix [B] is the transpose of the static matrix [A]. This characteristic is always found in all cases solved by this method.

Therefore, $$[B] = [A^T] \qquad (2.5)$$

Hence, it is not necessary to establish directly matrix [B] as it can be indirectly obtained by the transpose of the static matrix [A]. Sometimes, it is worthwhile to write out a few elements of [B] to check the correctness of [A].

2.2.3 STIFFNESS MATRIX [S]

The internal end moments M_a and M_b at the ends of an initially straight prismatic member ab (as shown in Fig.2.6) can be expressed in terms of the two internal end rotations θ_a and θ_b by using the slope-deflection equation;-

$$M_a = \frac{4EI}{L}\theta_a + \frac{2EI}{L}\theta_b$$

$$M_b = \frac{2EI}{L}\theta_a + \frac{4EI}{L}\theta_b \qquad (2.6)$$

where E and I are the Young's modulus and the moment of inertia of the member respectively, and are constant throughout its length. The elastic end rotation θ is considered positive when

the rotation is clockwise.

The total angle of rotation of semi-rigid connected member ab subjected respectively to couples M_a and M_b is, [Appendix I] [5]

$$\theta_a = \frac{M_a L}{3EI} - \frac{M_b L}{6EI} + \frac{M_a}{J} \qquad (2.7a)$$

$$\theta_b = \frac{-M_a L}{6EI} + \frac{M_b L}{3EI} + \frac{M_b}{J} \qquad (2.7b)$$

where J is the joint modulus*.

Solving eqns. (2.7a) and (2.7b) for M_a and M_b, we get [Appendix I] [7][8]

$$M_a = 6EI \frac{2L'}{4L'^2 - L^2}\theta_a + 6EI \frac{L}{4L'^2 - L^2}\theta_b$$

$$M_b = 6EI \frac{2L'}{4L'^2 - L^2}\theta_b + 6EI \frac{L}{4L'^2 - L^2}\theta_a \qquad (2.8)$$

where $L' = L + 3EIZ$

and $Z = 1.0 / J$

---

* The joint modulus J, or the rotational spring constant is a property of the joint. Mathematically speaking, it is the applied moment M divided by the relative rotation Ø of the connection when behaviour is elastic, i.e. M/Ø. The relationship between M and Ø is shown in Fig. 2.7. The joint modulus is usually measured in in-kips per radian.

When $J=\infty$ for the case of rigid connections, Eqn.(2.8) coincides with Eqn.(2.6) .

Hence, the slope-deflection equations for the chord members are given by Eqn.(2.6). Whereas, for the web members, Eqn.(2.8) are used.

By using Eqns.(2.6) and (2.8) , the relationship between the end moments and the end rotations for each member in the truss can be written as ;-

$$
\begin{aligned}
M_1 &= \frac{4EI}{L}\theta_1 + \frac{2EI}{L}\theta_2 \\
M_2 &= \frac{2EI}{L}\theta_1 + \frac{4EI}{L}\theta_2 \\
M_3 &= \frac{4EI}{L}\theta_3 + \frac{2EI}{L}\theta_4 \\
M_4 &= \frac{2EI}{L}\theta_3 + \frac{4EI}{L}\theta_4 \\
&\vdots \qquad\qquad \vdots \\
M_{33} &= 6EI\,\frac{2L'}{4L'^2 - L^2}\theta_{33} + 6EI\,\frac{L}{4L'^2 - L^2}\theta_{34} \\
M_{34} &= 6EI\,\frac{L}{4L'^2 - L^2}\theta_{33} + 6EI\,\frac{2L'}{4L'^2 - L^2}\theta_{34} \\
&\vdots \qquad\qquad \vdots \\
M_{50} &= 6EI\,\frac{L}{4L'^2 - L^2}\theta_{49} + 6EI\,\frac{2L'}{4L'^2 - L^2}\theta_{50}
\end{aligned}
\tag{2.9}
$$

Arranging Eqn.(2.9) in matrix notation, we have

$$\underset{(50\times1)}{\{M\}} = \underset{(50\times50)}{[S]}\ \underset{(50\times1)}{\{\theta\}} \qquad (2.10)$$

[S] is call the <u>stiffness matrix</u> in which the internal end moments are expressed in terms of the internal end rotations. [S] is a square matrix of order (50X50), its elements are given as the coefficients of $\{\theta\}$ in Eqn.(2.9) .

2.2.4 MATRIX $\{P\}$

Matrix $\{P\}$ had been defined in Section 2.2.1 as a column matrix showing values of unblanced moments at the joints and unbalanced linear forces. Now, returning to the real situation, the truss is only subjected to loading in which all P's are zero except P_{20}, P_{21}, P_{22}, P_{23}, P_{24}, P_{25}, P_{26} of equal magnitude acting at the panel points. Reference is made to Fig. 2.1

Therefore, matrix $\{P\}$ can be quickly established as

$$\underset{(26\times1)}{\{P\}} = \begin{Bmatrix} 0 \\ 0 \\ 0 \\ \vdots \\ P_{20} \\ P_{21} \\ P22 \\ P_{23} \\ \vdots \\ P_{26} \end{Bmatrix} \qquad (2.11)$$

The matrix $\{P\}$ can also be extended to include many different kinds of loading conditions. Each column of matrix $[P]$ is for each loading condition. If there are four different loading conditions, the matrix $[P]$ will then have four columns. Therefore $[P]$ is no longer a column matrix if the loading condition is a combination of loads.

2.3 MATRIX OPERATIONS

Three matrices $[A]$, $[S]$and $\{P\}$, which have been discussed in previous Sections, are all input matrices which have to be established before solving the problem. The solutions, or the output matrices are the displacement matrix $\{X\}$ and the internal-end-moment matrix $\{M\}$.

The operation of the matrix calculation is given as follows.

From the static equilibrium condition

$$\{P\} = [A]\{M\} \tag{2.3}$$

From the condition of deformation

$$\{\theta\} = [B]\{X\} \tag{2.4}$$

$$= [A^T]\{X\} \tag{2.4a}$$

Since $[B] = [A^T]$ (2.5)

From the slope-deflection equations

$$\{M\} = [S]\{\theta\} \tag{2.10}$$

Substituting Eqn.(2.4a) into Eqn.(2.10), yields

$$\{M\} = [S\ A^T]\{X\} \tag{2.12}$$

Substituting Eqn.(2.12) into Eqn.(2.3), we get

$$\{P\} = [A\ S\ A^T]\{X\} \tag{2.13}$$

Rearranging matrix equation(2.13), we obtain the output matrix $\{X\}$

$$\text{i.e. } \{X\} = [A\ S\ A^T]^{-1}\{P\} \tag{2.14}$$

Substituting the known matrix $\{X\}$ into Eqn.(2.12), we finally obtain another output matrix $\{M\}$.

With the results of $\{X\}$ and $\{M\}$, the analysis is thus complete.

A set of the solutions for a particular case(see the detail in Fig.(2.8a)) is plotted on the truss as shown in Figs.(2.8b) and (2.8c).

2.4 LIMITATIONS ON DEFLECTION

A computer programme [Appendix II] has been set up to analyse the truss with joint moduli varying from $J = 1 \times 10^4$ to 1×10^8 (in-kips/rad.) and with constant panel point concentrated loads. The dimensions of the adopted HSS are 4X4 for the web members and 8X8 for the chord members. Thickness of 1/4" and 1/2" are used. The panel length and the height of the truss is

8 ft. in the case of $\frac{1}{2}$" thick material and 13 ft. for $\frac{1}{4}$" material.

It is recognised that, with the adding of semi-rigid connections on the joints, the behaviour of the truss becomes flexible. That is to say, when the modulus decreases, the flexibility of the joint increases. As a result, the maximum deflection of the truss at the central point becomes more and more conspicuous. With certain limits on deflection set for the truss, the limits of joint modulus and loads can be found.

Figs.(2.9) are plots of the central deflection versus joint modulus to show the influence of joint modulus on the deflection of trusses. As can be seen from the Figures. the curves start to become flat when $J > 1 \times 10^6$ in-kips/rad. . Therefore, the connections can be regarded as rigid when J exceeds 1×10^6 in-kips/rad. .[6]

The limitations on deflection set by National Building Code (NBC)[9] are as follows,

(i) $\delta_{max.} < \frac{L}{360}$ for plastered ceilings

(ii) $\delta_{max.} < \frac{L}{320}$ for floor beams

(iii) $\delta_{max.} < \frac{L}{240}$ for asphalt roofing

(iv) $\delta_{max.} < \frac{L}{180}$ for metal or elastic membrane type roofing

where L is the span of a simply supported beam or truss.

With certain limitations on deflection in mind, the designer can choose his joint modulus within the required limits.

From Eqn.(2.13), the deflections and rotations for any joint can be found. Of primary interest is X_{23} which represents the central vertical deflection of the truss. From the results of the computer programme (Appendix II) and employing the particular examples of the Vierendeel trusses whose geometries were specified earlier, Table 2.3 illustrates the deflections at mid span with rigid($J = \infty$) and semi-rigid($J = 1 \times 10^4$ in-k/rad) connections for 1 kip loading at each panel point. The NBC limiting deflections for the specific trusses are also given.

2.5 STRENGTH LIMITATIONS

The computer programme referred to earlier (Appendix II) also defines the elastic stresses at all member ends according to the formula

$$\sigma = \frac{M}{S} + \frac{F}{A} \qquad (2.15)$$

where σ is the outer fibre stress in ksi at the critical

point considered

M is the associated bending moment in in-kips

F is the pertinent axial force in kips

A is the cross sectional area in $in.^2$

and S is the section modulus in $in.^3$

For the two trusses A* and B* considered, Figs.(2.10a) and (2.10b) indicate the stresses at each critical point for panel point loadings of 4.2 kips and 2.5 kips respectively for materials that yield at 55ksi. Note that Egn.(2.15) has been used in each case limiting the loading such that the maximum stress is equal to the maximum value at the most highly stressed section. In each case the critical section is the exterior web member. For truss A, plate slenderness is sufficiently small that the critical buckling stress is approximately equal to the yield stress. For truss B, although the critical buckling is somewhat less than yield because of increased slenderness, there is very little reduction in the maximum stress. A more complete description of the critical stress for plate buckling is described in Chapter III. Note that the flexibility at the web member ends alters the stress somewhat. For semi-rigid connections, the chord members carry a greater share of the load than do the web members. Consequently the critical point mentioned has a slightly reduced stress.

A simplified design for the examples will follow in the

* Truss A is 8 ft. deep using 1/2 in. thick HSS
* Truss B is 13 ft. deep using 1/4 in. thick HSS

next Section permitting the designer to employ joint flexibility as a parameter.

2.6 DESIGN PROCEDURES

For purposes of indicating the method design, the simplest possible geometry and sizing of members are assumed. The top and bottom chords are assumed to be parallel and of the same cross section. All web members are assumed to be of identical section, although it was evident from the previous Section that stiffer end web members would have improved the overall stress balance of the truss. However, since a deflection criterion is normally important, the examples are merely an attempt to illustrate the need to consider both strength and deflection in design.

Sections 2.4 and 2.5 describe deflection and strength criteria in the design process. For truss A, it is evident from Figs.(2.10) that a limiting panel point loading of 4.2 kips is necessary to prevent failure at a section (viz. sections 34 and 50 in Fig.(2.3) .

Deflection criteria are normally based on working stress levels rather than computed maximum values. Consequently to relate the panel point loadings from a strength point of view to deflection limitations, a reduction to 60% of capacity is required. When the deflection limitation of L/180 is imposed under working loads, it is evident from Table 2.3 that for $J = \infty$ the actual deflection for 2.5 kips(i.e. 4.2/1.67 kips)

is less than the limiting value. However, for $J = 1 \times 10^4$ in-k/rad the actual deflection of 0.521 ft. exceeds that of L/180 and is therefore not acceptable. A value of $J = 2.5 \times 10^4$ in-k/rad just satisfies the deflection criterion. Note that the stress at sections 34 and 50 are reduced somewhat and hence an iteration process may be attempted to refine the correct panel point loading and associated J value. This was not pursued in this study because the stress changes were rather small.

For truss B, similar results are evident. The limiting panel point loading is 2.5 kips to cause a stress of nearly 55 ksi at the critical section. Again, from either Table 2.3 or Figs.(2.10), when $J = 5 \times 10^4$ in-k/rad., the limiting deflection of L/180 for 1.5 kips(=2.5/1.67 kips) per panel point is reached with little change in the stresses throughout.

	Truss A	Truss B
Chord Member	8"x 8"x $\frac{1}{2}$"	8"x 8"x $\frac{1}{4}$"
Web member	4"x 4"x $\frac{1}{2}$"	4"x 4"x $\frac{1}{4}$"
Panel length	8 ft.	8 ft.
Truss Depth	8 ft.	13 ft.

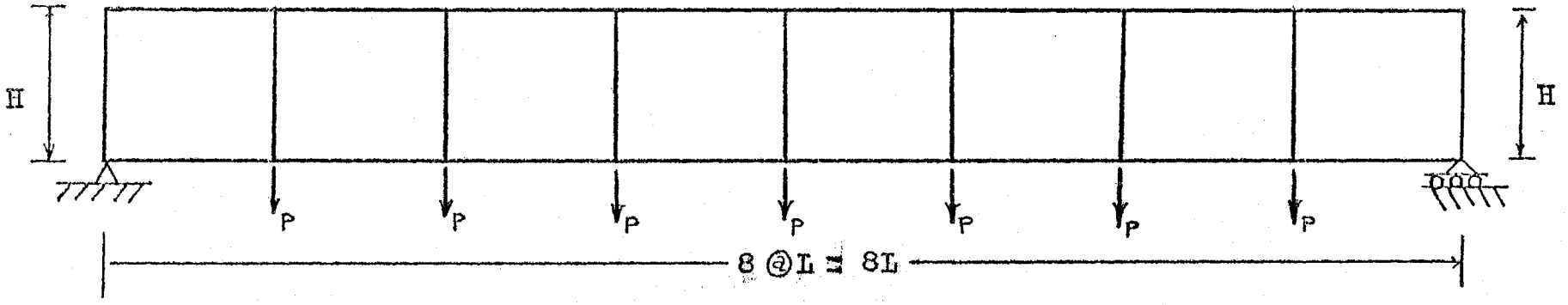

Fig. 2.1 Vierendeel Truss With Panel Point Loads

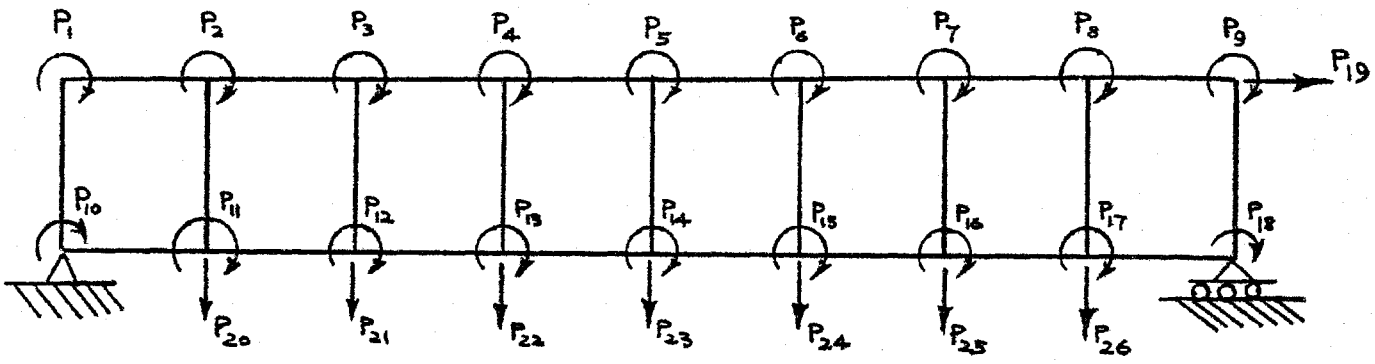

Fig. 2.2 A Diagram showing Unbalanced Forces and Displacements (Displacements X's are in the same directions as unbalanced forces P's)

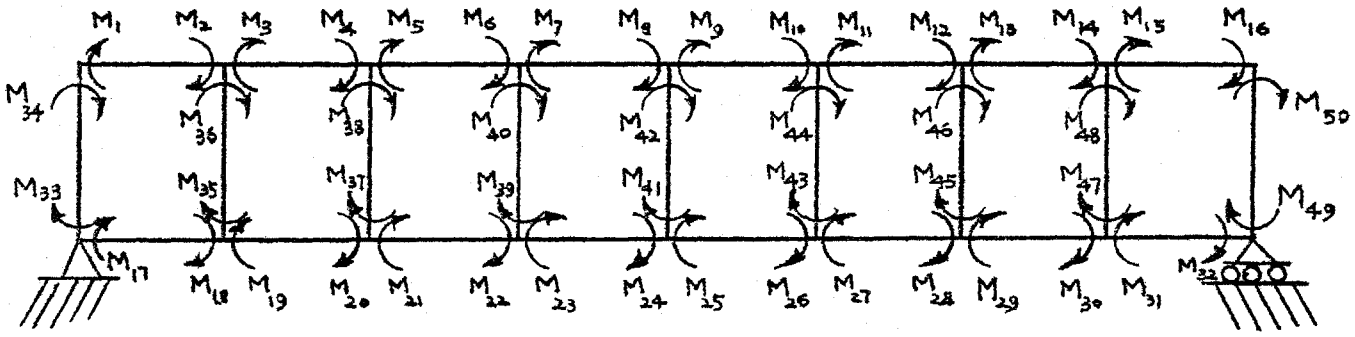

Fig. 2.3 End Moments

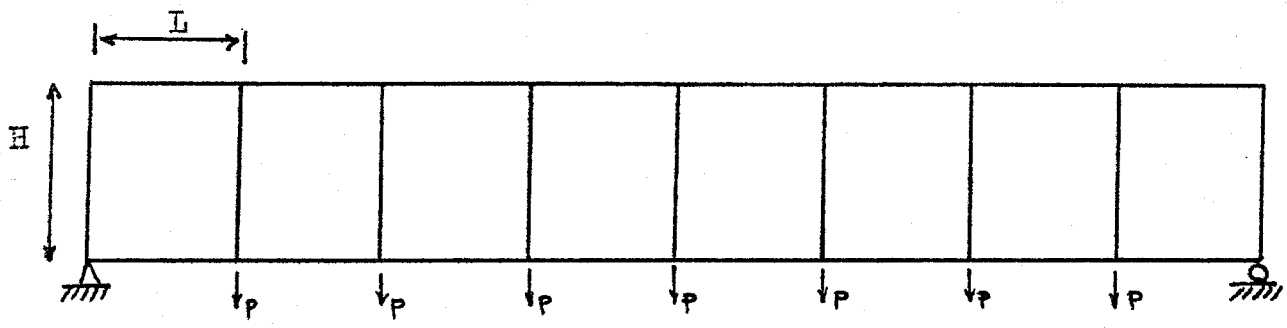

Fig. (2.4.a) Vierendeel Truss With Panel Point Loading

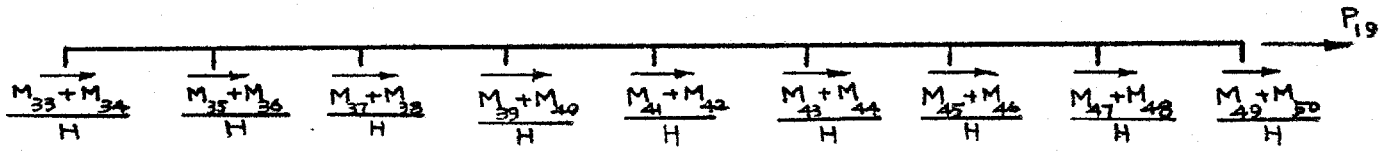

Fig.2.4.b Top Chord's Free Body Diagram For $\Sigma F_x = 0$

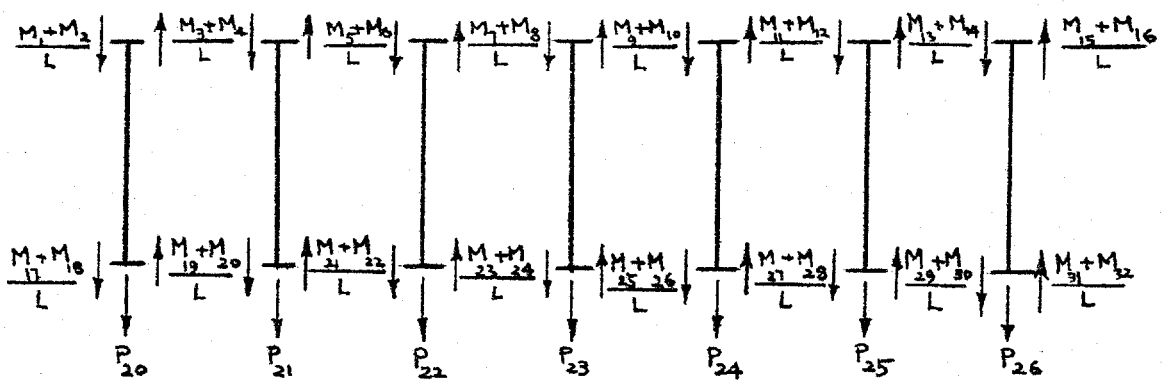

Fig. 2.4.c Free Body Diagrams For Web Members For $\Sigma F_y = 0$

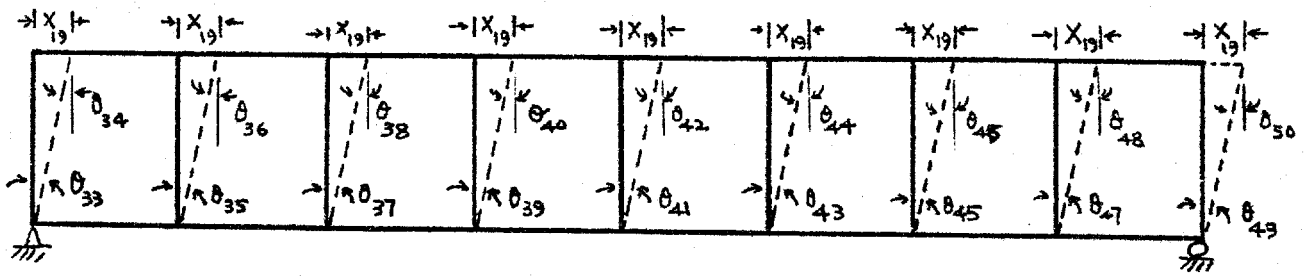

Fig. 2.5.a Effect of X_{19} on Internal End Rotations While Other X's are Zero

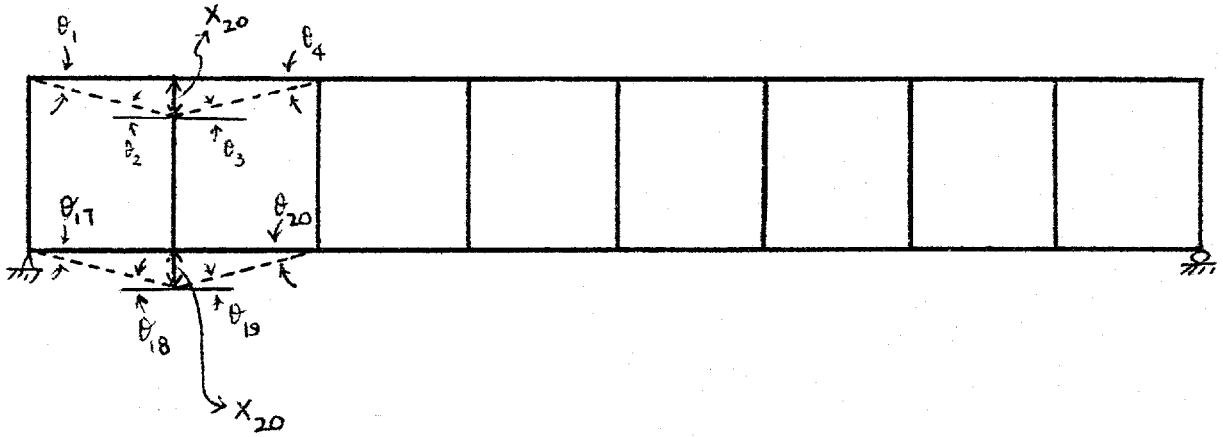

Fig. 2.5.b Effect of X_{20} on Internal End Rotations While Other X's are Zero

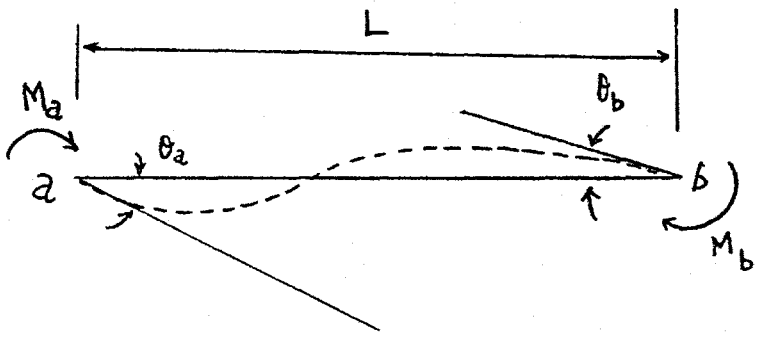

Fig. 2.6 Bending of A Member ab

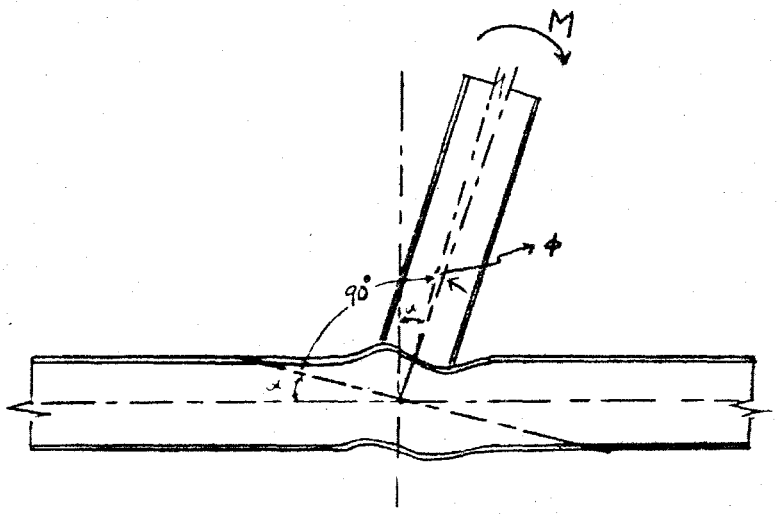

Fig. 2.7.a Semirigid Connection with Relative Rotation

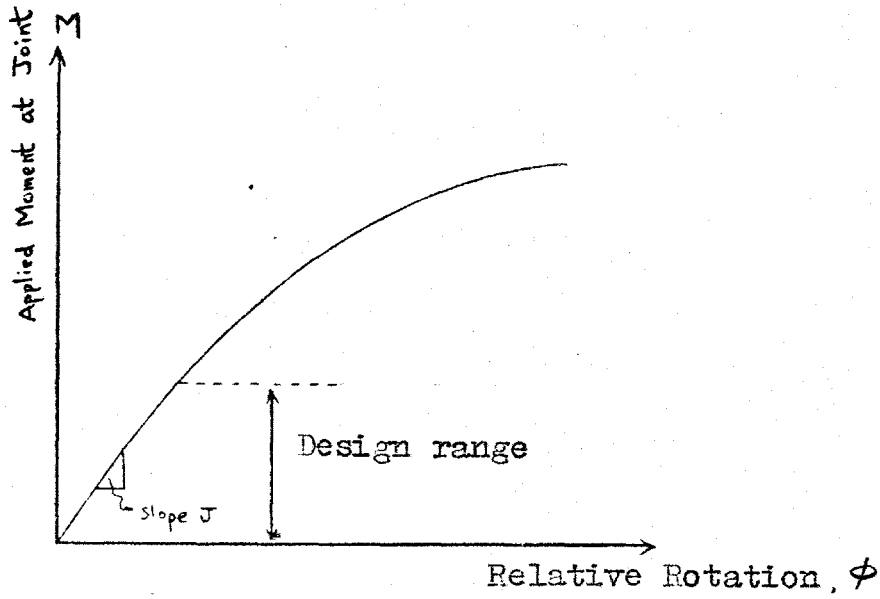

Fig. 2.7.b Moment-Rotation Curve For A Semirigid Connection

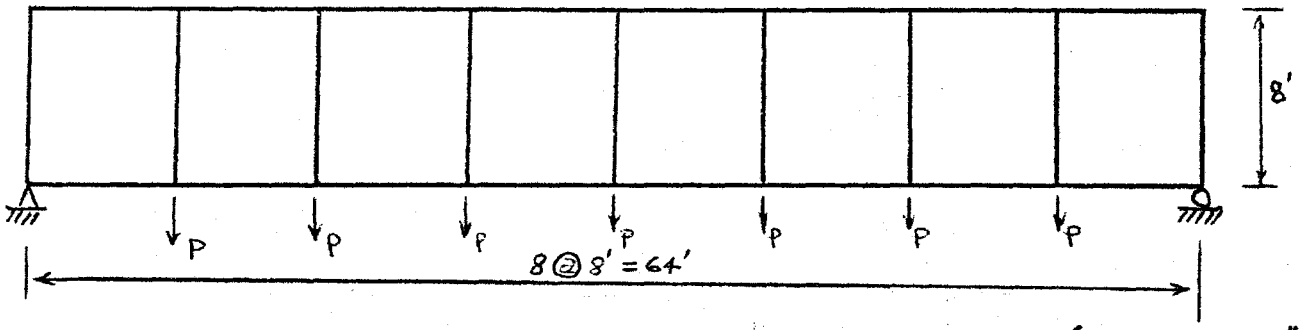

(a) Truss with Panel Load P = 1 Kip (Chord Member : 8"×8"×½"
Web Member : 4"×4"×½")

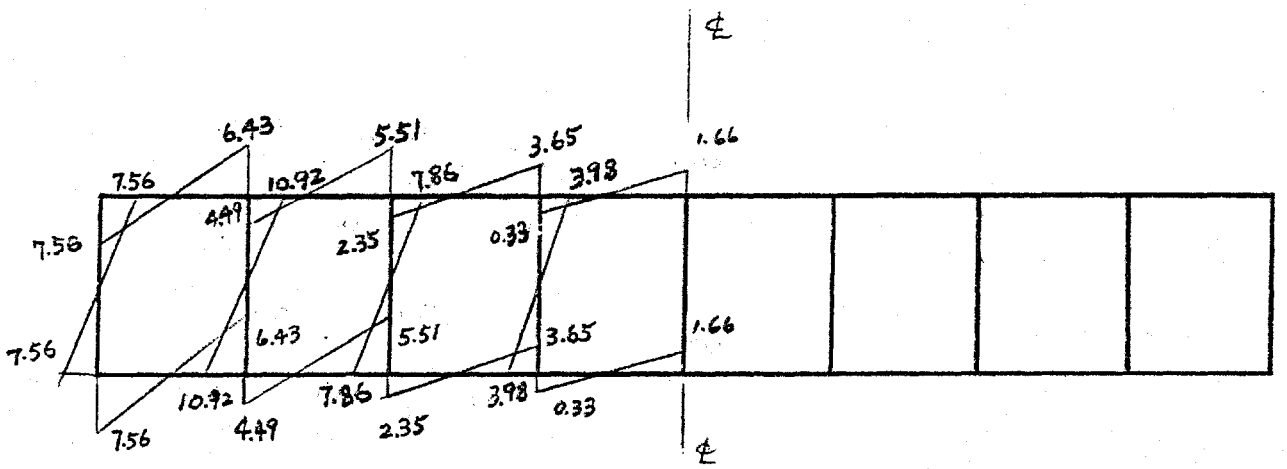

(b) Moment Distribution (ft-Kips)

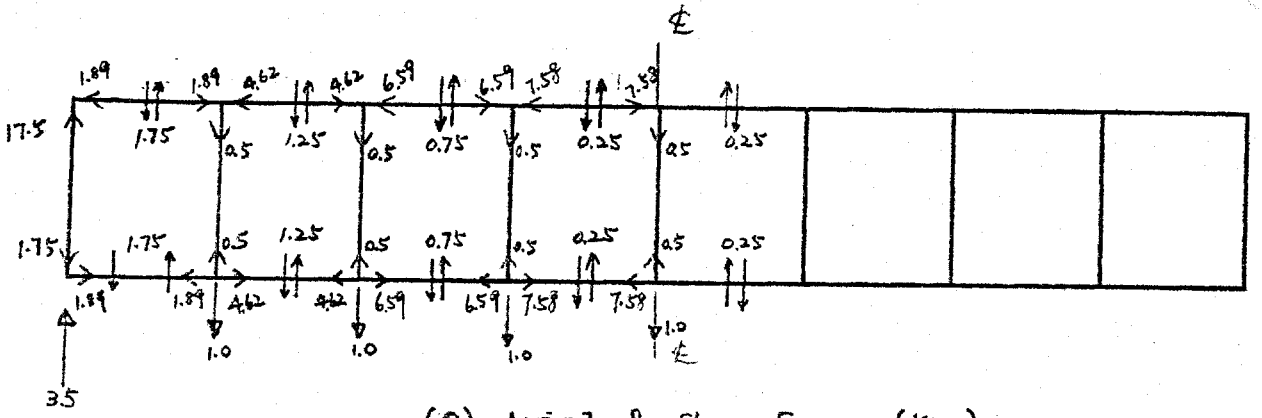

(c) Axial & Shear Forces (Kips)

Fig. 2.3 A Set of Solution For Panel Load P = 1 K

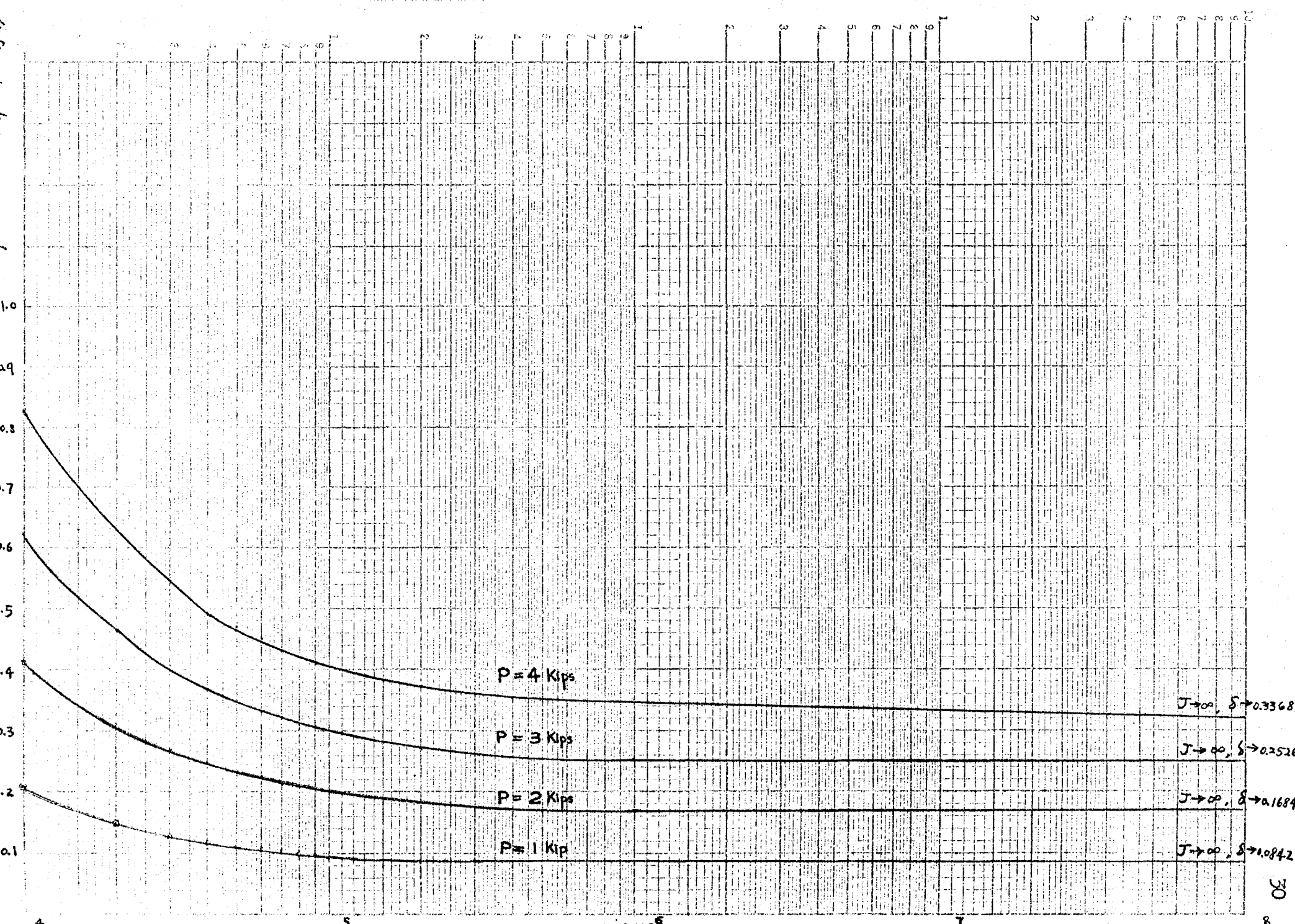

Fig. 2.9.a Plot of Deflection Versus J for Truss A

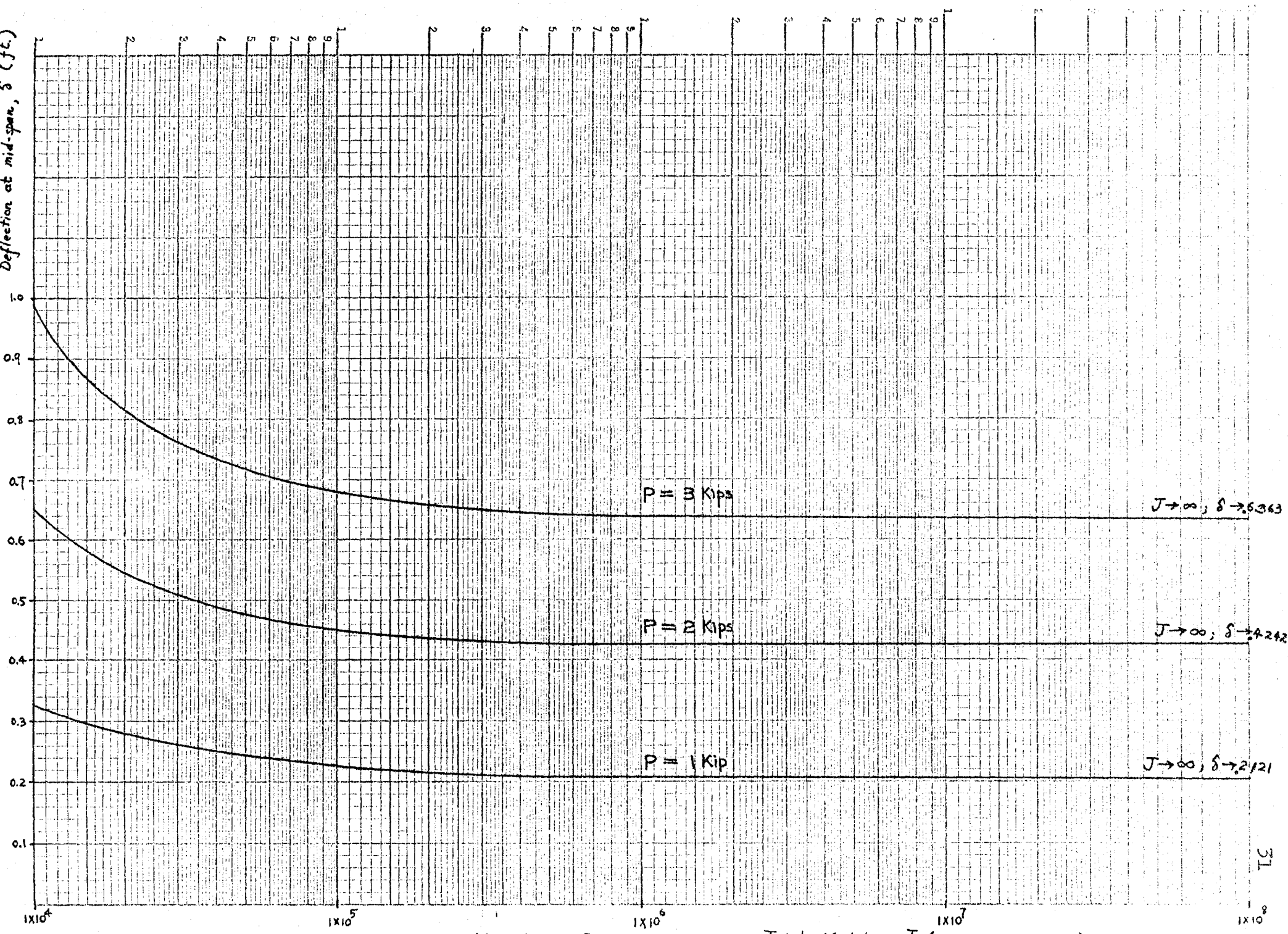

Fig. 2·9·b Plot of Deflection Versus J For Truss B

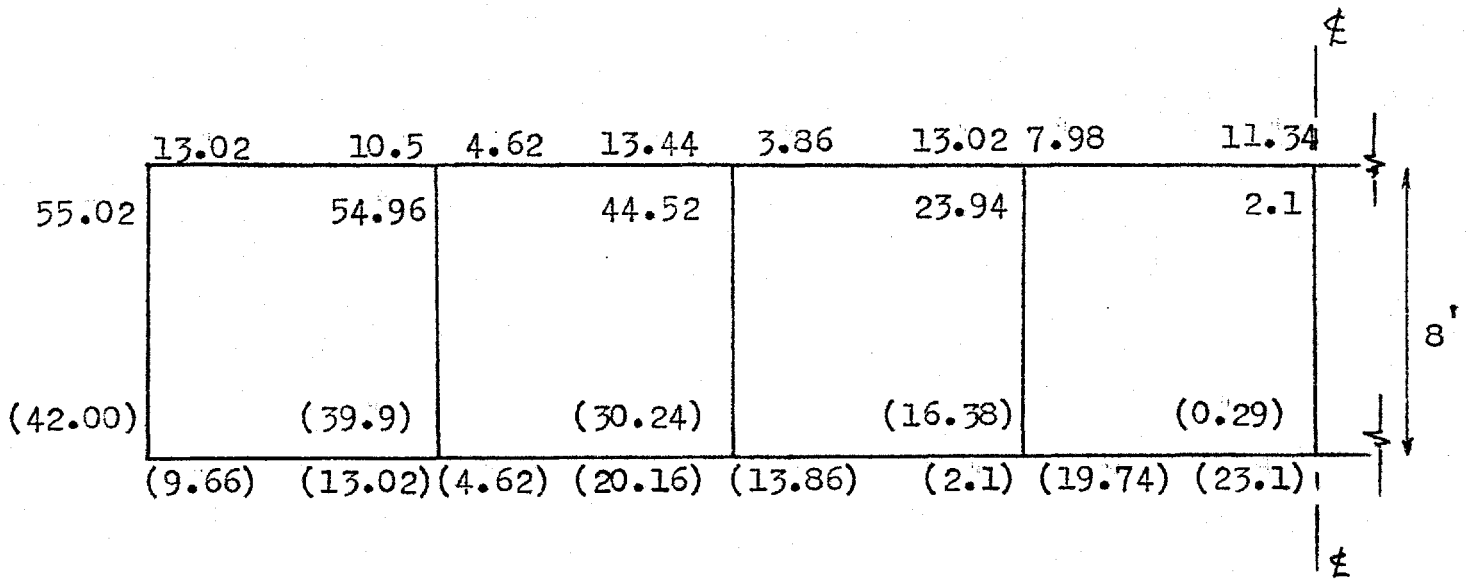

Fig. 2.10a : Stresses For Panel Point Loads of 4.2 Kips For truss A

(Note: Bracketed Nos. Refer to $J=1x10^4$ in-k/rad

Plain Nos. Refer to $J=\infty$)

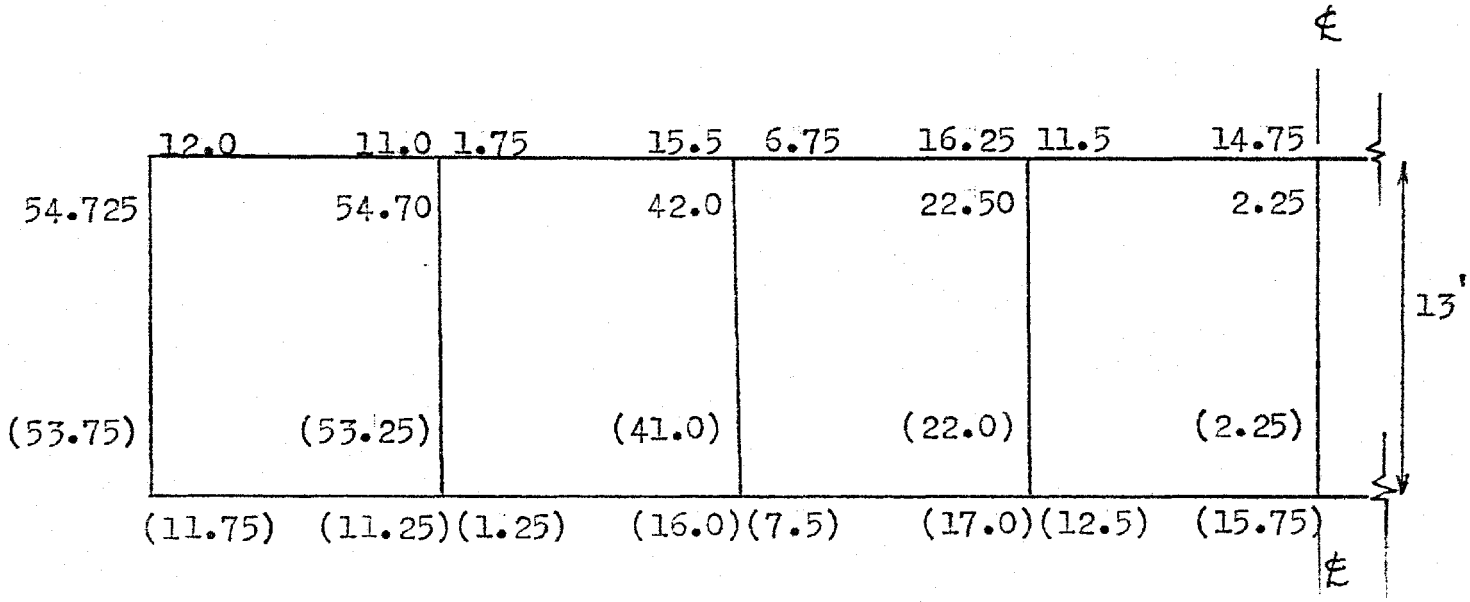

Fig. 2.10b : Stresses for Panel Loads of 2.5 Kips for Truss B

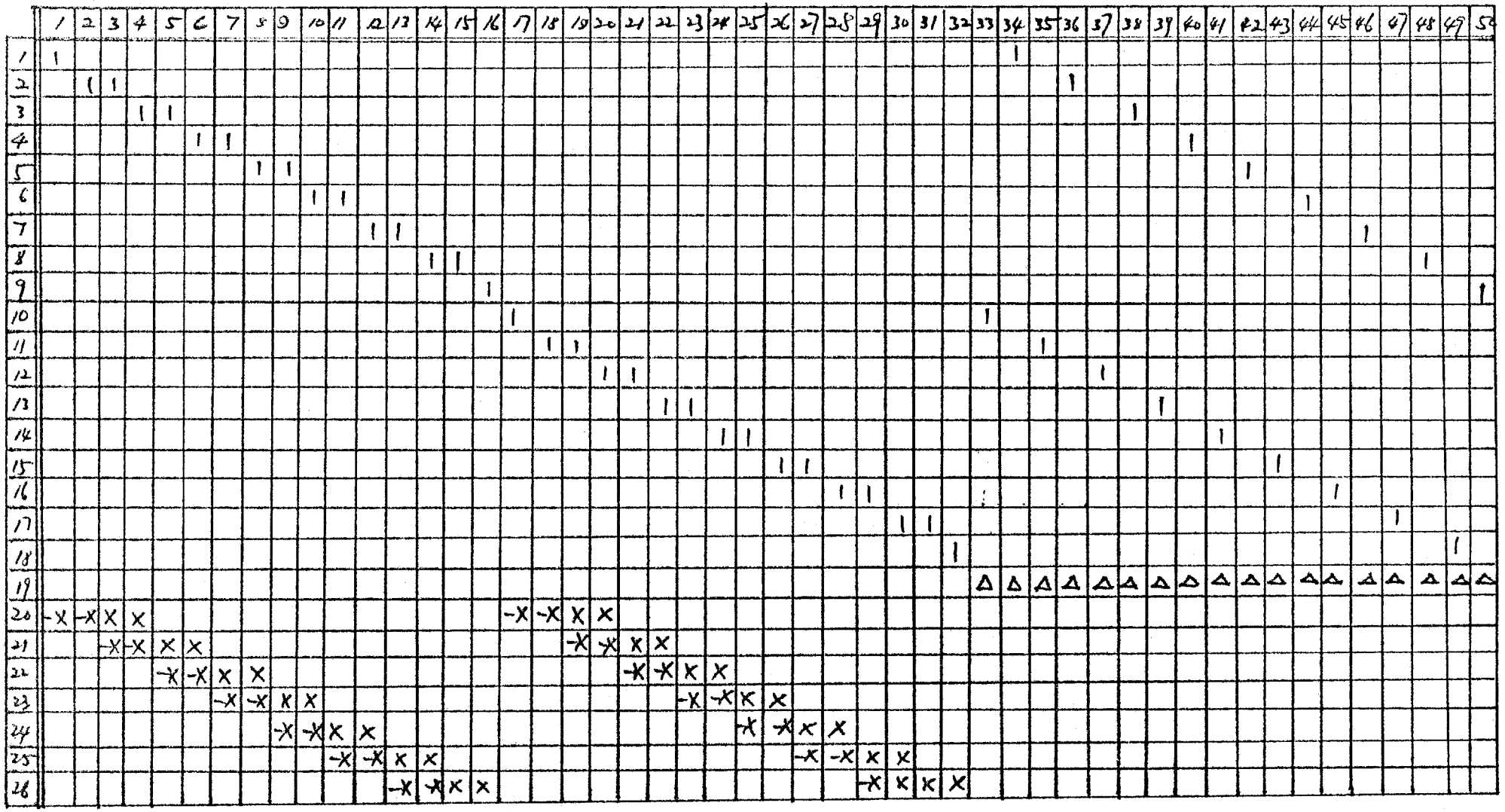

Table 2.1 Static Matrix [A]

where : $\Delta = \frac{-1}{H}$

$X = \frac{1}{L}$

H = Height of the truss (ft.)

L = Span Length of the truss (ft.)

Blank block means zero

Table 2·2 Deformation Matrix [B]

where $\Delta = -\frac{1}{H}$
$X = 1/L$
H = Height of truss (ft.)
L = Span Length (ft.)

	1	2	3	4	5	6	7	8	9	10	11	12	13	14	15	16	17	18	19	20	21	22	23	24	25	26
1	1																			-X						
2		1																		-X						
3		1																		X	-X					
4			1																	X	-X					
5			1																		X	-X				
6				1																	X	-X				
7				1																		X	-X			
8					1																	X	-X			
9					1																		X	-X		
10						1																	X	-X		
11						1																		X	-X	
12							1																	X	-X	
13							1																		X	-X
14								1																	X	-X
15								1																		X
16									1																	X
17										1										-X						
18											1									-X						
19											1									X	-X					
20												1								X	-X					
21												1									X	-X				
22													1								X	-X				
23													1									X	-X			
24														1								X	-X			
25														1									X	-X		
26															1								X	-X		
27															1									X	-X	
28																1								X	-X	
29																1									X	-X
30																	1								X	-X
31																	1									X
32																		1								X
33										1									Δ							
34	1																		Δ							
35											1								Δ							
36		1																	Δ							
37												1							Δ							
38			1																Δ							
39													1						Δ							
40				1															Δ							
41														1					Δ							
42					1														Δ							
43															1				Δ							
44						1													Δ							
45																1			Δ							
46							1												Δ							
47																	1		Δ							
48								1											Δ							
49																		1	Δ							
50									1										Δ							

	Truss A*	Truss B*	J value
Deflections for 1 kip at Panel Points (ft.)	0.20828	0.32869	1×10^4 in-K/rad
	0.08420	0.2120	∞ "

Deflection Criterion	δ (ft)	Panel Point Loads		J Value in-K/rad.
		Truss A*	Truss B*	
$\delta < L/360$	0.178	2.11 K.	0.83 K.	∞ in-Kip/rad.
		0.85 K.	0.54 K.	1×10^4 "
$\delta < L/320$	0.200	2.37 K.	0.94 K.	∞ "
		0.96 K.	0.61 K.	1×10^4 "
$\delta < L/240$	0.267	3.17 K.	1.26 K.	∞ "
		1.28 K.	0.81 K.	1×10^4 "
$\delta < L/180$	0.355	4.21 K.	1.67 K.	∞ "
		1.70 K.	1.08 K.	1×10^4 "

Table 2.3 Central Deflections and Code Limitations

* Truss A is 8' deep using $\frac{1}{2}$" thick HSS

* Truss B is 13' deep using $\frac{1}{4}$" thick HSS

CHAPTER III

THE BUCKLING PROBLEM OF THE HSS MEMBERS SOME DISTANCE AWAY FROM THE JOINT

3.1 GENERAL INTRODUCTION

In addition to the attention paid in the preceding Section to the limitation on deflection, one of the important facts for the design of a long-span Vierendeel truss is the relationship between the load capacity and the geometry of the section. These relationships are mostly a function of instability. As the adopted sections are HSS which consist of thin plate assemblages, the instability problem of the section becomes more prominent. The top chord member at mid-span is often critical. However, as the last Chapter showed the ends of the outside web members are stressed most severely for the trusses examined.

Thus the problem is to find the permissible ratio b/t of the plate element of the compression flange.

The foregoing mentioned buckling problem is referred to the section some distance away from the joint. The buckling problem of the section right under the joint is beyond the scope of this volume and will not be included in the following discussion.

3.2 LOCAL BUCKLING OF PLATE ELEMENT OF HSS COMPRESSION FLANGE

THE GOVERNING EQUATION OF PLATE UNDER AXIAL LOAD

The governing equation of the plate of dimensions a×b under the action of forces in its middle plane(see Fig.3.1) is [10]

$$D\left(\frac{\partial^4 W}{\partial x^4}+2\frac{\partial^4 W}{\partial x^2\partial y^2}+\frac{\partial^4 W}{\partial y^4}\right)+t\left(\sigma_x\frac{\partial^2 W}{\partial x^2}+\sigma_y\frac{\partial^2 W}{\partial y^2}+2\tau_{xy}\frac{\partial^2 W}{\partial x\partial y}\right)=0 \qquad (3.1)$$

where D = Flexural rigidity of plate per unit width
$= \frac{Et^3}{12(1-\nu^2)}$

ν = Poisson's ratio, and is 0.3 for steel

t = Plate's thickness

W = Transverse deflection of plate

σ_x, σ_y = Normal stresses in x and y directions respectively

τ_{xy} = Shearing stress in the plane of the plate

Note that the x and y are orthogonal coordinates in the plane of the plate, x being parallel to the chord member axis.

In the present case of HSS compression flange, only a uniformly distributed compressive stress σ_x exists. Eqn.(3.1) becomes

$$D\left(\frac{\partial^4 W}{\partial x^4}+2\frac{\partial^4 W}{\partial x^2\partial y^2}+\frac{\partial^4 W}{\partial y^4}\right)+\sigma_x t\frac{\partial^2 W}{\partial x^2}=0 \qquad (3.2)$$

Eqn.(3.2) is only valid within the elastic limit. When σ_x exceeds the elastic limit, Eqn.(3.2) has to be modified. Beyond the elastic limit, the tangent-modulus E_t will be effective in the x-direction while in the y-direction Young's modulus E can be assumed to remain valid as $\sigma_y = 0$. Introducing $\tau = E_t/E$, Eqn.(3.2) is generalised as

$$D\left(\tau\frac{\partial^4 W}{\partial x^4} + 2\sqrt{\tau}\nu\frac{\partial^4 W}{\partial x^2 \partial y^2} + \frac{\partial^4 W}{\partial y^4}\right) + \sigma_x t\,\frac{\partial^2 W}{\partial x^2} = 0 \qquad (3.3)$$

When σ_x is within elastic zone, τ is equal to 1.0 as $E_t = E$, thus Eqn.(3.3) returns to Eqn.(3.2) .

The moments in the x and y directions can be expressed as

$$M_x = -D\left(\tau\frac{\partial^2 W}{\partial x^2} + \nu\sqrt{\tau}\frac{\partial^2 W}{\partial y^2}\right)$$
$$M_y = -D\left(\nu\sqrt{\tau}\frac{\partial^2 W}{\partial x^2} + \frac{\partial^2 W}{\partial y^2}\right) \qquad (3.4)$$

GENERAL SOLUTION OF THE GOVERNING EQUATION

The general solution of the governing Equation (3.3) can be obtained by using the boundary conditions of which the conditions on the loaded edges are first considered.

(A) The B. C. on The Loaded Edges

The loaded edges are assumed simply supported. The B. C. are thus

$$W\Big]_{\substack{x=0\\x=a}} = 0 \quad ; \quad \frac{\partial^2 W}{\partial x^2}\Big]_{\substack{x=0\\x=a}} = 0 \qquad (3.5)$$

Where a is the length of the plate in x-direction, b, appears later, is the width of the plate in y-direction.

The second portion of Eqn.(3.5) is due to the first of Eqn.(3.4) where $M_x = 0$ and $\partial^2 w/\partial y^2 = 0$.

$$\text{Assume} \qquad W = Y \sin \frac{n\pi x}{a} \qquad (3.6)$$

which satisfies the above mentioned B.C.. Y is a function of y.

Substituting Eqn.(3.6) into the governing partial differential equation(3.3) and solving the resulting ordinary differential equation leads to the full expression of Eqn.(3.6) as given below

$$W = (c_1 \cosh k_1 y + c_2 \sinh k_1 y + c_3 \cos k_2 y + c_4 \sin k_2 y) \sin \frac{n\pi x}{a} \qquad (3.7)$$

where $k_1 = \frac{n\pi}{a}\sqrt[4]{\tau}\sqrt{\mu+1}$, $k_2 = \frac{n\pi}{a}\sqrt[4]{\tau}\sqrt{\mu-1}$,

$= \frac{\sigma_c t}{D\tau}\left(\frac{a}{n\pi}\right)^2$, σ_c = buckling stress

The constant terms c_1, ... c_4 are to be determined by using the B. C. of the unloaded edges

(B) <u>The B. C. on The Unloaded Edges</u>

The unloaded edges have the following B. C. ;-

(i) The web plates of HSS exert equal elastic restraint on the unloaded edges. The deflection, W, corresponding to the smallest value of σ_c is an even function of y. Thus c_2 and c_4 in Eqn.(3.7) vanish.

(ii) The unloaded edges remain straight.

(iii) The angle of rotation at the edge of the buckling plate is equal to the angle of rotation of the adjoining restraining web plate.

Using the above mentioned B. C. leads to the buckling condition, namely

$$\sqrt{\mu+1}\,\tanh\left(\frac{\pi}{2}\sqrt{\mu+1}\,\frac{n\sqrt[4]{\tau}}{\alpha}\right)+\sqrt{\mu-1}\,\tan\left(\frac{\pi}{2}\sqrt{\mu-1}\,\frac{n\sqrt[4]{\tau}}{\alpha}\right)+\pi\varsigma\mu\,\frac{n\sqrt[4]{\tau}}{\alpha}=0 \qquad (3.8)$$

where $\alpha = a/b$ and ς is the <u>coefficient of restraint</u>. $\varsigma = 0$ when the edge is rigidly fixed, and $\varsigma = \infty$ when the edge is simply supported.

(C) <u>Equation for Buckling Stress σ_c</u>

A solution of buckling-condition Eqn.(3.8) for the elastically restrained plate (where $0 < \varsigma < \infty$) leads to an equation for σ_c

$$\sigma_c = \frac{\pi^2 E\sqrt{\tau}}{12(1-\nu^2)}\left(\frac{t}{b}\right)^2\left[p+2\sqrt{q}\right] \qquad (3.9)$$

$$\text{or } \sigma_c = \frac{\pi^2 E\sqrt{\tau}}{12(1-\nu^2)}\left(\frac{t}{b}\right)^2 k \qquad (3.9)$$

where p and q are constants depending on the coefficient of restraint ψ and k is called the plate coefficient.

The value of k for a square HSS is 5.79 as can be found from the curve in Fig. 3.2 prepared by Hudoba [11] .

Determinations of Buckling Stress in the Inelastic Range And the b/t Ratio

In the elastic range where $\tau = 1.0$, the buckling stress can be determined directly from Eqn.(3.9) .

In the inelastic range, τ is an unknown as it depends on σ_c

$$\text{i.e.} \qquad \tau = \frac{(\sigma_y - \sigma_c)\sigma_c}{(\sigma_y - \sigma_p)\sigma_p} \qquad (3.10)$$

where σ_y = yield stress ; σ_p = proportional limit stress therefore, a method of trial and error will be necessary by using

$$\frac{\sigma_c}{\sqrt{\tau}} = \frac{\pi^2 E}{12(1-\nu^2)}\left(\frac{t}{b}\right)^2 k \qquad (3.11)$$

The procedure of calculation is as follows.

For a given HSS section, we can precalculate the value on the right-hand side of Eqn.(3.11), and then, a table is set up for the τ- values computed from Eqn.(3.10) with given σ_y

and σ_p and for the corresponding value of $\sigma_c/\sqrt{\tau}$. When the value of $\sigma_c/\sqrt{\tau}$ in the table is closely approaching the pre-calculated value on the right-hand side of Eqn.(3.11), the required buckling stress is found. For HSS steel σ_y =55 ksi and σ_p = 48 ksi . These values are based on the results of tensile tests carried out by Hudoba [11] and pertain to the example in Chapter II. Such a table for these values is given below

σ_c	τ	$\sigma_c/\sqrt{\tau}$
48.0	1.0000	48.0
49.0	0.8750	52.5
50.0	0.7450	58.0
51.0	0.6070	65.4
52.0	0.4640	76.5
54.0	0.1600	135.0
54.8	0.0326	303.0
55.0	0.0000	∞

In the above table it can be seen that τ-values vary from 1.0 to zero. Hudoba showed that when the total strain is 0.5% that τ= 0.1 . The corresponding buckling stress σ_c is about $0.99\sigma_y$ and thus the designed τ value of 0.1 can be considered reasonable for calculation of the critical b/t ratio in allowable stress design. For this τ-value of 0.1 the corresponding value of $\sigma_c/\sqrt{\tau}$ is 200, the critical b/t ratio can then be calculated as

$$b/t = \sqrt{\frac{\pi^2 E K}{12(1-\nu^2)}} \frac{\sqrt{\tau}}{\sigma_c}$$

$$= 28$$

where $E = 29600$ ksi

$\nu = 0.3$ (for steel)

$k = 5.79$ (for square HSS)

$\sigma_c/\sqrt{\tau} = 200$ ksi

For our examples of Vierendeel trusses whose members' dimensions were given in Chapter II, we can determine the buckling stress for the web members by using the following data and Table 3.1 .

$\sigma_y = 55$ ksi $\qquad \sigma_p = 48$ ksi

$E = 29600$ ksi $\qquad \nu = 0.3, \quad K = 5.79 , \quad b = 4"$

$t = \frac{1}{4}"$ and $\frac{1}{2}"$

$$\therefore \frac{\sigma_c}{\sqrt{\tau}} = \frac{\pi^2 E}{12(1-\nu^2)}\left(\frac{t}{b}\right)^2 k \quad = 605.219 \text{ ksi (for } \tfrac{1}{2}" \text{ material)}$$

$$= 2420.8 \text{ ksi (for } \tfrac{1}{2}" \text{ material)}$$

For these calculations, it is evident that assuming the yield stress of 55 ksi for each case was in close agreement with the critical stresses for buckling.

Although the stress of the top chord member was not critical in the matrix analysis given in Chapter II, it is necessary to check that the 8 x $\frac{1}{4}$ plate does not have a critical stress substanially below the yield value. Since the behaviour is purely elastic up to 48 ksi , a simple elastic calculation is given below.

When $\tau = 1$, Eqn.(3.9) gives

$$\sigma_c = \frac{\pi^2 \times 29600}{12(1-0.09)} \left(\frac{1}{32}\right)^2 \times 5.79 = 151.3 \text{ ksi}$$

Since this value exceeds 48 ksi (proportional limit), it is apparent that the buckling stress for the inelastic case will be between 48 ksi and 55 ksi. Hence the top chord for truss B is not critical. Truss A need not be checked because of the $\frac{1}{2}$" thick material .

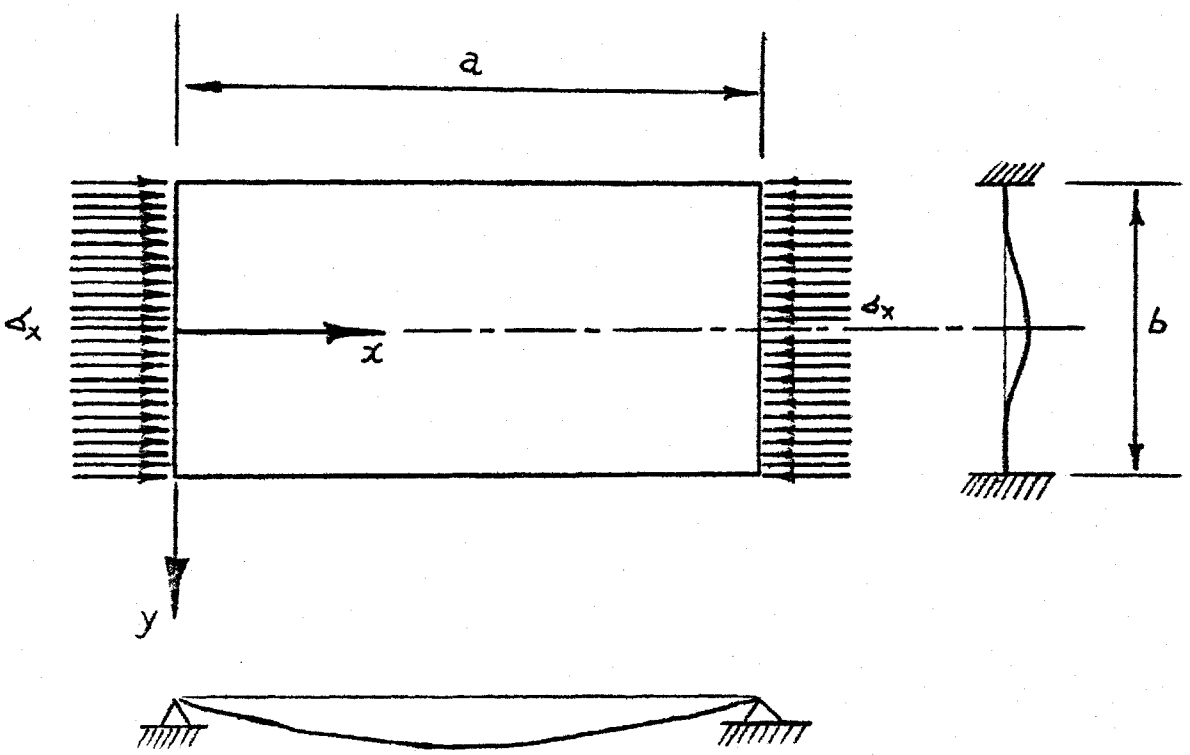

Fig. 3.1 A Rectangular Plate Subjected to Compressive Axial Stress

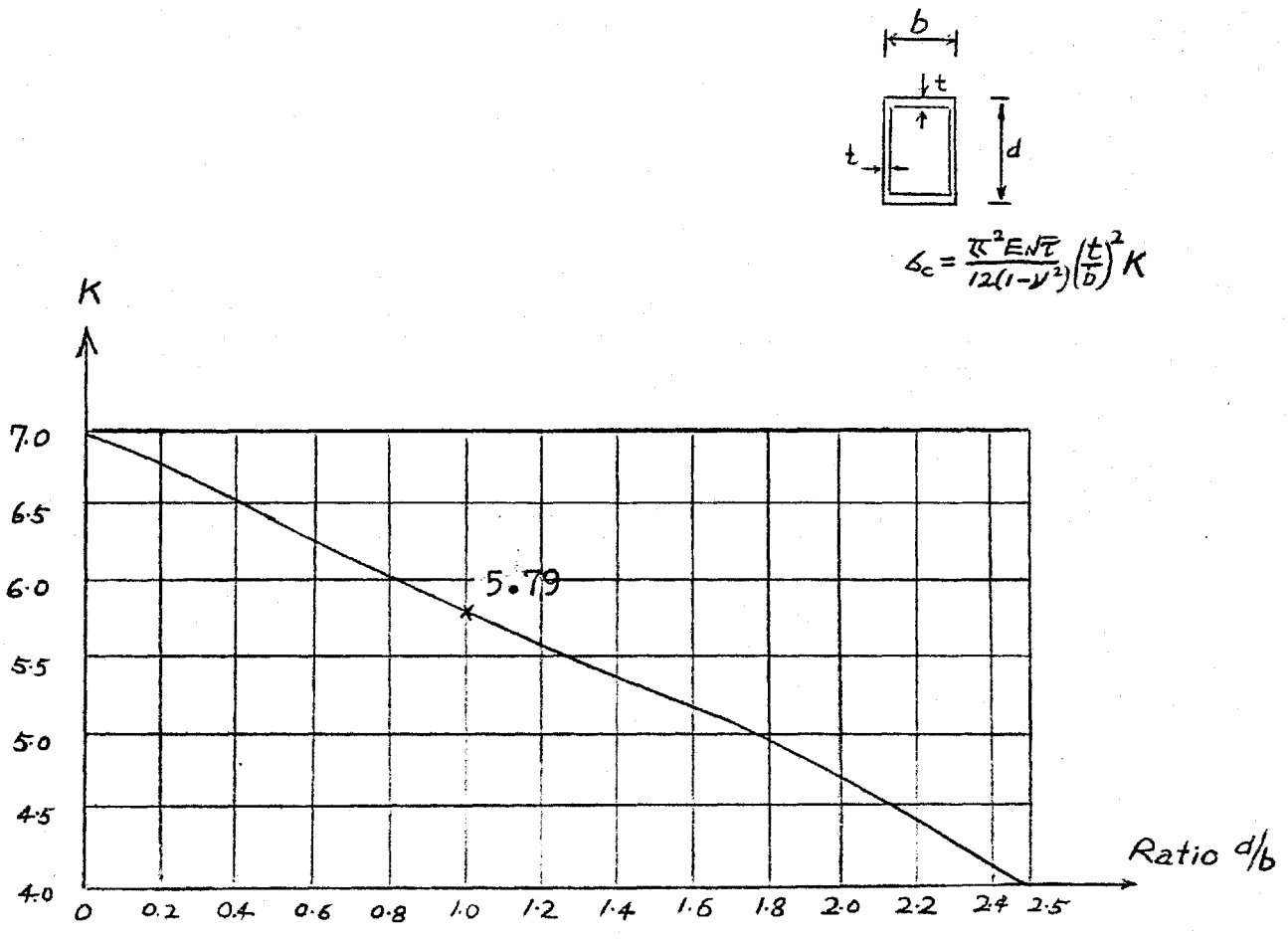

Fig. 3.2 Plate Coefficient K as Function of d/b

Table 3.1 Estimation of Buckling Stress

σ_c ksi.	τ	$\sqrt{\tau}$	$\sigma_c/\sqrt{\tau}$ ksi.
48.0	1.0	1.0	48.0
49.0	0.875000	0.93600	52.5
54.0	0.160000	0.40000	135.0
54.21	0.127450	0.35700	151.8
54.93	0.011440	0.10700	513.36
54.945	0.008990	0.09490	578.977
54.950	0.008170	0.09060	606.512 *
54.970	0.004000	0.06300	782.540
54.990	0.001636	0.04000	1374.750
54.995	0.000818	0.02860	1922.900
54.9969	0.000507	0.02258	2435.600 *

*(From above Table, the buckling stresses for the web members of $\frac{1}{4}$" and $\frac{1}{2}$"thickness material are 54.95 ksi. and 54.9969 ksi. respectively.)

CHAPTER IV

STRUCTURAL BEHAVIOUR OF UNEQUAL-WIDTH CONNECTIONS

4.1 ELASTIC BEHAVIOUR

The theoretical and experimental investigation of the elastic behaviour of the unequal-width connections had been carried out by Redwood [12] [13] .

As mentioned in Chapter I, when the width ratio d/b is less than 1.0 , the joint problem is one of plate flexure with certain loads and boundary conditions. In addition to the localised bending just described, the chord member is subjected to bending and axial load from the rest of the truss. However, a length of plate about four times the width is considered to be sufficiently 'long' that end-effects might be ignored. Therefore, in the work described in this volume, particular attention is devoted to the localised bending of the connecting flange of the chord member.

Theoretical and experimental values of joint stiffness obtain by Redwood are plotted in Fig. (4.1) where D and ϕ were defined earlier for applied moment. The detail of the joint used in the tests is given in Table 4.1

In Fig. (4.1), the stiffness incorporated in appropriate non dimensional form is shown to increase rapidly with the joint parameter λ (λ = d/b)

At relatively low loads, the load-displacement curves

become non-linear. But in most cases, there is a large reserve of strength which has not yet been fully utilised. Therefore, the elastic analysis expressed in Fig.(4.1) can give little information on the strength of the joint.

Since the end web members are critical for the examples used(see Section 2.5), a plastic analysis of the joint is attempted to estimate its collapse load to determine whether stiffening procedures are required to establish full moment capacity.

4.2 THE STRENGTH OF JOINTS ESTIMATED BY PLASTIC METHOD

Use is made of Johansen's square yield criterion [14] for the plastic analysis of the joint. Although the square yield criterion is mostly applied to reinforced concrete structures, it has been shown by Wood [14] that the method applied fairly well for steel plates.

A collapse mechanism is assumed on the loaded plate. By using the principle of virtual work, the collapse load can be calculated. As the collapse load estimated by this method is an upper-bound value, the lowest value of all calculated collapse loads corresponding to various assumed mechanisms is the most 'correct' one.

JOINT SUBJECTED TO APPLIED MOMENT

Initially, the assumed collapse mechanism for the plate subjected to moment transmitted from the web member is shown in Fig.(4.2) in which the dotted lines are the yield lines

The region of the plate enclosed by the web member is assumed to be rigid as it rotates through, say, a unit angle. The amount of rotation of plate elements about the yield lines and their lengths are tabulated in Table 4.2 . Note that the values on one side of the center line are numerically equal to the other side.

The equation of virtual work associated with the mechanism is

$$M \cdot 1 = 2bm_p \left(1-\lambda+\frac{2\lambda^2}{1-\lambda}+\frac{2\lambda\tan\alpha}{1-\lambda}+2\lambda\cot\alpha\right) \qquad (4.1)$$

for a unit angle rotation of the square enclosed by the web member, and where m_p is the internal moment per unit length along the yield line. Using the condition $dM/d\alpha = 0$, we get

$$\tan\alpha = \sqrt{1-\lambda}$$

Substituting into Eqn.(4.1) , we obtain the minimum value of M

$$\text{i.e.} \quad M = 2bm_p \left(1-\lambda+\frac{2\lambda^2}{1-\lambda}+\frac{4\lambda}{\sqrt{1-\lambda}}\right) \qquad (4.2)$$

Lower values of the collapse moment M were attempted by employing other patterns of mechanism with 'fans' of yield lines as shown in Fig.(4.3) .

The equation of virtual work works out to be

$$M = 2bm_p \left[2\lambda(\pi/2 - \alpha-\beta) + 1 + 2\lambda(\tan\alpha + \tan\beta) + \frac{2\lambda^2\cos\beta}{(1-\lambda)\cos\alpha} + \frac{2\lambda^2}{1-\lambda} \right] \qquad (4.3)$$

The minimum value of M is obtained by setting $\partial M/\partial \alpha$ and $\partial M/\partial \beta$ equal to zero.

$$\therefore \quad M = 2bm_p \left(1 + \lambda\pi + \frac{4\lambda^2}{1-\lambda}\right) \qquad (4.4)$$

In the range $0 < \lambda < 0.635$ Eqn.(4.2) gives a smaller value of M than that given by Eqn.(4.4) .

Equations (4.2) and (4.4) are plotted on Fig.(4.4) showing values of $\frac{M}{0.5bm_p}$ with various values of λ. (Note that $\frac{M}{0.5bm_p}$ is equal to four times the value in the parenthesis of Eqn.(4.2) or (4.4).)

4.3 COMPARISON BETWEEN THEORETICAL AND EXPERIMENTAL COLLAPSE LOADS

The experimental results from the tests performed in the University of Bristol [12] [13] plotted in Fig.(4.5) is used to compare with the theoretical results derived above. Fillet welded connections were made between two square HSS and were subjected to applied moment. The specimens were of Grade 16 steel to BS 15 : 1961. The average yield stress was 18.5 ton/in.^{2} which was used to compute the m_p of the specimens.

In using the theoretical equations for calculating the collapse loads, the width b was taken as the outside dimensions of the section minus twice the thickness of the wall. And also, two values of λ for each tested joint were taken; one corresponds to the nominal size of the web member, the other is the nominal size plus weld material.

Details of the connections are summarised in Table 4.1 .

In Fig.(4.5), the estimated collapse loads show some agreement with the measured loads especially for the smaller web member.

When the web member becomes larger, the estimated collapse load based on the nominal web size becomes increasingly conservative. Onthe other hand, the larger load, based on the nominal size plus weld, overestimates the strength of the joint. The latter discrepancy is probably as a result of the unconnected web plates of chord member failing before the connected flange plate for large sized web members.

For the trusses A and B(see Chapter II) where the critical sections are the ends of the web members, the results of the yield line method and experimental results quoted herein are important. For the truss A, the moment capacity of the 4"x 4"x $\frac{1}{2}$" web member is 508.75* in-kips, and the moment capacity by yield line theory is 240 in-kips. For the truss B, the moment capacity for the 4"x 4"x $\frac{1}{4}$" member is 290.46 in-kips, and the moment capacity by yield line method is 60.0 in-kips. From these figures, we know that the strength capacity of the web member is not fully utilized. Furthermore, the experimental results of Redwood [12][13] show that for small values of λ(width ratio), the joint capacity is less than the web member capacity.

Therefore, on these two counts, the joints require stiffening if the panel point loadings as computed in Chapter II are to be realized.

---

* Based on steel that yields at 55 ksi. .

An extension of the yield line method will be used to study the strength of reinforced joints in Chapter VI.

Table 4.1 Detail Dimensions of Joints [12], [13]

Main Member	Branch Member	Weld Size (in.)	λ (d/b) Excl. Weld	λ (d/b) Incl. Weld
5 x 5 x3/16	$2\frac{1}{2}$x$2\frac{1}{2}$x0.16	5/16	0.541	0.677
5 x 5 x3/16	1 x 1 x 0.128	$\frac{1}{4}$	0.217	0.325
5 x 5 x3/16	$1\frac{7}{8}$x$1\frac{7}{8}$x0.160	$\frac{5}{16}$	0.412	0.546
5 x 5 x3/16	$2\frac{3}{4}$x$2\frac{3}{4}$x0.16	$\frac{5}{16}$	0.605	0.739
5 x 5 x3/16	$3\frac{1}{2}$x$3\frac{1}{2}$x0.192	$\frac{3}{8}$	0.758	0.920

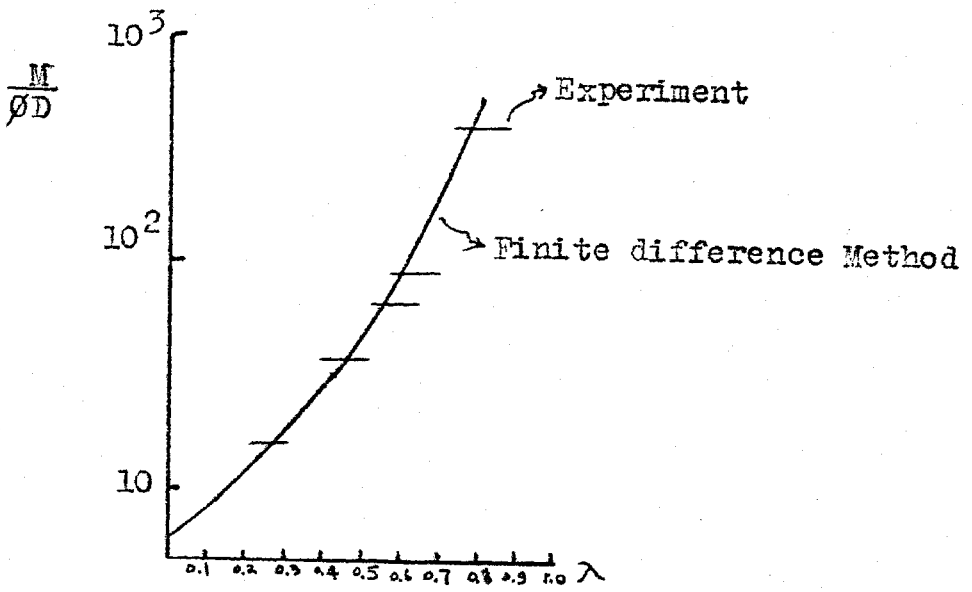

Fig. 4.1 Joints with applied Moment*

*(Reference is made to [12][13])

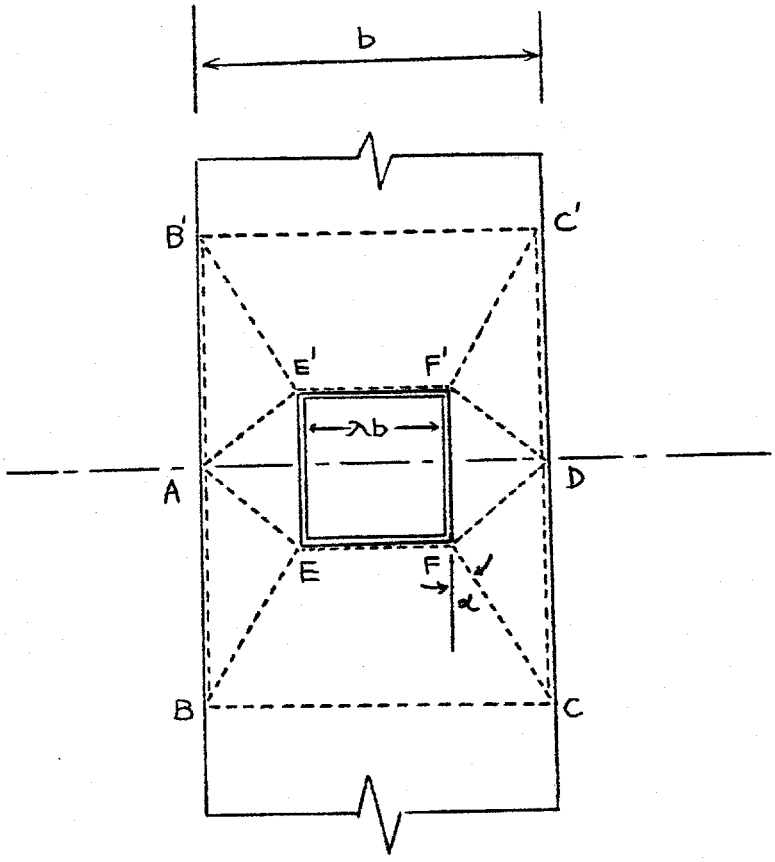

Fig. 4.2 A Yield-line Pattern for Applied Moment

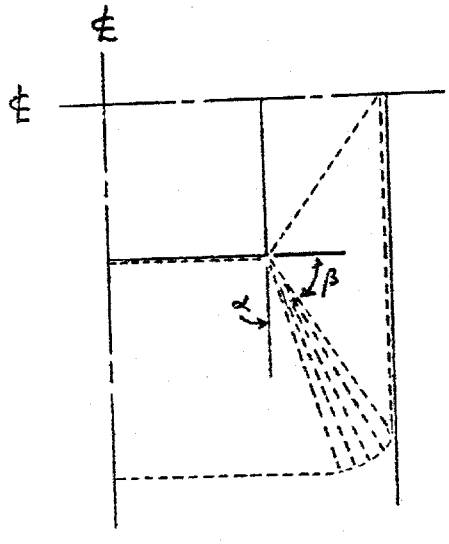

Fig. 4.3 Alternative Yield Pattern for Applied Moment

Table 4.2 Lengths and Angles of Rotation of Yield Lines

Yield Line	Angle of Rotation	Length
AB, CD	$\frac{\lambda}{1-\lambda}$	$\frac{b(1-\lambda)}{2\tan\alpha} + \frac{\lambda b}{2}$
BC	$\frac{\lambda}{1-\lambda}\tan\alpha$	b
EF	"	λb
BE, CF	$\frac{\lambda\cos\alpha}{1-\lambda} + \frac{\lambda\sin\alpha\tan\alpha}{1-\lambda}$	$\frac{b(1-\lambda)}{2\sin\alpha}$
AE, DF	$\frac{1-\lambda}{\sqrt{2\lambda^2-2\lambda+1}} + \frac{\lambda}{(1-\lambda)\sqrt{2\lambda^2-2\lambda+1}}$	$\frac{b}{2}\sqrt{2\lambda^2-2\lambda+1}$

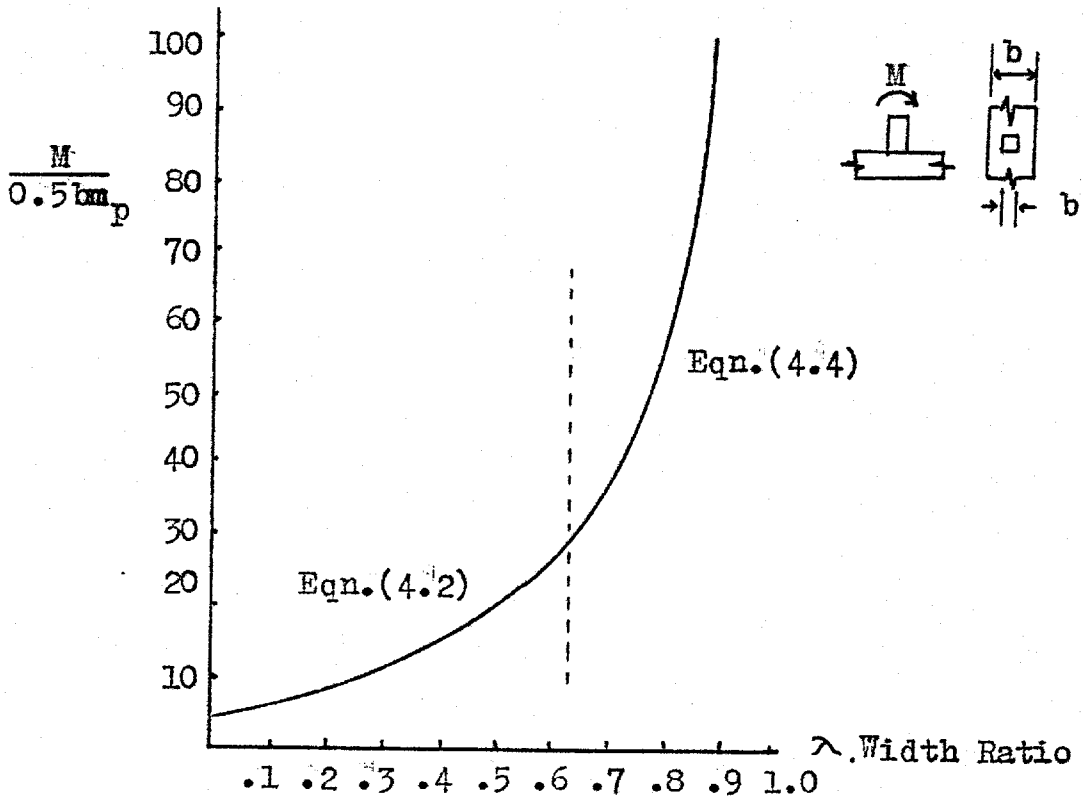

Fig. 4.4 Theoretical Applied Moment for Collapse

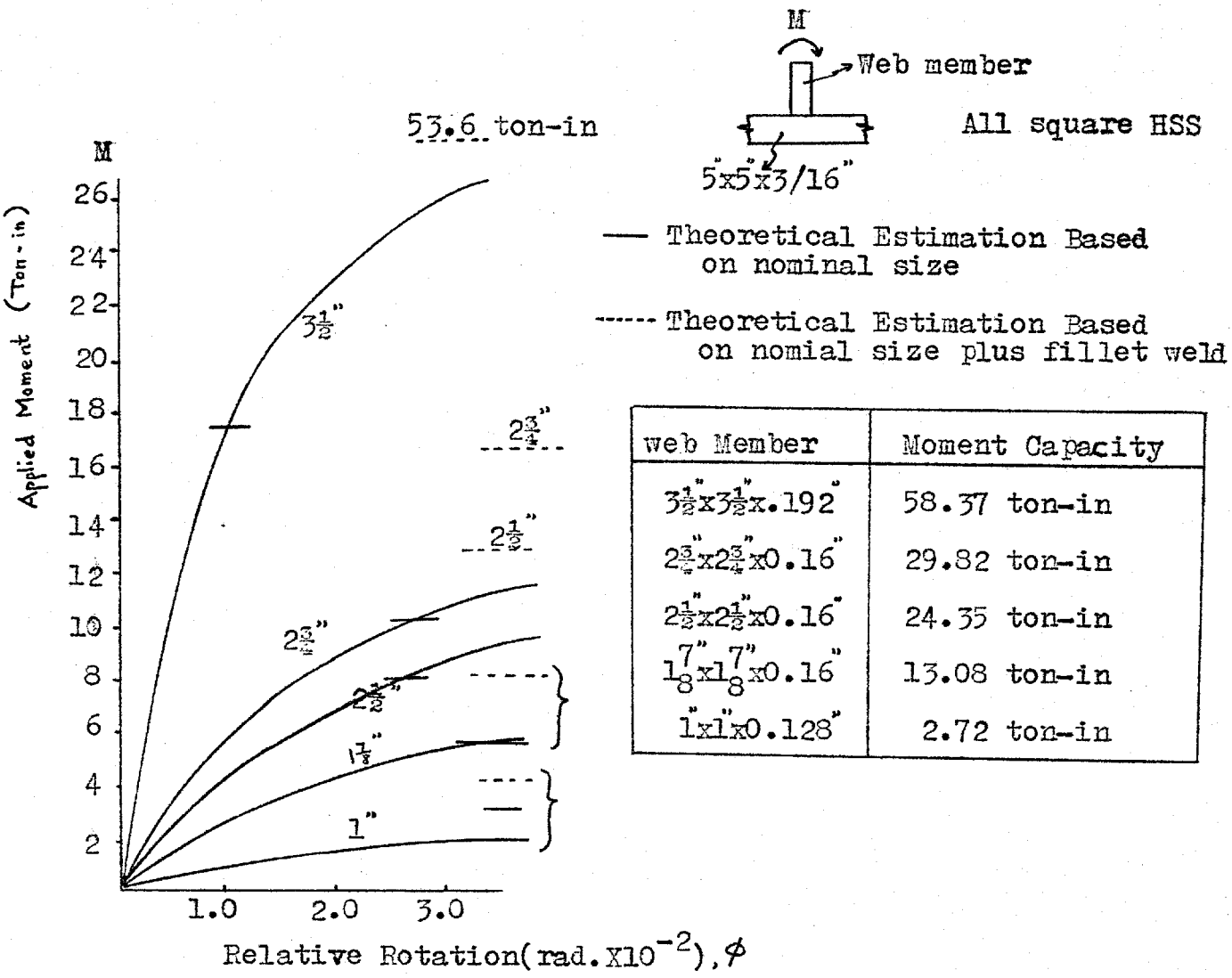

web Member	Moment Capacity
3½"x3½"x.192"	58.37 ton-in
2¾"x2¾"x0.16"	29.82 ton-in
2½"x2½"x0.16"	24.35 ton-in
1⅞"x1⅞"x0.16"	13.08 ton-in
1"x1"x0.128"	2.72 ton-in

Fig. 4.5 Applied Moment Versus Relative Rotation

(Experimental Results from University of Bristol [12][13])

CHAPTER V

THE INFLUENCE OF SOME MEMBER SIZING ON THE BEHAVIOUR OF JOINTS

5.1 GENERAL INTRODUCTION

This chapter presents a brief review of the dimensional parameters of the connecting members which are important for full web to chord member moment transfer. When certain ratio limits are achieved, no additional strengthening is necessary to obtain full working capacity of the truss. Chapter VI will discuss strengthening methods and will attempt to analyze joints for moment capacity.

It was mentioned earlier that, when the welded connections between two unequal-width square HSS at right angles to one another were formed the problem of the joint was mainly the bending of the connected plate, and that the strength and stiffness of the joint were thus greatly reduced.

There might be some improvements for the joint if the dimensions of the connected plate were carefully selected to match the given dimensions of the branch member (i.e. web member).

The experimental results by Redwood furnished in the preceding chapter were all with constant dimensions of the main member. These tests, therefore, have limited value in

terms of relating slenderness or thickness ratios to moment capacity. Based on the limited tests carried out at the Drexel Institute of Technology [15], some information in this aspect can be gathered.

5.2 THE INFLUENCE OF CHORD WIDTH-to-THICKNESS RATIO, b/t_c

The details of the tested joints at Drexel with various b/t_c ratio are tabulated in Table (5.1), and the experimental curves are plotted in Fig. (5.1).

In all these tests, the widths of the two members were kept constant; one was 4", the other 6". The thickness of the branch member was also kept unchanged. The only change was made to the thickness of the main member to form b/t_c ratios of 12, 16 and 24. (t_c is the thickness of the main member.) The joints with these ratios are labeled as J1, J2 and J3 respectively.

As shown in Fig. (5.1), J1 and J2 with the b/t_c ratio equal to 12 and 16 were capable of developing the fully plastic moment of the branch member even though d/b is less than 1.0 . J3 with b/t_c equal to 24 was unable to develop M_p or even M_y, the yield moment of the branch.

It is concluded that, backed with observations from several miscellaneous tests, the unequal-width connections can considerably be strengthened to develop M_y or even Mp if the width-to-thickness ratio, b/t_c is 16 or less.

5.3 THE INFLUENCE OF t_c/t_w

In the preceding Section, attention was paid to the fact that the joint with a b/t_c ratio equal to or less than 16 is able to develop M_y or even M_p .

Close examination of Table (5.1) shows that another important parameter affecting the joint strength is the t_c/t_w ratio. Where t_w is the thickness of the web member.

From Table (5.1), the t_c/t_w ratios for the above mentioned two 'strong' joints, J1 and J2, which were able to develop M_p , are greater than 1.0 , whereas t_c/t_w ratio for the 'weak' joint, J3, is equal to 1.0 .

Introduce another joint J4, with joint dimensions matching other joints as shown in Table (5.1) , to note the influence of t_c/t_w .

The experimental curves from the Drexel tests are plotted in Fig. (5.2) .

When a comparison is made, regardless of all the parameters except b/t_c , between J2 and J4, we might quickly claim that J2 and J4, should have the same joint resistance because they have the same b/t_c ratio. But, as a matter of fact, J4 is stronger than J2 even though the former has a smaller λ (as joint stiffness is proportional to λ).

The reason for this is claimed to be that J4 has a higher t_c/t_w ratio than J2 .

It is therefore concluded that the ratio t_c/t_w is also an important parameter for strengthening the unequal-width connections; the higher the tc/tw ratio, the stronger the joint. The unequal-width connections can be assured to develop M_p if $t_c/t_w \geq 2.0$ and at the same time $b/t_c \leq 16$. Clearly, the examples of the two trusses mentioned in Chapter II do not satisfy the first inequality and, in addition, truss B violates the second inequality.

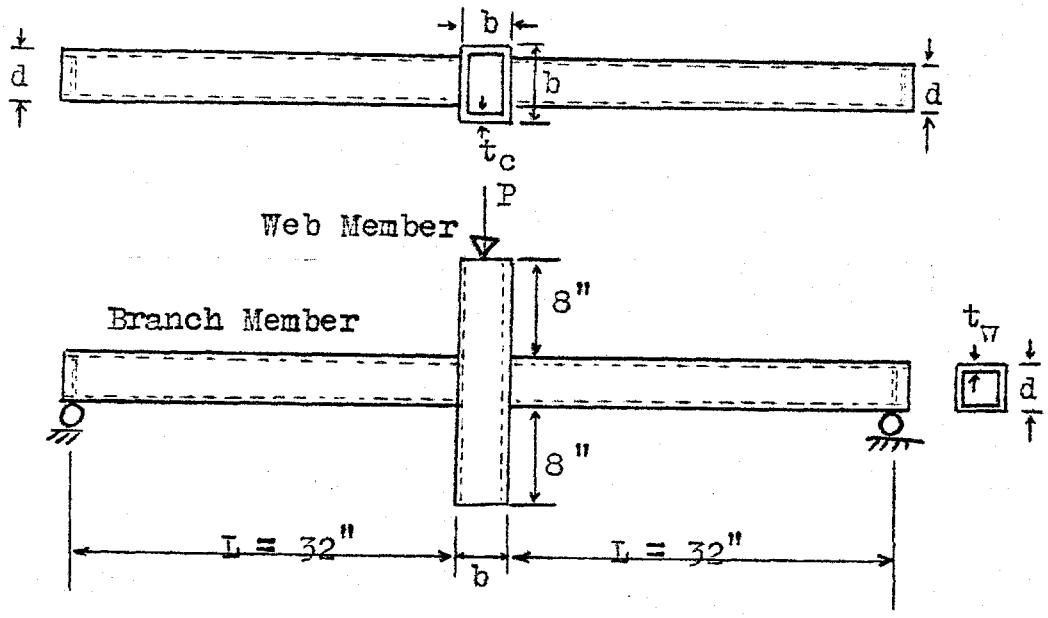

Table 5.1 Joint Details

Joint No	Main Member (in)	Branch Member (in)	$\lambda = \frac{d}{b}$	b/t_c	t_c/t_w
J 1	6 x 6 x 0.5	4 x 4 x 0.25	0.667	12	2.0
J 2	6 x 6 x0.375	4 x 4 x 0.25	0.667	16	1.5
J 3	6 x 6 x 0.25	4 x 4 x 0.25	0.667	24	1.0
J 4	8 x 8 x 0.5	4 x 4 x 0.25	0.5	16	2.0

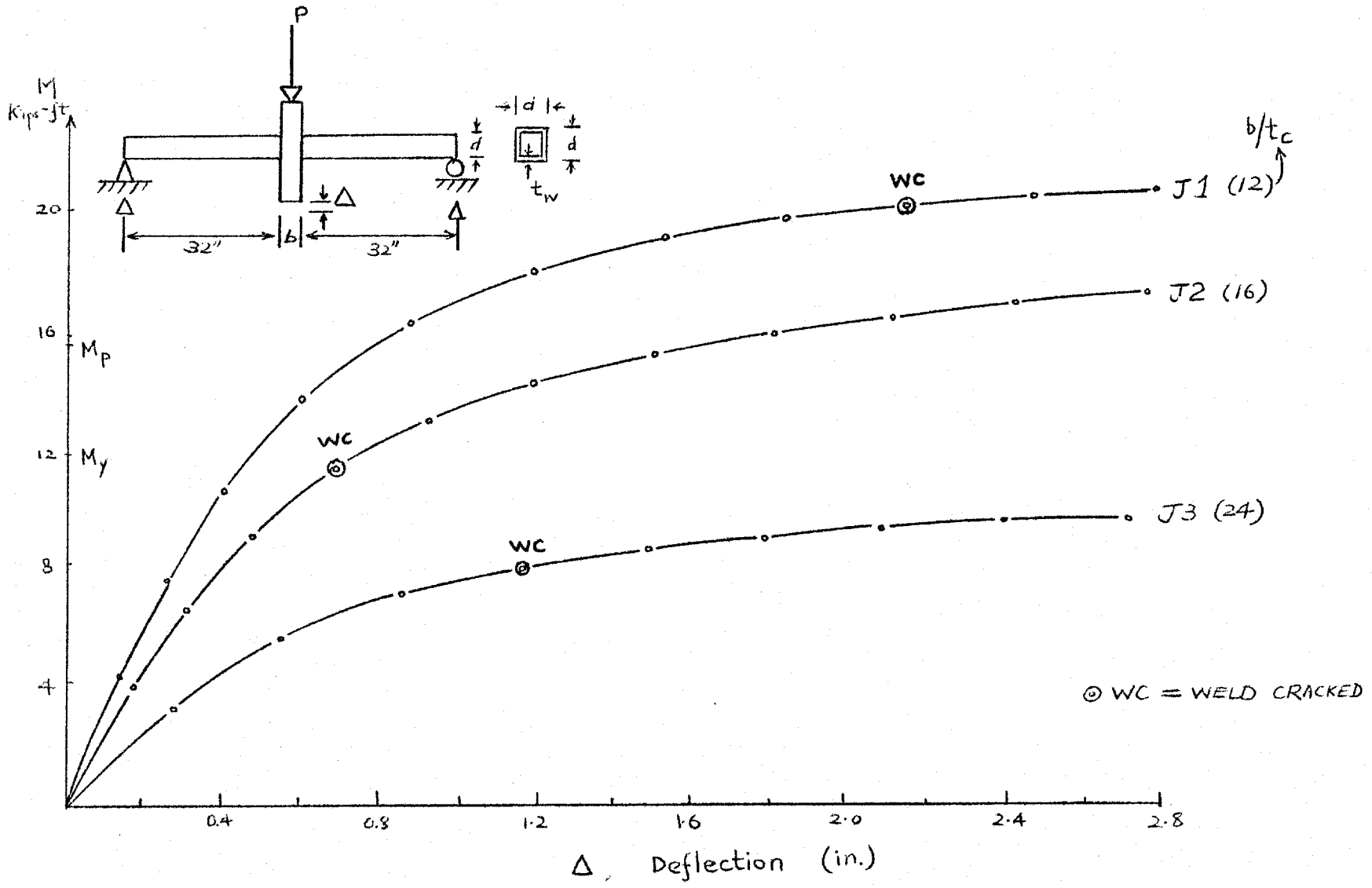

Fig. 5·1 Load - deflection Curves for b/t_c Effect (Drexel Research)

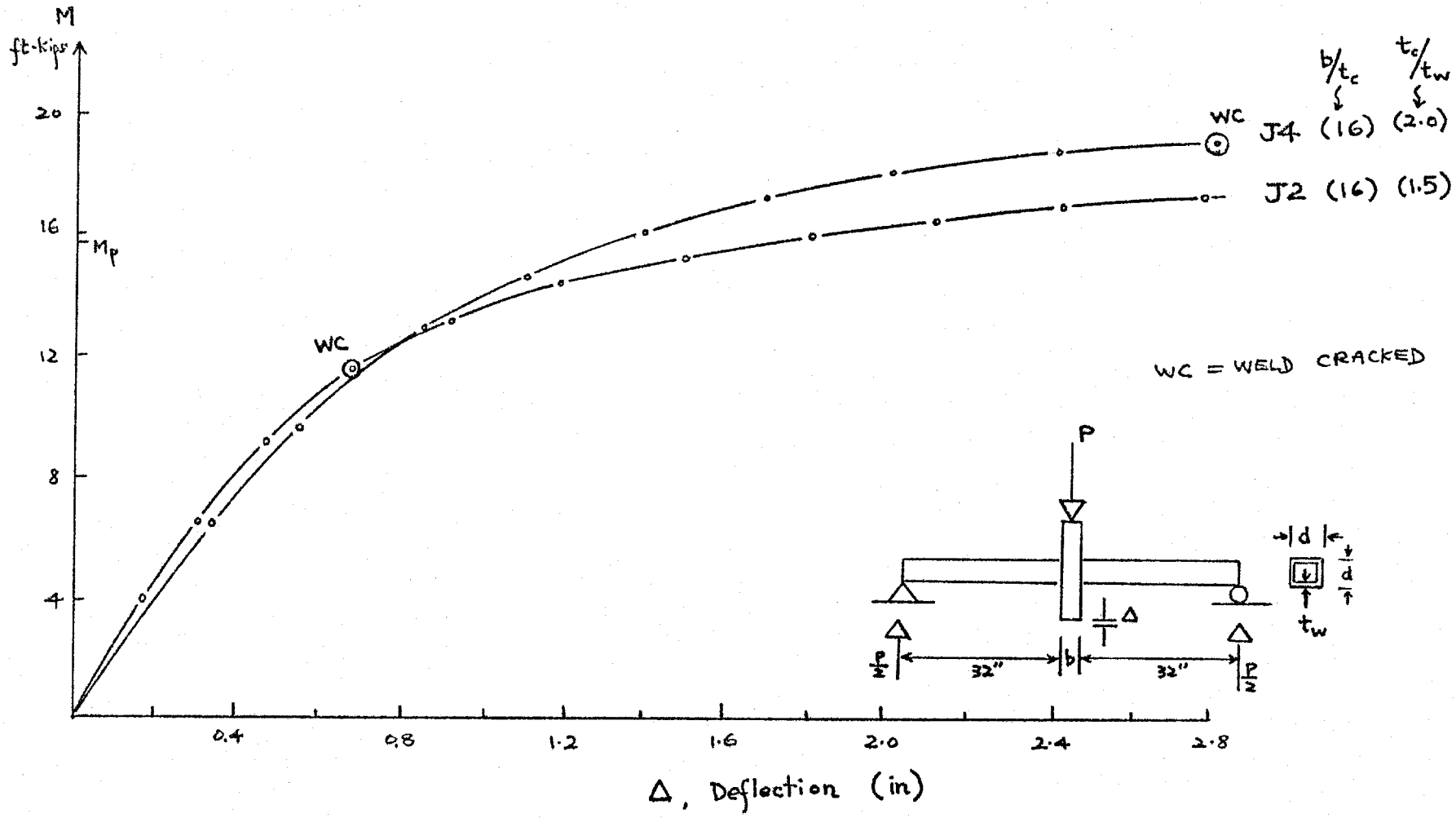

Fig. 5.2 : Load-deflection Curves For t_c/t_w Effect (DREXEL) [15]

CHAPTER VI

JOINTS WITH REINFORCEMENTS

6.1 GENERAL INTRODUCTION

When the ratio b/t_c is greater than 16 and t_c/t_w is less than 2.0 , the unequal-width joint is generally unable to develop the fully plastic moment of the smaller section (web member) unless reinforcement is applied to the joint.

Several kinds of reinforcement can be suggested such as the use of web flange plates, chord flange stiffeners(mounted on the chord flange), haunched plates etc. as shown in Fig. (6.1). Nevertheless, these forms of reinforcement should be consistent with the requirements of efficiency, feasibility and economy as a whole.

The following sections are devoted to various forms of reinforcement.

6.2.1 ANALYSIS OF FLANGE-PLATE REINFORCED JOINT

An approximate analysis of the Flange Plate Reinforcement is discussed in this section.

Consider an unequal-width connection reinforced by two flat plates welded on the flanges of the branch member as shown in Fig. (6.1a). A moment is applied on the joint through the branch member.

The relative rotation of the joint as a result of the applied moment can be found by dividing the maximum vertical deflection of the chord flange plate by one half the depth of the branch member.

The vertical deflection of the joint consists of two parts; one part is attributed to the shortening (or elongation at tension side) of the reinforcing plate, the other part is the deflection of the connected plate of the main member subjected to line load transmitted from reinforcement. The former part is small as compared to the latter part.

The exact distribution of line load transmitted from reinforcement is not fully known. But, it is quite safe, with some reasonable approximation, to say that the distribution of loading falls somewhere between two extreme cases; one is the uniform distribution, the other is of parabolic shape with zero intensity at the center. However, the areas of two distributions should be equal to each other.

6.2.2 SHORTENING (OR ELONGATION) OF THE REINFORCING PLATE

On the compression side of the joint subjected to applied moment, the reinforcing plate of dimensions b x h x t is assumed to be subjected to concentrated load of magnitude P as shown in Fig.(6.2a). Since all motion is supposed to occur in the plane of the paper, a unit thickness of the plate is taken in the discussion.

This type of plane stress problem is best solved by the lower bound theorem of limit analysis [16] [17] which states that if an equilibrium state of stress below yield can be found which satisfies the stress boundary conditions, then the loads imposed can be carried without collapse by a stable body composed of elastic-perfectly plastic material.

Instead of the plate, we suppose that a triangular pinned truss is imagined to carry the load inside the body as shown in Fig. (6.2b). The forces in the members of the truss can easily be determined as

$$C = \frac{P}{2 \cos \theta} \quad , \qquad T = C \sin \theta = \frac{P}{2} \tan \theta \tag{6.1}$$

where θ is half the angle made by two inclined legs.

The cross-sectional area of each member is to be chosen in such a manner as to give a safe or permissible axial stress. Here the stress must be chosen at or below 2k, where k is the yield stress in shear, if a lower bound on the limit load is to be found or if the safety of applying P to the plate is to be realized.

To maximize the lower bound loading, all members of the truss are taken at yield. The width of each member and the principal stress in the overlap regions are all indicated in Fig.(6.2c)

The compressive force in the inclined legs and the lower bound for the limit value of P can be written as

$$C = 2k\lambda b \cos\theta \quad , \quad P = 2C \cos\theta = 4k\lambda b \cos^2\theta$$

The vertical projection of the shortening of the inclined bar is equal to the change in the height of the truss. For simplicity, we assume the change in the height of the truss is approximately equal to the shortening of the plate.

Therefore, by using Hooke's law, the shortening of the bar is

$$\delta' = \frac{CL}{AE} = 2k \frac{b(1-\lambda)}{2 \sin\theta} \frac{1}{E}$$

where $C/A = 2k$, $L = b(1-\lambda)/2 \sin\theta$

The change in the height of the truss or the shortening of the plate is

$$\begin{aligned} \delta &= \delta' \cos\theta = \frac{kb(1-\lambda)}{E} \cot\theta \\ &= \frac{kb(1-\lambda)}{E} \frac{h}{b(1-\lambda)/2} \\ &= \frac{2kh}{E} \end{aligned} \tag{6.2}$$

As can be seen from the above expression, the shortening of the plate is proportional to its length, h. As will be seen later, this shortening is small as compared to the deflection of the connected plate of the chord member and can thus be neglected.

6.2.3 DEFLECTION OF THE CONNECTED PLATE OF MAIN MEMBER

Two extreme cases of loading distributions on the plate

will be considered. One is the uniform line load, the other is parabolic line load with zero intensity at center.

The long edges of the connected plate of the main member are assumed to remain straight and are subjected to restraining moments from the web plates. The effect of these restraining moments is disregarded for the purpose of counterbalancing the assumption that all plates are rigid which in reality have some flexibility.

A length of four times the width of the plate could be regarded as sufficiently long to simulate the chord flange as mentioned in section 4.1 . So the length of the long edge is assumed to be of this amount. And thus the loading conditions at both ends of the plate of this length could be neglected, and so the deflection is zero.

The middle of this length is the center of rotation of the joint where deflection is zero. This middle line is anti-symmetrical in relation to the forces. Taking one half of the length of this long plate into consideration, a rectangular plate of dimensions bx2b with four edges simply supported, subjected to either uniform line load or parabolic line load is the main topic of discussion that follows.

The details of the rectangular plate are shown in Fig. (6.3) .

6.2.4 SIMPLY SUPPORTED RECTANGULAR PLATE SUBJECTED TO UNIFORM LINE LOAD

The problem of a rectangular plate with all edges

simply supported subjected to transverse loading can be best solved by Navier's method [18].

Navier's method for plate problems is essentially explained as follows.

Consider a simply-supported rectangular plate of dimensions AxB with coordinate axes as shown in Fig. (6.4).

The governing equation [19] is

$$\frac{\partial^4 w}{\partial x^4} + 2\,\frac{\partial^4 w}{\partial x^2 \partial y^2} + \frac{\partial^4 w}{\partial y^4} = \frac{q}{D} \tag{6.3}$$

where q= intensity of transverse loading, w and D having been defined earlier.

The boundary conditions for all sides simply supported are

$$\left.\begin{aligned} w\Big|_{\substack{x=0\\x=A}} &= 0 \quad ; \quad \frac{\partial^2 w}{\partial x^2}\Big|_{\substack{x=0\\x=A}} = 0 \\ w\Big|_{\substack{y=0\\y=B}} &= 0 \quad ; \quad \frac{\partial^2 w}{\partial y^2}\Big|_{\substack{y=0\\y=B}} = 0 \end{aligned}\right\} \tag{6.4}$$

Suppose a deflection, which satifies the B.C. is equal to

$$w = C_{11} \sin\frac{\pi x}{A} \sin\frac{\pi y}{B} \tag{6.5}$$

Substituting the above equation into the governing equation (6.3), the loading needed to produce this deflection (6.5) is

$$q = DC_{11}\left[\frac{\pi^4}{A^4} + \frac{2\pi^4}{A^2B^2} + \frac{\pi^4}{B^4}\right] \sin\frac{\pi x}{A} \sin\frac{\pi y}{B} \qquad (6.6)$$

Similarly, suppose a deflection which satisfies all B.C. is

$$W = C_{mn} \sin\frac{m\pi x}{A} \sin\frac{n\pi y}{B} \qquad (6.7)$$

The loading needed to produce this deflection (6.7) must be

$$q = DC_{mn}\left[\frac{m^4\pi^4}{A^4} + \frac{2m^4n^4\pi^4}{A^2B^2} + \frac{n^4\pi^4}{B^4}\right] \sin\frac{m\pi x}{A} \sin\frac{n\pi y}{B} \qquad (6.8)$$

It is seen that a transverse loading of the form $\sin\frac{\pi x}{A} \sin\frac{\pi y}{B}$ applied to an all-sided simply supported plate will produce a deflection which is also of the form $\sin\frac{\pi x}{A} \sin\frac{\pi y}{B}$.

Hence, a procedure for solving this type of plate problem can be summarised as follows;

(i) Express the transverse loading into trigonometric series as

$$\sum_{m=1,2,3..}^{\infty} \sum_{n=1,2,3...}^{\infty} q_{mn} \sin\frac{m\pi x}{A} \sin\frac{n\pi y}{B}$$

(ii) The deflection of the plate will then be

$$W = \sum_{m=1,2,3..}^{\infty} \sum_{n=1,2,3...}^{\infty} C_{mn} \sin\frac{m\pi x}{A} \sin\frac{n\pi y}{B}$$

where $$C_{mn} = q_{mn}/D\left\{\frac{m^4\pi^4}{A^4} + \frac{2m^2n^2\pi^4}{A^2B^2} + \frac{n^4\pi^4}{B^4}\right\}$$

$$= q_{mn}/D\pi^4\left(\frac{m^2}{A^2} + \frac{n^2}{B^2}\right)^2$$

Turning to the case of a simply-supported plate of dimensions $b \times 2b$, subjected to uniform line load of intensity q_o at ρ from one edge is [Appendix IV],

$$q = \frac{4q_o}{\pi b}\sum_{n=1,2,3..}^{\infty}\sum_{m=1,3,5...}^{\infty}\frac{1}{m}\sin\frac{n\pi\rho}{2b}\sin\frac{n\pi x}{2b}\sin\frac{m\pi y}{b} \qquad (6.9)$$

$$= \sum_{n=1,2,3..}^{\infty}\sum_{m=1,3,5...}^{\infty} q_{mn}\sin\frac{n\pi x}{2b}\sin\frac{m\pi y}{b}$$

where $$q_{mn} = \frac{4q_o}{\pi b}\frac{1}{m}\sin\frac{n\pi\rho}{2b}$$

Following the procedure described above, the deflection of the plate can quickly be found as

$$W = \sum_{n=1,2,3..}^{\infty}\sum_{m=1,3,5...}^{\infty} C_{mn}\sin\frac{m\pi y}{b}\sin\frac{n\pi x}{2b} \qquad (6.10)$$

where $$C_{mn} = q_{mn}/D\pi^4\left\{\frac{m^2}{b^2} - \frac{n^2}{4b^2}\right\}^2$$

6.2.5 SIMPLY SUPPORTED RECTANGULAR PLATE SUBJECTED TO PARABOLIC LINE LOAD

Next, consider the simply supported plate of dimensions bx2b subjected to a parabolic line load of maximum intensity $3q_o$ at both ends and zero intensity at the centre acting at ρ distance from one edge. The quantity $3q_o$ is determined in such a way that the area of parabolic line load is equal to that of the uniform line load.

The equation [Appendix III] for this parabolic line load can be expressed as

$$q = \frac{48q_o}{\pi b} \sum_{m=1,3,5..}^{\infty} \sum_{n=1,2,3...}^{\infty} \frac{1}{m}\left(\frac{1}{4} - \frac{2}{m^2\pi^2}\right) \sin\frac{n\pi\rho}{2b} \sin\frac{m\pi y}{b} \sin\frac{n\pi x}{2b}$$

$$= \sum_{m=1,3,5...}^{\infty} \sum_{n=1,2,3...}^{\infty} q_{mn} \sin\frac{m\pi y}{b} \sin\frac{n\pi x}{2b} \qquad (6.11)$$

where $$q_{mn} = \frac{48q_o}{\pi b}\frac{1}{m}\left(\frac{1}{4} - \frac{2}{m^2\pi^2}\right) \sin\frac{n\pi\rho}{2b}$$

$$= \frac{4q_o}{\pi b}\frac{1}{m}\left(3 - \frac{24}{m^2\pi^2}\right) \sin\frac{n\pi\rho}{2b}$$

Following Navier's method, the deflection of the plate can be found as

$$W = \sum_{m=1,3,5..}^{\infty} \sum_{n=1,2,3...}^{\infty} C_{mn} \sin\frac{m\pi x}{b} \sin\frac{n\pi y}{2b} \qquad (6.12)$$

where $C_{mn} = q_{mn}/D\pi^4\left(\frac{m^2}{b^2} + \frac{n^2}{4b^2}\right)^2$

Substituting $\rho = (2-0.5\lambda)b$, $x = (2-0.5\lambda)b$ and $y = 0.5b$ into Eqns. (6.10) and (6.12), we can find the deflections of the plate at the middle of two different line loads. The actual deflection of the plate falls between these two values, i.e.

$$\delta_{(6.12)} < \delta_{act.} < \delta_{(6.10)}$$

Three terms of either Eqn. (6.10) or Eqn. (6.12) are sufficient for an approximate value of deflection. By using the above mentioned values of ρ, x, y and $q_o = M/db = M/\lambda b^2$ and different λ, values of deflection from Eqns. (6.10) and (6.12) are obtained. The obtained values are then changed into relative rotations of the joint by dividing them by 0.5d or $0.5\lambda b$. The contribution of deflection or relative rotation made by Eqn. (6.2) is small and is invariably within 8% of Eqn. (6.12). As the deflection by Eqn. (6.12) is already small, the 8% value could be neglected. A graph with relative rotation ϕ versus λ is plotted on Fig.(6.5) to show the flexibility of the reinforced joint with respect to λ.

6.3 CHORD FLANGE STIFFENER

A stiffening plate mounted to the chord flange with its centre coincident with the centre of the joint is shown in Fig.(6.1b)

It has been recognised that the loading transmitted from the web member to the joint is mostly resisted by the connecting flange plate when λ is less than 1.0 . An additional plate above the connected plate will automatically tend to increase the flexural rigidity of the joint. This increase will be by a factor of eight if the thickness of the stiffener is the same as that of the chord flange.

A test of this type of reinforcement had been carried out in the Drexel Institute of Technology (15). The details of the joints and the test results are shown in Table (6.2) and Fig. (6.6) respectively.

In the test, the stiffening plate of dimensions 5x5x5/16 was fillet welded to the 6" face of the main member of dimensions 6x4x1/4, the branch member was then centrally fillet welded to the stiffener.

As can be seen from Fig.(6.6), the moment resisted by the joint with reinforcement is 175% that resisted by the same joint without reinforcement. Therefore, the chord flange stiffener may provide efficient reinforcement for unequal-width connections. In addition, the adding of this stiffener is not objectionable from an aesthetic viewpoint.

6.4 HAUNCHED REINFORCEMENT

The haunch consists of HSS wedges cut at 45^{o} with a right angle to match that of the web and chord member.

The details of the haunches for reinforcement are shown in Fig.(6.7).

To the knowledge of the author, the experimental tests on this type of reinforcement for unequal-width connection has not yet been reported. The tests carried out in Corby, England [20], on this type of reinforcement were solely for equal-width connections.

In order to obtain design information for haunched reinforcements for unequal-width connections, an experimental programn is currently being carried out in McMaster University under the supervision of Dr. R.M. Korol with the sponsorship of CIDECT.

6.5 PLASTIC MECHANISM FOR REINFORCED JOINTS

As an extension of yield-line theory described in Chapter 4, an analysis will be made of reinforced joints loaded to failure.

FLANGE PLATE REINFORCEMENT

The details of the flange-plate reinforced joint are shown in Fig.(6.1a) in which two rectangular or trapezoidal flat plates are welded to the flanges of the branch member.

The collapse yield line pattern for this reinforced joint subjected to applied moment is similar to that of the unreinforced one (Fig. 4.2)

Like Eqn. (4.1), the internal virtual work done by the yield lines when the joint rotates through a unit angle of rotation is

$$2bm_p \left(1 - \lambda + \frac{2\lambda^2}{1-\lambda} + \frac{2\lambda \tan\alpha}{1-\lambda} + 2\lambda \cot\alpha \right) \qquad (6.13)$$

Considering the reinforcing plate (Fig.6.8) on the tension side of the joint, the shearing stress does the work of lifting two triangular parts of the plate when the joint rotates through unit angle of rotation. As the plate is assumed of rigid plastic material, the lifting only occurs when the shearing stress reaches its ultimate value as shown in Fig.(6.9).

Therefore, the total work done by the shearing stress in two reinforcing plates is

$$4\int \tau \gamma t \, dA \qquad (6.14)$$

where $t, \tau = \sigma_Y/2$ and $\gamma = \frac{\delta}{\frac{b-d}{2}} = \frac{d/2}{(b-d)/2} = \frac{\lambda b/2}{(b-d)/2}$ are constants.

Eqn.(6.14) becomes

$$4\frac{\sigma_Y}{2}\frac{\lambda b/2}{(b-d)/2} t \int dA$$

$$= 4\frac{\sigma_Y}{2}\frac{\lambda b/2}{(b-d)/2} t \left(\tfrac{1}{2} \frac{b-d}{2} h\right)$$

$$= \tfrac{1}{2} \sigma_Y \lambda bth \qquad (6.15)$$

Equating the internal work to external work, we get

$$M = 2bm_p \left(1 - \lambda + \frac{2\lambda^2}{1-\lambda} + \frac{2\lambda \tan\alpha}{1-\lambda} + 2\lambda \cot\alpha \right) + \tfrac{1}{2}\sigma_y \lambda b t h$$

With the condition $dM/d\alpha = 0$, we get $\tan\alpha = \sqrt{1-\lambda}$

Thus we obtain the minimum M as

$$M = 2bm_p \left(1 - \lambda + \frac{2\lambda^2}{1-\lambda} + \frac{4\lambda}{\sqrt{1-\lambda}} \right) + \tfrac{1}{2}\sigma_y \lambda b t h \qquad (6.16)$$

It is obvious that the last term of the above equation is due to the reinforcing plates which add more strength to the joint

CHORD FLANGE STIFFENER

A chord flange stiffener is a rectangular (usually square) plate of dimensions b x l x t welded between the chord flange and the web member with its center coincident with the center of the web member as shown in Fig.(6.1b) .

It is well known that if the fully plastic moment of a plate of thickness t is m_p per unit length, a plate of thickness 2t should have moment capacity equal to $4m_p$. However, complete composite action is unlikely, hence it is useful to also consider as a limit the case of no bond between reinforcing plate and chord flange. For this case, the two-layer plate has a moment capacity of $2m_p$. Our actual case will be between these two extremes.

The yield line pattern for this type of reinforced joint is essentially the same as that of the unreinforced joint with only a slight difference. The diagonal yield lines may propagate beyond the edges of the stiffening plate. Whether or not the diagonal yield lines spread beyond the edges of the stiffener is dependent on the length of the stiffener. In view of this phenomenon, the yield-line patterns are classified into the following three cases.

(i) EXTENSIVE YIELD LINES SPREAD

The collapse mechanism with diagonal yield lines spread beyond the edges of the stiffening plate is shown in Fig.(6.10). The yield lines occuring on a single-layered plate are acted upon by m_p, such as BB', CC', BC, BC', B'G' ..... etc.. The others occuring on double-layered plates have a moment capacity of $2m_p$ or $4m_p$. The angle of yield-line rotations and their lengths are the same as in Table 4.2 .

The equation of virtual work for the $2m_p$ case is

$$M = 2bm_p \left[\frac{2\lambda \tan\alpha_1}{1-\lambda} + \frac{\lambda^2 \tan\alpha_1}{1-\lambda} + 2\lambda \cot\alpha_1 + \frac{2\lambda^2}{1-\lambda} + 2(1-\lambda) + \frac{\lambda l}{b} \frac{(1+\tan^2\alpha_1)}{1-\lambda} - \frac{\lambda^2 \tan^2\alpha_1}{1-\lambda} \right] \qquad (6.17)$$

To find the minimum M, we let $dM/d\alpha_1 = 0$ which yields

$$\frac{2\lambda}{1-\lambda}\sec^2\alpha_1+\frac{\lambda^2}{1-\lambda}\sec^2\alpha_1 - 2\lambda\,\mathrm{cosec}^2\alpha_1$$

$$+ \frac{2\lambda l}{b(1-\lambda)}\tan\alpha_1\cdot\sec^2\alpha_1 - \frac{2\lambda^2}{1-\lambda}\tan\alpha_1\cdot\sec^2\alpha_1 = 0$$

or $$\frac{2\lambda}{1-\lambda}+\frac{\lambda^2}{1-\lambda} - 2\lambda\cot^2\alpha_1 + \frac{2\lambda l}{b(1-\lambda)}\tan\alpha_1 - \frac{2\lambda^2}{1-\lambda}\tan\alpha_1 = 0$$

On further simplifying, the above equation becomes

$$\tan^3\alpha_1 - \left(\frac{2+\lambda}{2}\right)\left(\frac{b}{\lambda b-l}\right)\tan^2\alpha_1 - (1-\lambda)\left(\frac{b}{\lambda b-l}\right) = 0 \qquad (6.18)$$

Equation (6.18) can also be written as

$$\tan^3\alpha_1 = \left(\frac{b}{\lambda b-l}\right)\left[\left(\frac{2+\lambda}{2}\right)\tan^2\alpha_1 - (1-\lambda)\right]$$

For the case being studied a square reinforcing plate is assumed such that $l = b$. Also $\lambda = 0.5$ since the web member is 4" and the chord member is 8" . The solution for $\tan\alpha_1$ from the above equation is $\tan\alpha_1 = 0.57$ and hence $\alpha_1 = 29^\circ 41'$.

With $l = b$ and $\lambda = 0.5$, Eqn.(6.17) becomes

$$M = 2bm_p\,(\,2.5\,\tan\alpha_1 + \cot\alpha_1 + 0.5\,\tan^2\alpha_1 + 3\,)$$

Substituting $\tan\alpha_1 = 0.57$ into above equation, we obtain

$$M = 2bm_p\cdot(\,6.33) \qquad (6.18)$$

In similar way, the minimum M for $4m_p$ case is $2bm_p\cdot(10.1)$ with $\tan\alpha_1 = 0.45$ for $l = b$ and $\lambda = 0.5$.

(ii) DIAGONAL YIELD LINES THROUGH THE CORNERS OF STIFFENER PLATE

The yield-line pattern for this case is shown in Fig.(6.11) . There are only four yield lines, namely BC , B'C' , BB' and CC' having moment capacity m_p, the others have $2m_p$ for the no bond state.

The equation of virtual work is

$$M = 2bm_p \left[\frac{3\lambda \tan\alpha_2}{1-\lambda} + 3\lambda \cot\alpha_2 + \frac{3\lambda^2}{1-\lambda} + 2(1-\lambda) \right]$$

Using $dM/d\alpha_2 = 0$, we get $\tan\alpha_2 = \sqrt{1-\lambda}$

Substituting $\tan\alpha_2 = \sqrt{1-\lambda}$, we obtain the min. M as

$$M = 2bm_p \left[\frac{6\lambda}{\sqrt{1-\lambda}} + \frac{3\lambda^2}{1-\lambda} + 2(1-\lambda) \right]$$

For $\lambda = 0.5$ as our previous example of truss A or B, the min. M becomes

$$M = 2bm_p \cdot (6.64)$$

(iii) CONFINED YIELD LINES

The collapse yield-line pattern confined to the region of the stiffener is shown in Fig.(6.12). As can be seen from the Figure, only BB' and CC' have moment capacity of m_p, the other have moment capacity $2m_p$.

The equation of virtual work is

$$M = 2bm_p \left[\frac{4\lambda \tan\alpha_3}{1-\lambda} + 3\lambda \cot\alpha_3 + \frac{3\lambda^2}{1-\lambda} + 2(1-\lambda) \right]$$

By using $dM/d\alpha_3 = 0$, we get $\tan\alpha_3 = \sqrt{\frac{3}{4}(1-\lambda)}$

The min. M is thus

$$M = 2bm_p \left[\frac{4\sqrt{3}\lambda}{\sqrt{(1-\lambda)}} + \frac{3\lambda^2}{1-\lambda} + 2(1-\lambda) \right]$$

For $\lambda = 0.5$, $M = 2bm_p \cdot (7.4)$

The 'fan' yield-line mechanism for above three cases was not attempted because of its comlexity. In addition, the adjustment to M would be slight and therefore the attempt is not justified.

Table 6.3 compares joint moment capacities with web member values for the two cases studied. Comparing the joint moment capacities obtained for the flange plate reinforcement and the chord flange stiffener we observe that flange plate reinforcement provides a value of moment capacity intermediate between the extremes of full chord plate action and complete sliding action.* No definitive statement can be made as to which method of reinforcement is superior. A test series such as that currently underway in the A.D.L. will hopefully answer that question. For the case of truss A, the reinforcement methods appear to be sufficient to develop the required M_p for the web member. This is not the case for truss B where the 1/4" plates are insufficient to develop the required web member moment.

---

* For Truss A only

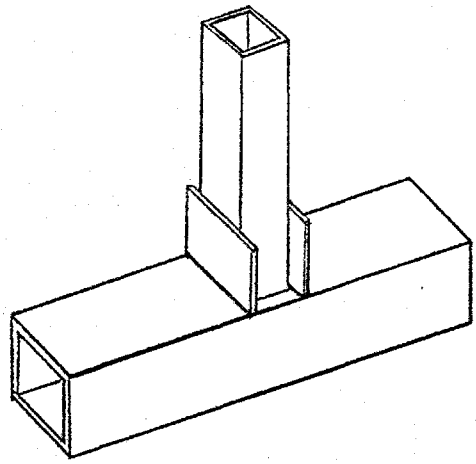

Fig. 6.1a Flange Plate Reinforcement

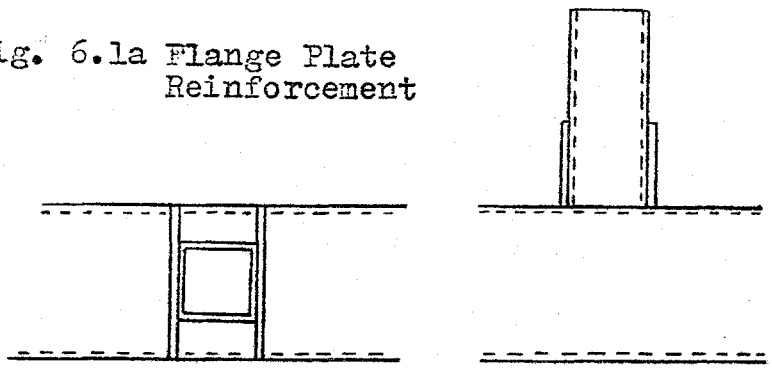

Flange Plate Reinforcement Plan View Side View

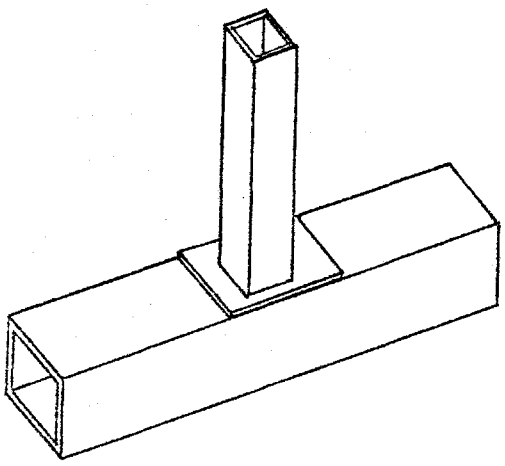

Fig. 6.1b Chord Flange Stiffener

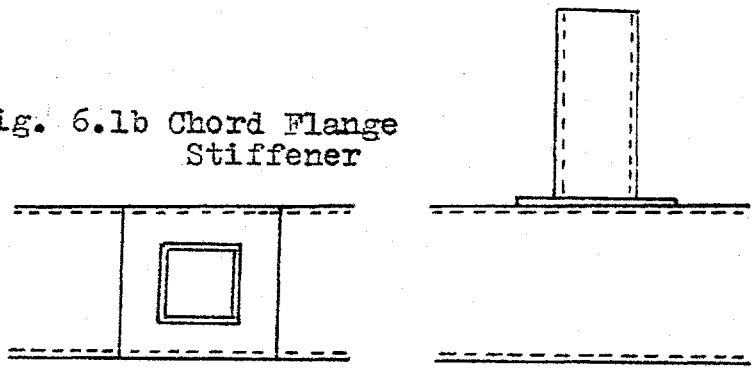

Chord Flange Stiffener Plan View Side View

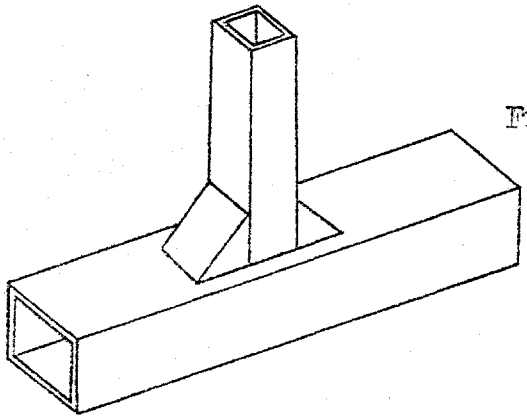

Fig.6.1c Haunched Reinforcement

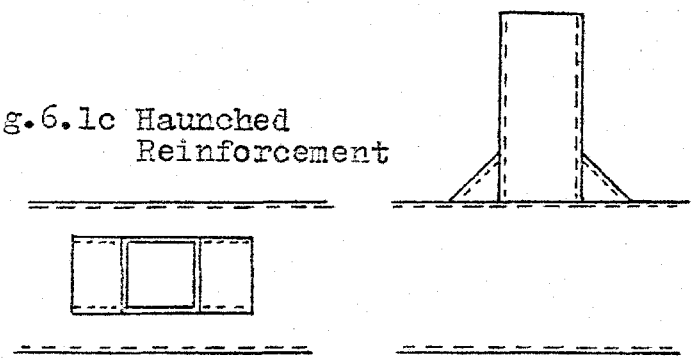

Huanched Reinforcement Plan View Side View

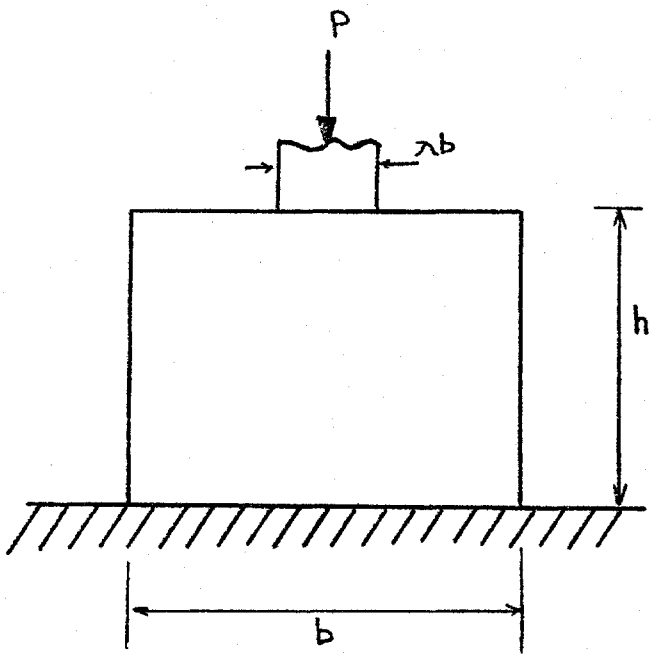

Fig. 6.2a Reinforcing Plate Subjected
To Modified Concentrated Load

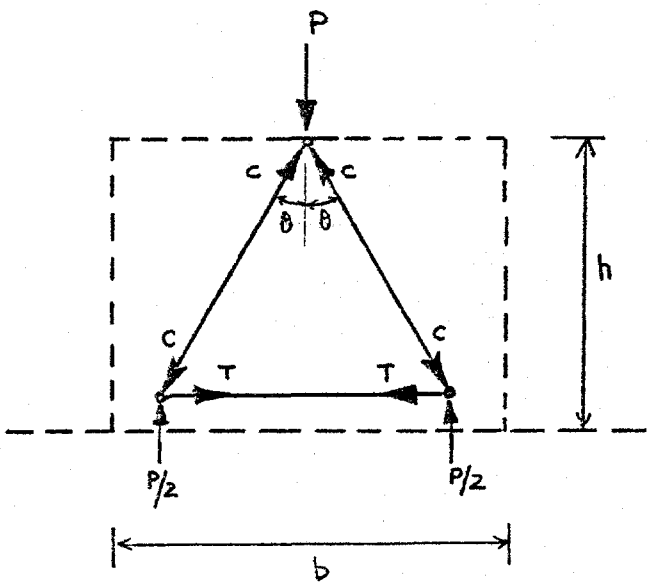

Fig. 6.2b Triangular Pinned Truss
in Plate

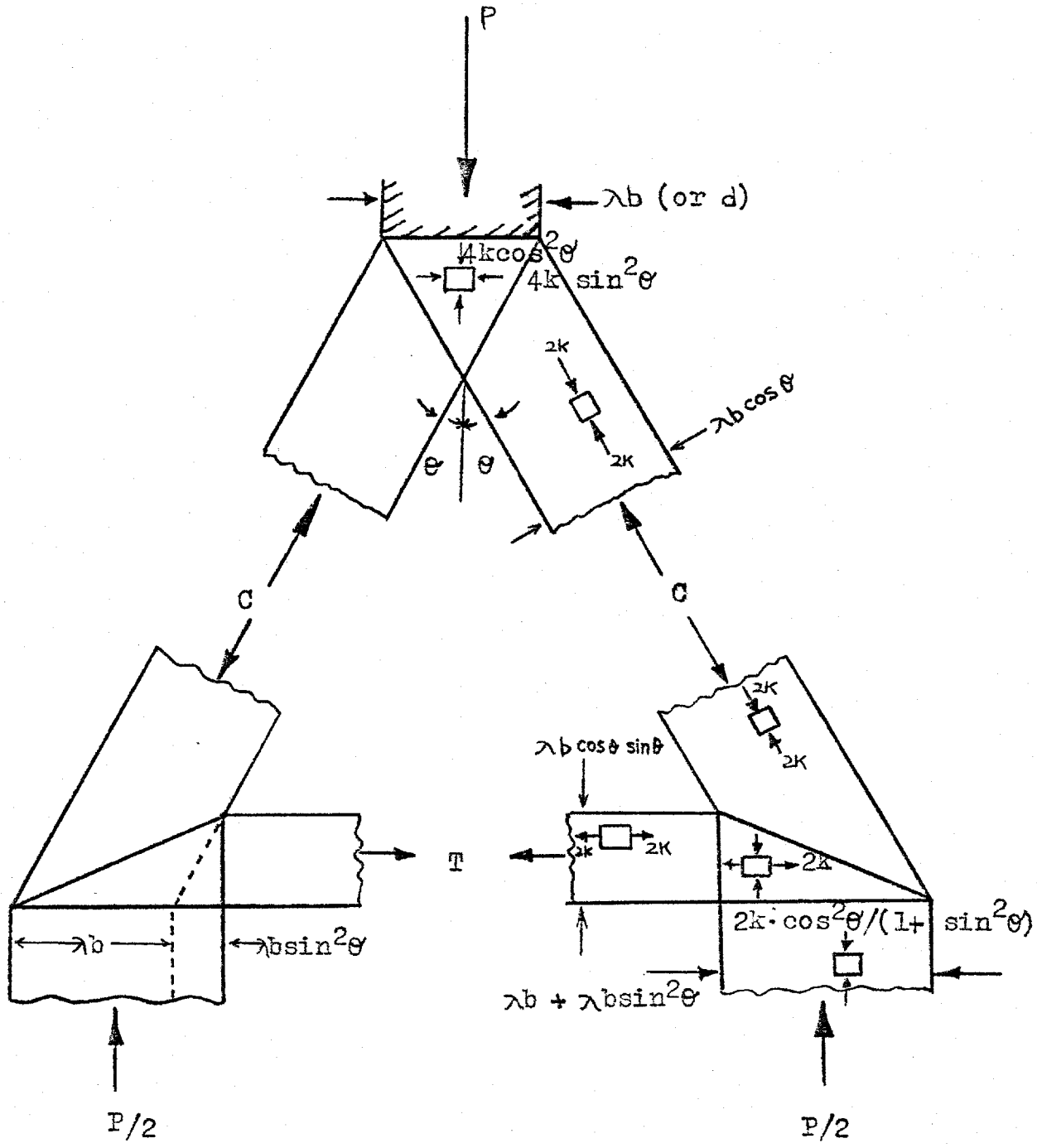

Fig. 6.2c Triangular Pinned Truss

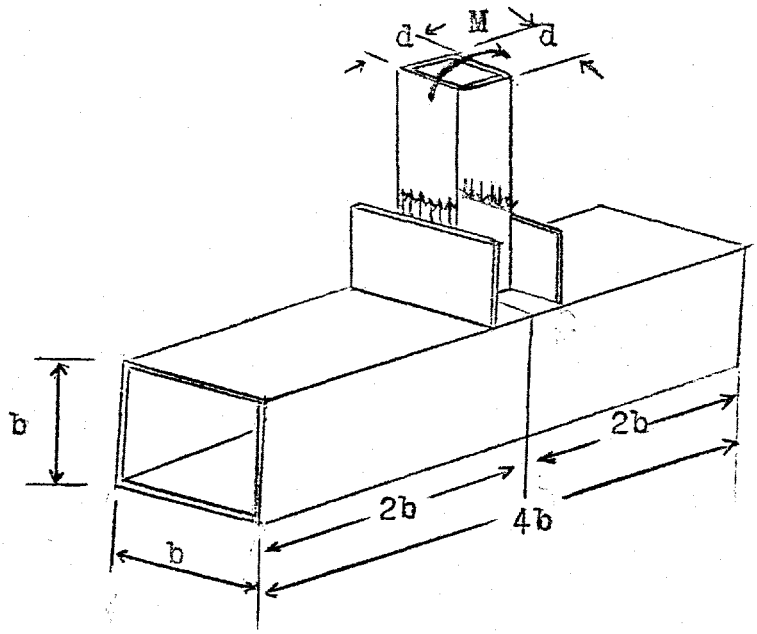

Reinforced Joint Under Applied Moment

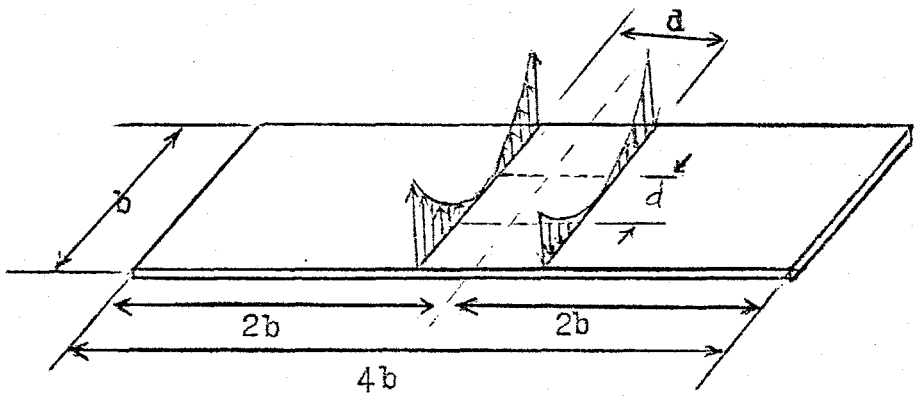

Isolation of Loaded Plate

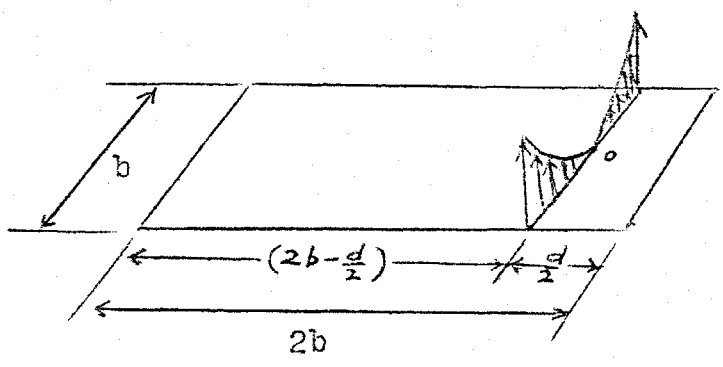

Fig.6.3 A Rectangular Plate Subjected to Transverse Line load

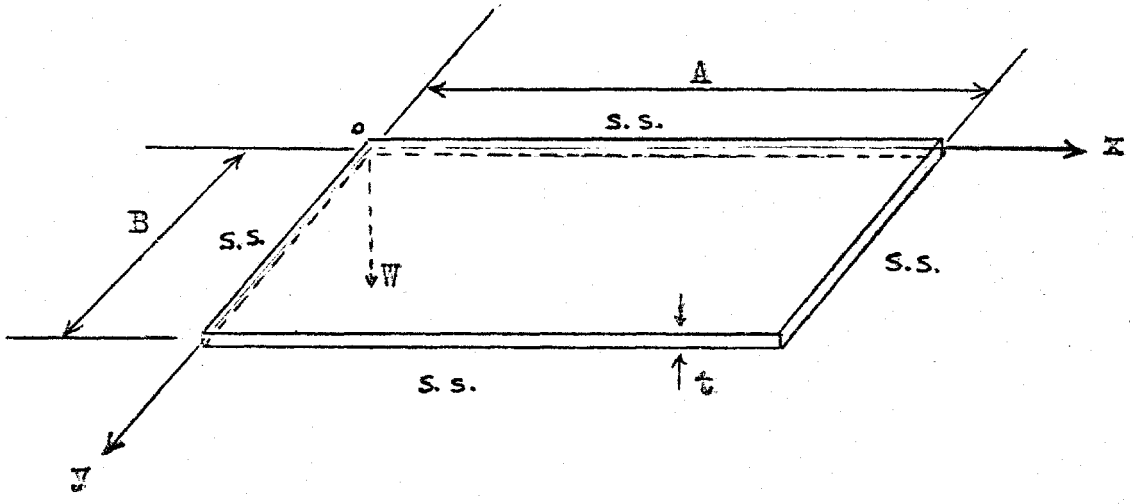

Fig. 6.4; A Simply-supported Plate and its x-y Axes

Table 6·1 * : Relative Rotations $\left(\phi \times \frac{D}{M}\right)$ with various values of λ

	$\lambda=0.1$	$\lambda=0.2$	$\lambda=0.3$	$\lambda=0.4$	$\lambda=0.5$	$\lambda=0.6$	$\lambda=0.7$	$\lambda=0.8$	$\lambda=0.9$	$\lambda=1.0$
Uniform Line Load	0.0391	0.0381	0.0362	0.0338	0.0309	0.0276	0.0246	0.0215	0.0185	0.016
Parabolic line Load	0.0244	0.0216	0.0206	0.0193	0.0176	0.0159	0.0141	0.0124	0.0107	0.00925

* Figures in this Table are used in plotting the curves in Fig. 6·5

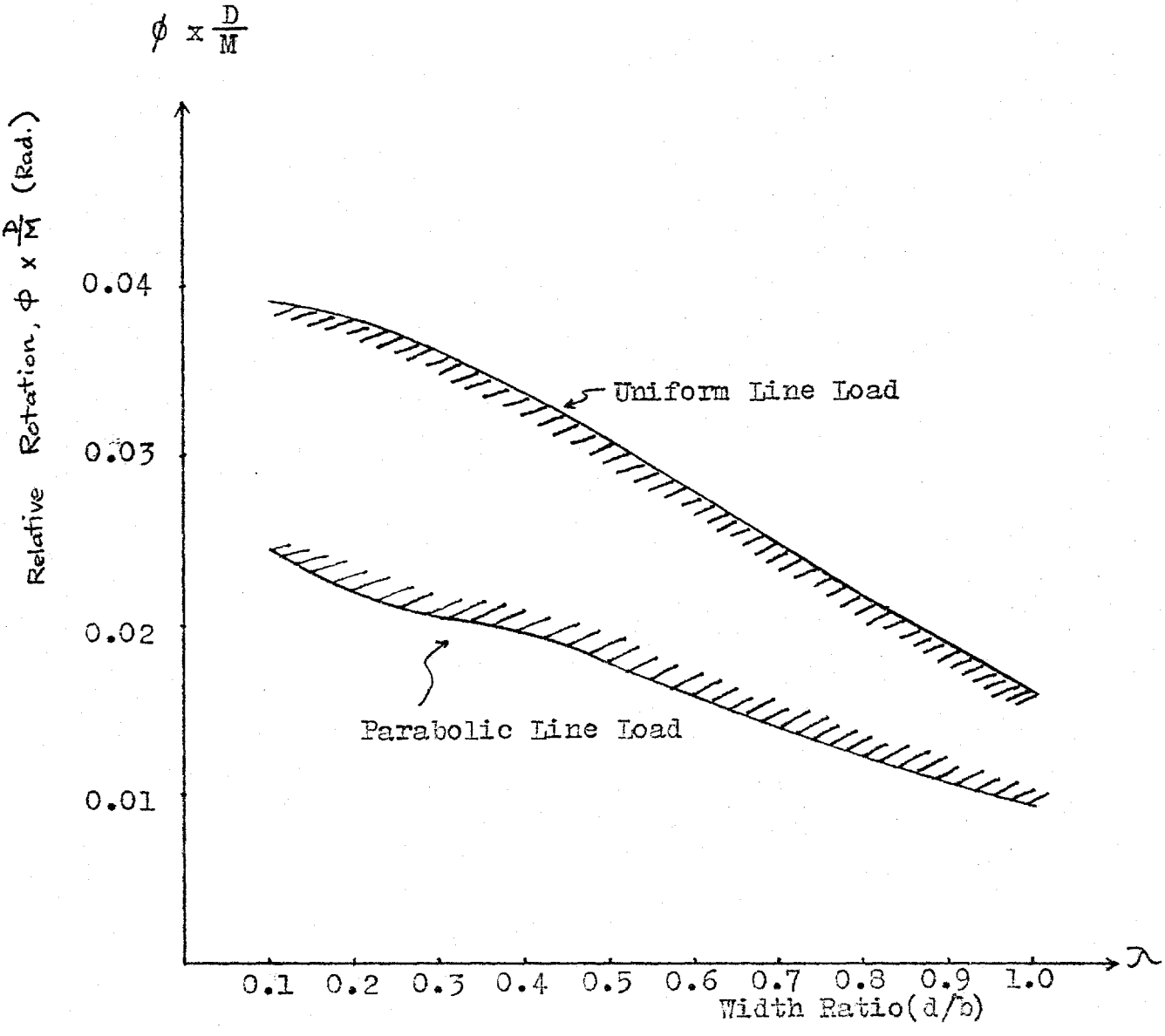

Fig. 6.5 : A Plot of Relative Rotations Versus λ

Table 6.2 : Joint Dimensions

Joint No	Main Member (in)	Branch member (in)	$\lambda = \frac{d}{b}$	b/t_c	t_c/t_w	Reinforcement
J5R	6 x 4 x0.25	4 x 4 x 0.25	0.67	24	1.0	5x5x$\frac{5}{16}$ PL
J5	6 x 4 x0.25	4 x 4 x0.25	0.67	24	1.0	NONE

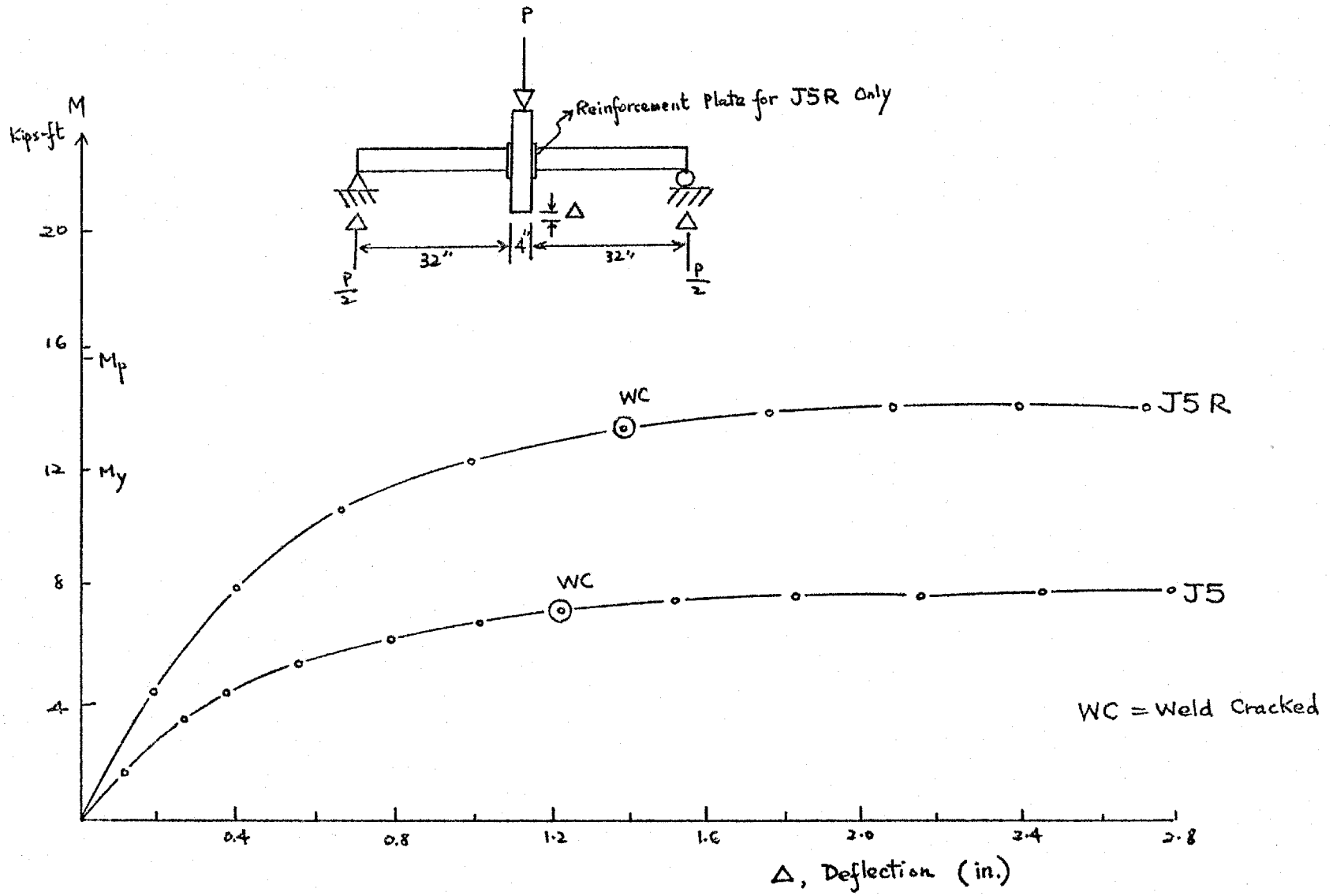

Fig. 6.6 : Load - Deflection Curves

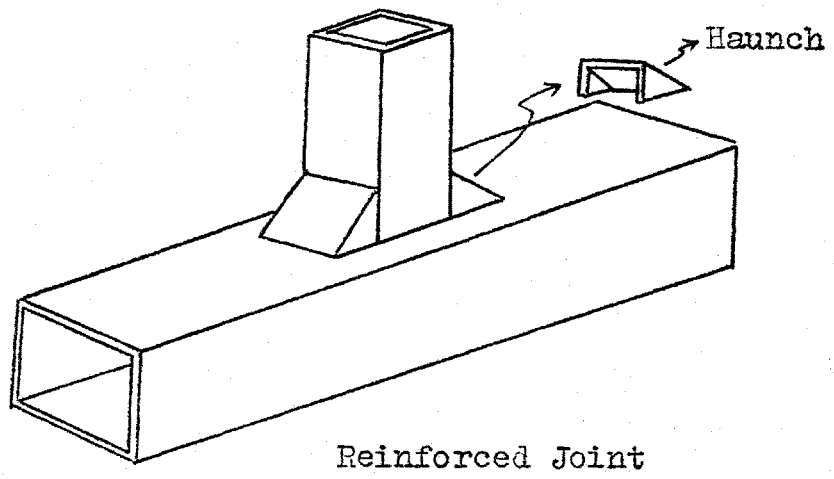

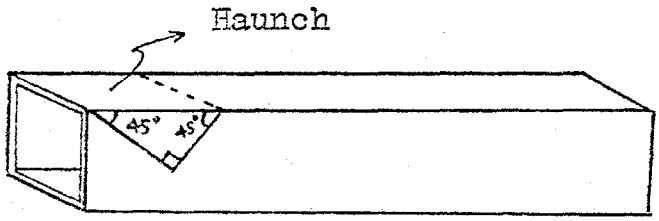

Fig. 6.7 : Haunch Cuttings

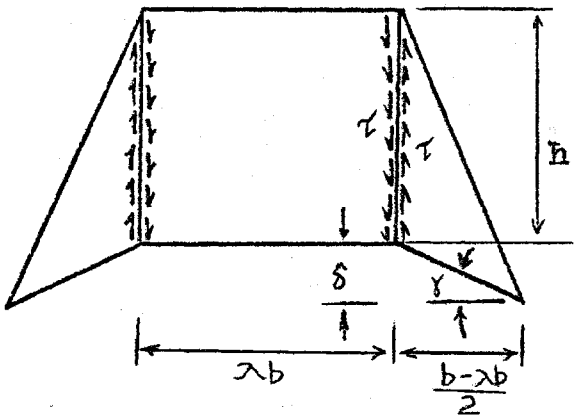

Fig.6.8 Deformed Flange Plate Reinforcement On the Tension Side of Joint

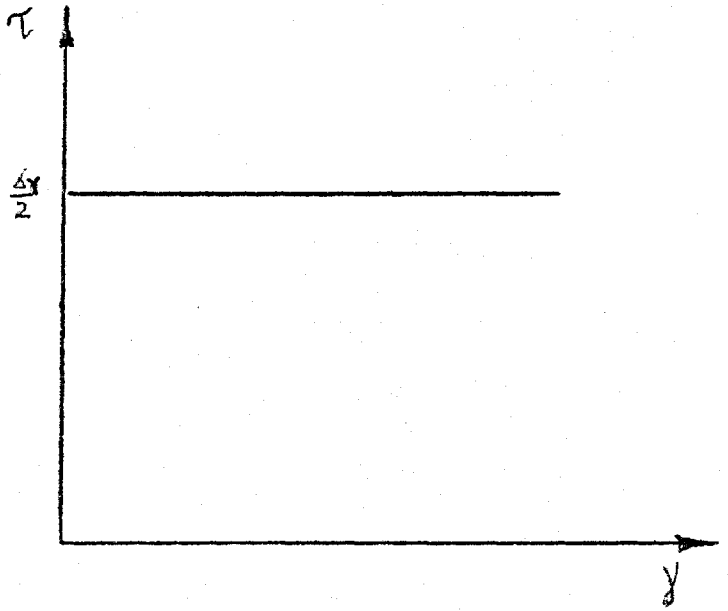

Fig.6.9 Relationships Between Shearing Stress And Strain for Rigid Plastic Material

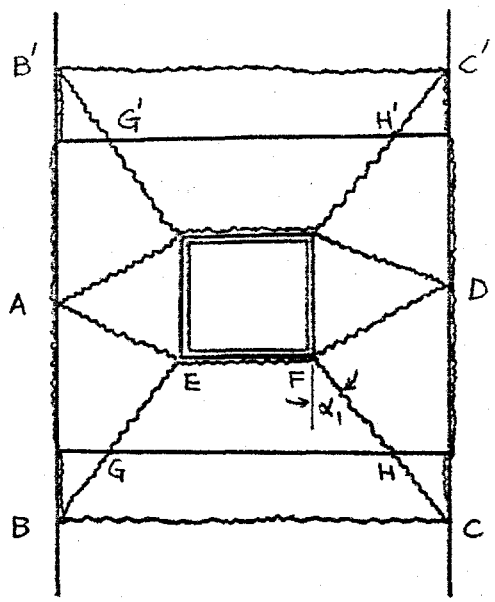

Fig. 6.10 Case (i)

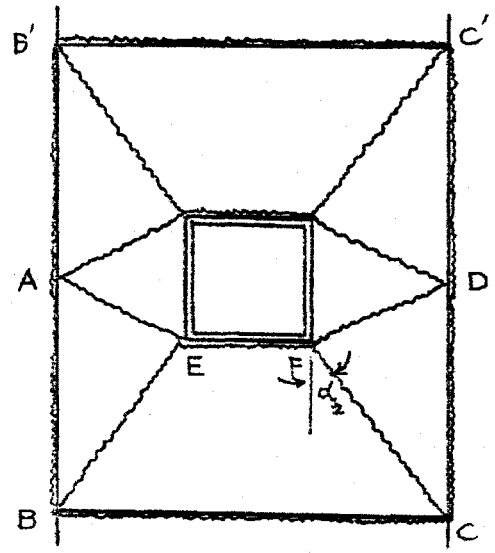

Fig. 6.11 Case (ii)

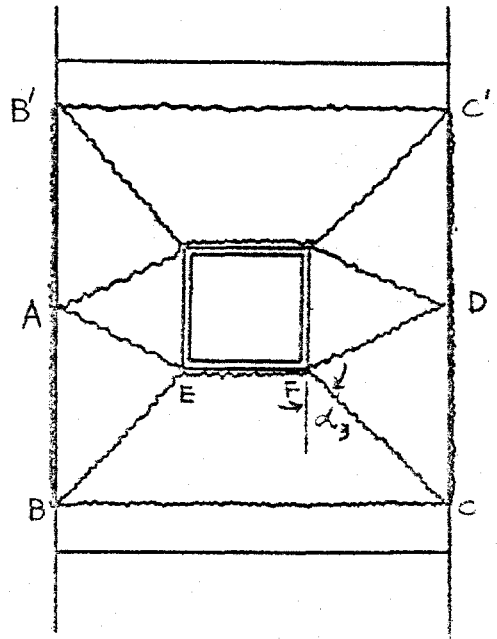

Fig. 6.12 Case (iii)

Yield Line Patterns for Chord Flange Stiffener

Table 6.3 Moment Capacities of Joint and Web Members

	Moment Capacity of Joint by Yield-line Theory *				Moment Capacity of Web Member (where $Z_p = \frac{1}{4}(d^3 - d_i^3)$)
	Unreinforced Joint	Chord Flange Stiffener		Flange Plate Reinforcement	
		Lower Extreme	Upper Extreme		
Truss A Chord 8" x 8" x ½" Web 4" x 4" x ½"	$M = 2b m_p \cdot (4.32)$ $= 240$ in-Kips	$M = 2b m_p \cdot (6.33)$ $= 348.15$ in-Kips	$M = 2b m_p \cdot (10.1)$ $= 556$ in-Kips	$M = 2b m_p \cdot (4.32) + \frac{1}{2} \sigma_y \lambda b t h$ ** $= 458$ in-Kips	$M = Z_p \sigma_y$ $= 508.75$ in-Kips
Truss B Chord 8" x 8" x ¼" Web 4" x 4" x ¼"	60 in-Kips	87.0 in-Kips	139.0 in-Kips	170 in-Kips	290.46 in-Kips

* $m_p = 3.44$ in-Kips/unit width (for ½" thickness material)
$= 0.86$ in-Kips/unit width (for ¼" thickness material)

** $h = d$ (or λb)
$\sigma_y = 55$ Ksi

CHAPTER VII

SUMMARY AND CONCLUSIONS

Connections made between two unequal width square HSS welded at right angles are regarded as semi-rigid. This condition is caused by purely flexural action of the connected chord flange due to internal loads transmitted to the joint by the web member.

Vierendeel trusses composed of unequal width square HSS were used as examples utilizing this type of connection and were analysed by a matrix method taking semi-rigidity into consideration. The trusses were of equal 8@8' panel widths, parallel chords 8' and 13' apart and uniform size of web members, 4" x 4" x $\frac{1}{2}$" for one case and 4" x 4" x $\frac{1}{4}$" for the other. Associated chord sizes were 8" x 8" x $\frac{1}{2}$" and 8" x 8" x $\frac{1}{4}$" respectively.

A computer programme was set to estimate the maximum deflection of the truss subjected to constant panel-point concentrated loads. With varying joint modulus, the maximum deflections were calculated and were plotted against the joint modulus to facilitate the designers choice of joint modulus or dimensions.

Buckling of the compressive top chord member was unlikely in the two examples considered in Chapters II and III. Instead of the top chord member, the end web members were critical

and needed to be increased in size due to the presence of high stresses there.

The loading acting on the joint was confined to the transmission of loads from the web member only. A length of four times the width of the chord member could be considered as sufficiently long for the chord flange plate analysis for rotation under applied moment.

The behaviour of the joint becomes non-linear even at relatively low loads due to the very high stresses at the corners of the joint. However, this yielding is quite insignificant if the ultimate load capacity of the joint is required. Thus, the plastic analysis of the joints was attempted to estimate the ultimate strength of the joints.

As an ordinary unequal width connection is weak to develop M_p or even M_y, several reinforcing techniques have been suggested, such as flange-plate reinforcing, chord flange stiffener and haunched plate reinforcing. An approximate elastic analysis of flange-plate reinforcement was attempted. An extension of the yield line method was also used to estimate the strength of the reinforced joints. Moment capacities of the reinforced and unreinforced joints were then calculated to compare the moment capacity of the web member. In each case, it was found that the moment capacity of the joint is usually lower than the moment capacity of web member. Hence, reinforcement is deemed necessary if the strength of the web member is to be fully utilized.

The following conclusions can be made based on the study described;

(1) Vierendeel trusses are aesthetically pleasing and are generally economical in a number of applications such as for pedestrian walkways and as roof trusses.

(2) Deflection criteria may be at least as important to the designer as are strength considerations. Greater economies are achieved with the use of unequal web members welded to chord members in HSS material. However, this type of design reduces the overall stiffness because of semi-rigid connections and may result in excessive deflections under working loads.

(3) In each of the two trusses analysed, the web member width to chord member width was equal to 0.5(i.e.λ). Analyses were carried out to show that the web to chord welded joints were inadequate in two respects, i.e.,

(i) Strength as determined by a yield line solution,

(ii) Stiffness, from the point of view of deflection.

An adequate design could only be achieved by employing one of these joint strengthening techniques described herein.

(4) Reducing λ while desirable in material saving may be offset by costs incurred from joint stiffening. No cost analysis was attempted but experience in the use of HSS trusses will tend to suggest optimum λ in relation to other geometrical properties of the members and the associated joint stiffening procedures most desirable.

APPENDIX I

SEMI-RIGID CONNECTION EQUATION [5,7,8]

Consider a prismatic member ab with semi-rigid connections of joint moduli J_a and J_b (For defination of J see footnote on pp. 13) at ends a and b respectively. The internal end moments M_a and M_b due to the external loadings or support settlement somewhere in the structure are acting at ends a and b respectively.

The total angles of rotation at both ends are determined by adding the rotations of the member without elastic rotational spring subjected to M_a and M_b with the additional rotations due to the existance of the elastic rotational springs.

The first part of the rotations of the member a b without elastic spring subjected to M_a and M_b can be determined by the Conjugate Beam Method. [26] [27]

Consider Fig.A which shows the real beam a b and the conjugate beam. The bending moment diagram of the real beam with a multiplier 1/EI is regarded as 'loading' acting on the conjugate beam. To find the reaction force of the conjugate beam at the support a, we take moments about b, thus

$$R_a L + \left(\frac{M_b L}{3EI}\right)\frac{L}{3} - \left(\frac{M_a L}{2EI}\right) = 0$$

$$\therefore \quad R_a = M_a L/3EI - M_b L/6EI$$

As the shear force of the conjugate beam at any particular

point is equal to the slope of the elastic line of real beam. Thus, the rotation at a is

$$\theta'_a = M_a L/3EI - M_b L/6EI$$

Similarly, by taking moments about a, we get the rotation of the beam at b

$$\theta'_b = - M_a L/6EI + M_b L/3EI$$

The other part of the rotations due to the elastic rotational springs are

$$\theta''_a = M_a/J_a$$

$$\theta''_b = M_b/J_b$$

where J_a and J_b are the joint moduli at ends a and b respectively.

Hence the total angles of rotation at both ends of the beam are

$$\theta_a = \theta'_a + \theta''_a = M_a L/3EI - M_b L/6EI + M_a/J_a \qquad (A.1)$$

$$\theta_b = \theta'_b + \theta''_b = -M_a L/6EI + M_b L/3EI + M_b/J_b \qquad (A.2)$$

Taking out the common factors M_a and M_b, two above equations can be re-arranged as

$$\theta_a = \left(\frac{LJ_a + 3EI}{3EIJ_a} \right) M_a - \left(L/6EI \right) M_b \qquad (A.3)$$

$$\theta_b = - \left(L/6EI \right) M_a + \left(\frac{LJ_b + 3EI}{3EIJ_b} \right) M_b \qquad (A.4)$$

Multiplying both sides of Eqn.(A.4) by $2(LJ_a + 3EI)/LJ_a$ and adding it to Eqn.(A.3), we get

$$\theta_a + \frac{2(LJ_a + 3EI)}{LJ_a}\theta_b = \left[\frac{4(LJ_a + 3EI)(LJ_b + 3EI) - J_aJ_bL^2}{6EIJ_aJ_bL}\right]M_b$$

Let $L_a = L + (3EI/J_a)$

& $L_b = L + (3EI/J_b)$

M_b can be written as

$$M_b = 6EI\,\frac{L'}{4L_aL_b - L^2}\,\theta_a + 6EI\,\frac{2L_a}{4L_aL_b - L^2}\,\theta_b \qquad (A.6)$$

Similarly, M_a can be written as

$$M_a = 6EI\,\frac{2L_b}{4L_aL_b - L^2}\,\theta_a + 6EI\,\frac{L}{4L_aL_b - L^2}\,\theta_b \qquad (A.7)$$

If $J_a = J_b = J$, then $L_a = L_b = L'$

Eqns.(A.6) and (A.7) can be written as

$$M_a = 6EI\,\frac{2L'}{4L'^2 - L^2}\,\theta_a + 6EI\,\frac{L}{4L'^2 - L^2}\,\theta_b \qquad (A.8)$$

$$M_b = 6EI\,\frac{L}{4L'^2 - L^2}\,\theta_a + 6EI\,\frac{2L'}{4L'^2 - L^2}\,\theta_b \qquad (A.9)$$

Eqns.(A.8) and (a.9) coincide with Eqn.(2.8) .

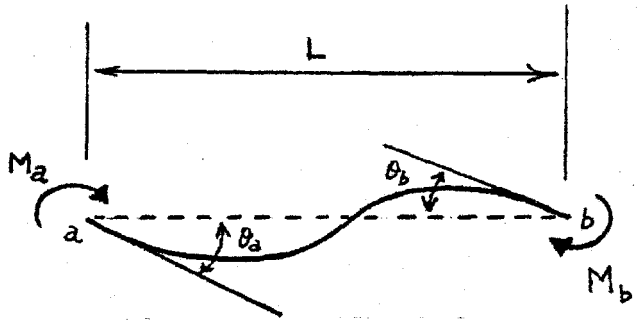

Real Beam Under Actions

of End Moments

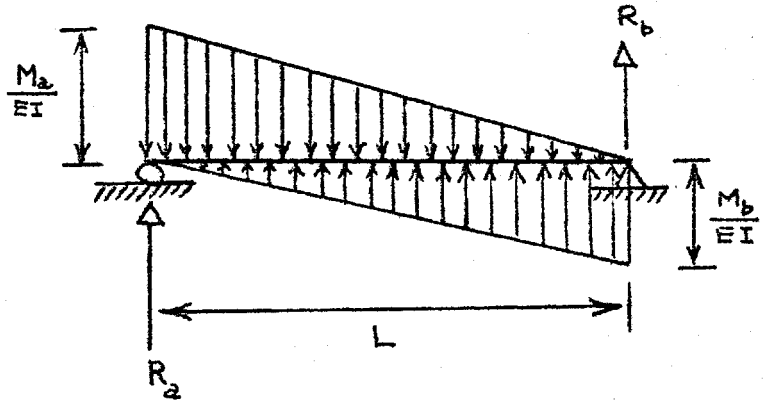

Conjugate Beam Under

Conjugate Loading

Fig. A Conjugate Beam

```
HRK7.T100.                                                    Y.K.LOO
FTN(R=3)
LGO.
'        6400 END OF RECORD
      PROGRAM TST (INPUT,OUTPUT,TAPE5=INPUT,TAPE6=OUTPUT)
C     THIS PROGRAMME IS USED FOR SOLVING THE VIERENDEEL TRUSS WITH SEMI-RIGID
C     CONNECTIONS AT BOTH ENDS OF THE WEB MEMBERS ****************************
      DIMENSION  A(26,50),S(100),ASAT(26,26),P(26,1),X(26,1),F(50,1),
     CSPRING(25),Z(25),WEBSL(25),STRESS(13,1),AXIAL(4,1),VERT(4,1)
      DIMENSION INDEX(26)
      READ  (5,101) NP,NF,NLC
  101 FORMAT    (3I5)
C     WHERE NP=NO. OF UNBALANCED MOMENTS AND UNBALANCED LINEAR FORCES AT JOINTS
C     NF=NO. OF END MOMENTS,     NLC=NO. OF LOADING CONDITIONS ON THE STRUCTURE
      READ (5,102)  ((A(I,J), J=1,NF), I=1,NP)
  102 FORMAT  (10F6.3)
      READ  (5,99)  ((P(I,J),   J=1,NLC),  I=1,NP)
   99 FORMAT  (1F4.0)
      WRITE  (6,104)
  104 FORMAT (13HOTHE MATRIX A)
      DO  105 I=1,NP
  105 WRITE  (6,106)  I,  (A(I,J), J=1,NF)
  106 FORMAT (4H ROW,I3,1X,1P4E16.7/(8X,1P4E16.7))
      WRITE  (6,110)
  110 FORMAT  (13HOTHE MATRIX P)
      DO 111 I=1,NP
  111 WRITE  (6,146)  I,  (P(I,J), J=1,NLC)
  146 FORMAT  (4H ROW,I3,1X,1F4.0)
C     THE PANEL LENGTH OF THE VIERENDEEL TRUSS IS 8FT AND ITS HEIGHT IS 13FT
C     THE DIMENSIONS OF CHORD AND WEB ARE 8X8X1/4 AND 4X4X1/4 RESPECTIVELY
      DO 71 I=1, 61, 4
   71 S(I)=7844.
      DO 72 I=4, 64, 4
   72 S(I)=7844.
      DO 73 I=2, 62, 4
   73 S(I)=3922.
      DO  74  I=3, 63, 4
   74 S(I)=3922.
      KK=0
      DO  3001  II=1,10
      KK=KK+1
      EI=30000.*8.18
      SPRING(KK)=FLOAT(II)*10.*10.*10.*10.*10./1.0
      Z(KK)=1./SPRING(KK)
      WEBSL(KK)=156.+3.*EI*Z(KK)
      DO  81  I=65, 97,  4
   81 S(I)=((6.*EI*2.*WEBSL(KK))/(4.*WEBSL(KK)*WEBSL(KK)-156.*156.))
     C/12.0
      DO  82  I=68,  100,  4
   82 S(I)=((6.*EI*2.*WEBSL(KK))/(4.*WEBSL(KK)*WEBSL(KK)-156.*156.))
     C/12.0
      DO  83  I=66,  98,  4
   83 S(I)=((6.*EI*156.)/(4.*WEBSL(KK)*WEBSL(KK)-156.*156.))/12.
      DO  84  I=67,  99,  4
   84 S(I)=((6.*EI*156.)/(4.*WEBSL(KK)*WEBSL(KK)-156.*156.))/12.
      DO 112  I=1,NP
      DO 112 J=1,NP
      ASAT(I,J)=0.
```

```
      DO  112 K=1,NF
      K1=(K-1)/2*2+1
      K2=(K+1)/2*2
      K3=2*K-1
      K4=2*K
  112 ASAT(I,J)=ASAT(I,J)+A(I,K)*(S(K3)*A(J,K1)+S(K4)*A(J,K2))
      DO 113 I=1,NP
  113 INDEX(I)=0
  114 AMAX=-1.
      DO  115 I=1,NP
      IF (INDEX(I)) 115, 116, 115
  116 TEMP=ABS(ASAT(I,I))
      IF (TEMP-AMAX) 115,115, 117
  117 ICOL=I
      AMAX=TEMP
  115 CONTINUE
      IF  (AMAX)  118,  3001,  119
  119 INDEX (ICOL)=1
      PIVOT=ASAT(ICOL,ICOL)
      ASAT(ICOL,ICOL)=1.0
      PIVOT=1./PIVOT
      DO  120  J=1,NP
  120 ASAT(ICOL,J)=ASAT(ICOL,J)*PIVOT
      DO 121 I=1,NP
      IF (I-ICOL)122, 121, 122
  122 TEMP=ASAT(I,ICOL)
      ASAT(I,ICOL)=0.0
      DO 123 J=1,NP
  123 ASAT(I,J)=ASAT(I,J)-ASAT(ICOL,J)*TEMP
  121 CONTINUE
      GO TO 114
  118 DO 124 I=1,NP
      DO 124 J=1,NLC
      X(I,J)=0.
       DO 124 K=1,NP
  124 X(I,J)=X(I,J)+ASAT(I,K)*P(K,J)
      DO  127 I=1,NF
      I1=(I-1)/2*2+1
      I2=(I+1)/2*2
      I3=2*I-1
      I4=2*I
      DO 127 J=1,NLC
      F(I,J)=0.
      DO 127 K=1,NP
  127 F(I,J)=F(I,J)+X(K,J)*(S(I3)*A(K,I1)+S(I4)*A(K,I2))
      AXIAL AND VERT ARE THE AXIAL FORCES OF CHORD AND WEB MEMBERS RESPECTIVELY
      DO  210  J=1,NLC
      AXIAL(1,J)=(.5*7.*P(20,J)*8.+F(2,J)+F(18,J))/13.0
      AXIAL(2,J)=(.5*7.*P(20,J)*16.-P(20,J)*8.+F(4,J)+F(20,J))/13.
      AXIAL(3,J)=(.5*7.*P(20,J)*24.-P(20,J)*(16.+8.)+F(6,J)+F(22,J))/13.
      AXIAL(4,J)=(.5*7.*P(20,J)*32.-P(20,J)*(24.+16.+8.)+F(8,J)
     C+F(24,J))/13.0
      VERT(1,J)=(F(1,J)+F(2,J))/8.
      VERT(2,J)=(F(3,J)+F(4,J)-F(1,J)-F(2,J))/8.
      VERT(3,J)=(F(5,J)+F(6,J)-F(3,J)-F(4,J))/8.
      VERT(4,J)=(F(7,J)+F(8,J)-F(5,J)-F(6,J))/8.
```

```
      VERT(5,J)=(F(9,J)+F(10,J)-F(7,J)-F(8,J))/8.
  210 CONTINUE
C     SM AND SM2 ARE THE SECTION MODULI OF CHORD AND WEB MEMBERS RESPECTIVELY
      SM=18.8
      SM2=4.09
C     THE CROSS SECTIONAL AREA OF THE CHORD MEMBER IS 7.59 SQ. IN.
C     THE CROSS SECTIONAL AREA OF THE WEB MEMBER IS 3.54 SQ. IN.
      DO  310  J=1,NLC
      STRESS(1,J)=ABS(F(1,J)*12./SM)+ABS(AXIAL(1,J)/7.59)
      STRESS(2,J)=ABS(F(2,J)*12./SM)+ABS(AXIAL(1,J)/7.59)
      STRESS(3,J)=ABS(F(3,J)*12./SM)+ABS(AXIAL(2,J)/7.59)
      STRESS(4,J)=ABS(F(4,J)*12./SM)+ABS(AXIAL(2,J)/7.59)
      STRESS(5,J)=ABS(F(5,J)*12./SM)+ABS(AXIAL(3,J)/7.59)
      STRESS(6,J)=ABS(F(6,J)*12./SM)+ABS(AXIAL(3,J)/7.59)
      STRESS(7,J)=ABS(F(7,J)*12./SM)+ABS(AXIAL(4,J)/7.59)
      STRESS(8,J)=ABS(F(8,J)*12./SM)+ABS(AXIAL(4,J)/7.59)
      STRESS(9,J)=ABS(VERT(1,J)/3.54)+ABS(F(34,J)*12./SM2)
      STRESS(10,J)=ABS(VERT(2,J)/3.54)+ABS(F(36,J)*12./SM2)
      STRESS(11,J)=ABS(VERT(3,J)/3.54)+ABS(F(38,J)*12./SM2)
      STRESS(12,J)=ABS(VERT(4,J)/3.54)+ABS(F(40,J)*12./SM2)
      STRESS(13,J)=ABS(VERT(5,J)/3.54)+ABS(F(42,J)*12./SM2)
  310 CONTINUE
      WRITE  (6,107)
  107 FORMAT (13H0THE MATRIX S)
      DO  108 I=1,NF
      I1=(I-1)/2*2+1
      I2=(I+1)/2*2
      I3=2*I-1
      I4=2*I
  108 WRITE  (6,109)  I, I1, S(I3), I2, S(I4)
  109 FORMAT (4H ROW,I3,5X,3HCOL,I3,1PE16.7,5X,3HCOL,I3,1PE16.7)
      WRITE  (6,1128)
 1128 FORMAT (13H0THE MATRIX F)
      DO 1129 I=1,NF
 1129 WRITE  (6,1136) I, (F(I,J), J=1,NLC)
 1136 FORMAT  (4H ROW,I3,1X, 1F14.4)
      WRITE  (6,1125)
 1125 FORMAT (13H0THE MATRIX X)
      DO  1126  I=1,NP
 1126 WRITE  (6,1136) I, (X(I,J), J=1,NLC)
      WRITE  (6,1820)
 1820 FORMAT (54H0THE ABSOLUTE VALUE OF STRESS IN THE MEMBERS OF TRUSS/)
      DO 1821  I=1,13
 1821 WRITE  (6,1830) I, (STRESS(I,J), J=1,NLC)
 1830 FORMAT  (7H STRESS, I3, 1X,  1F14.4)
      WRITE  (6,1840)
 1840 FORMAT  (52H1THE AXIAL FORCES IN CHORD AND WEB MEMBERS IN KIPS//)
      DO 1841  I=1,4
 1841 WRITE  (6,1850) I,  (AXIAL(I,J),  J=1,NLC)
 1850 FORMAT  (6H AXIAL, I3, 1X,  1F14.4)
      DO 1851  I=1,5
 1851 WRITE  (6,1860) I, (VERT(I,J), J=1,NLC)
 1860 FORMAT  (5H VERT, I4, 1X,  1F14.4)
 3001 CONTINUE
      STOP
      END
```

APPENDIX III

LOADING EQUATIONS EXPRESSED IN TRIGONOMETRIC SERIES

UNIFORMLY DISTRIBUTED LINE LOAD

Consider a uniformly distributed line load of intensity q_o acting at a location of a plate as shown in Fig. B .

This loading equation can be expressed into double trigonometric series. One component of the equation is expressed in x-direction, the other component is expressed in y-direction. The product of two components is the required double trigonometric series.

In y-direction, the loading can be regarded as U.D.L. of intensity q_o acting on a simply supported beam. For a structural element with simply supported ends the half range series which is most often used is the sine series. Therefore, the load may be represented as

$$q_o = q_1 \sin\frac{\pi y}{b} + q_2 \sin\frac{2\pi y}{b} + \ldots + q_n \sin\frac{n\pi y}{b} + \ldots \quad (A.10)$$

To find q_n multipy both sides of this equation by $\sin n\pi y/b$ and integrate from 0 to b. Noting that

$$\int_0^b \sin\frac{m\pi y}{b} \sin\frac{n\pi y}{b}\, dy = \begin{cases} 0, & \text{when } m \neq n \\ b/2, & \text{when } m = n \end{cases}$$

the resulting equation is

$$q_n\left(\frac{b}{2}\right) = \int_0^b q \sin\frac{n\pi y}{b}\, dy = \frac{qb}{n\pi}(1 - \cos n\pi)$$

From above equation

$$q_n = \frac{4q_0}{n\pi} \qquad \text{when n is odd}$$

and $q_n = 0$ when n is even

Therefore, Eqn.(A.10) is expressed as

$$q = \frac{4q_0}{\pi}\left(\sin\frac{\pi y}{b} + \frac{1}{3}\sin\frac{3\pi y}{b} + \ldots\right) \qquad \text{(A.11)}$$

In the x-direction, the loading can be regarded as a unit concentrated load (because of line load) acting at a distance ρ from one end of a simplied supported beam of length 2b. To derive the expression for this unit concentrated load, we can treat the loading as a UDL of intensity $1/2\epsilon$ between $x = \rho - \epsilon$ and $x = \rho + \epsilon$ (see Fig.B). The loading on the beam is then;

zero from $x = 0$ to $x = \rho - \epsilon$

1/2 from $x = \rho - \epsilon$ to $x = \rho + \epsilon$

zero from $x = \rho + \epsilon$ to $x = 2b$

Like Eqn.(A.10), the loading may be represented as $\sum q_n \sin n\pi x/2b$, multiplying both sides by $\sin n\pi x/2b$ and integrating between 0 and 2b we get

$$\int_0^{\rho-\varepsilon}(0)\sin\frac{n\pi x}{2b}\,dx + \int_{\rho-\varepsilon}^{\rho+\varepsilon}\frac{1}{2\varepsilon}\sin\frac{n\pi x}{2b}\,dx - \int_{\rho+\varepsilon}^{2b}(0)\sin\frac{n\pi x}{2b}\,dx$$
$$= \int_0^{2b} q_n \sin^2\frac{n\pi x}{2b}\,dx$$

Whence $$\frac{1}{2\varepsilon}\frac{2b}{n\pi}\left[\cos\frac{n\pi}{2b}(\rho-\varepsilon) - \cos\frac{n\pi}{2b}(\rho+\varepsilon)\right] = q_n\frac{2b}{2}$$

Using the cosine combination formula, this give

$$q_n = \frac{1}{\varepsilon n\pi}\cdot 2\cdot\sin\frac{n\pi c}{2b}\cdot\sin\frac{n\pi\varepsilon}{2b}$$

and since $\sin\frac{n\pi\varepsilon}{2b} \longrightarrow \frac{n\pi\varepsilon}{2b}$ as $\varepsilon \longrightarrow 0$

$$\therefore\quad q_n = \frac{1}{b}\sin\frac{n\pi\rho}{2b}$$

The expression for this unit concentrated load is thus [17]

$$\frac{1}{b}\sin\frac{\pi\rho}{2b}\sin\frac{\pi x}{2b} + \sin\frac{2\pi\rho}{2b}\sin\frac{2\pi x}{2b} + \cdots \qquad \text{(A.12)}$$

Multiplying Eqn.(A.11) with Eqn.(A.12), we obtain the required double trigonometric series for the uniform line load acting on the plate, i.e.

$$q = \frac{4q_o}{\pi b}\sum_{m=1,3,5\cdots}^{\infty}\sum_{n=1,2,3\cdots}^{\infty}\left(\frac{1}{m}\sin\frac{n\pi\rho}{2b}\sin\frac{m\pi y}{b}\sin\frac{n\pi x}{2b}\right)$$
$$= \sum_{m=1,3,5\cdots}^{\infty}\sum_{n=1,2,3\cdots}^{\infty} q_{mn}\sin\frac{m\pi y}{b}\sin\frac{n\pi x}{2b} \qquad \text{(A.13)}$$

where $q_{mn} = \frac{4q_o}{\pi b}\frac{1}{m}\sin\frac{n\pi\rho}{2b}$

Equation (A.13) coincides with Eqn.(6.9) .

PARABOLIC LINE LOAD

Consider a parabolic line load at a location of a plate as shown in Fig. C . The areas of this parabolic distribution and the U.D.L. in preceding Section must equal each other. The intensity of this parabolic distribution is found equal to $3q_o$ at both ends and zero at the center.

The double sine series for this parabolic line load can be decomposed into two components, namely x and y components.

Before dealing with the component equation, we would like to find the equation of a parabolic curve as shown in Fig. D where q is the vertical axis and y is the horizontal axis.

The general equation for the parabola in Fig(D) is[21]

$$(y - b/2)^2 = 4k (q - 0) \qquad (A.14)$$

where (b/2, 0) and (b/2, k) are the coordinates of the vertex and the focus respectively. The value of k can be found by substituting the boundary value of the curve, namely when $y = 0$, $q = 3q_o$. K is thus found equal to $b^2/48q_o$. Express q in terms of y, Eqn.(A.14) can be written as

$$q = (y - b/2)^2 \frac{12q_o}{b^2} \qquad (A.15)$$

Returning to the y-component equation, we can regard the loading in y-direction as a parabolic distribution load acting on a simply supported beam of length b. Let this load be represented as

$$q = q_1 \sin\frac{\pi y}{b} + q_2 \sin\frac{2\pi y}{b} + \cdots + q_m \sin\frac{m\pi y}{b} + \cdots \tag{A.16}$$

Where q_m can be found by multiplying both sides of above equation by $\sin m\pi y/b$ and integrating with respect to y from 0 to b.

Thus $$q_m = \frac{2}{b}\int_0^b q \sin\frac{m\pi y}{b}\, dy$$

Substituting q as expressed by Eqn.(A.16) into above equation, we get

$$q_m = \frac{24q_o}{m\pi}\left[\frac{1}{4} - \frac{2}{m^2\pi^2}\right]\left[1 - (-1)^m\right]$$

when m is odd $$q_m = \frac{48q_o}{m\pi}\left(\frac{1}{4} - \frac{2}{m^2\pi^2}\right)$$

when m is even $$q_m = 0$$

Therefore, Eqn.(A.16) can be written as

$$q = \sum_{m=1,3,5\cdots}^{\infty} \frac{48q_o}{m\pi}\left(\frac{1}{4} - \frac{2}{m^2\pi^2}\right) \sin\frac{m\pi y}{b} \tag{A.17}$$

which is the y-component of the parabolic line load acting on the plate.

As in preceding Section, the loading in x-direction can be regarded as a unit concentrated load acting at a distance ρ from one end of a simply supported beam of length 2b. The expression for this unit load is

$$\frac{1}{b}\left[\sin\frac{\pi\rho}{2b}\sin\frac{\pi x}{2b} + \sin\frac{2\pi\rho}{2b}\sin\frac{2\pi x}{2b} + \cdots\right]$$

The product of the two components gives the required double sine series, thus

$$q = \sum_{m=1,3,5\cdots}^{\infty} \sum_{n=1,2,3\cdots}^{\infty} \left(q_{mn} \sin \frac{m\pi y}{b} \sin \frac{n\pi x}{2b} \right) \qquad \text{(A.18)}$$

where $$q_{mn} = \frac{48 q_o}{b\pi} \frac{1}{m} \left(\frac{1}{4} - \frac{2}{m^2\pi^2} \right) \sin n\pi\rho/2b$$

$$= \frac{4q_o}{b\pi} \frac{1}{m} \left(3 - \frac{24}{m^2\pi^2} \right) \sin n\pi\rho/2b$$

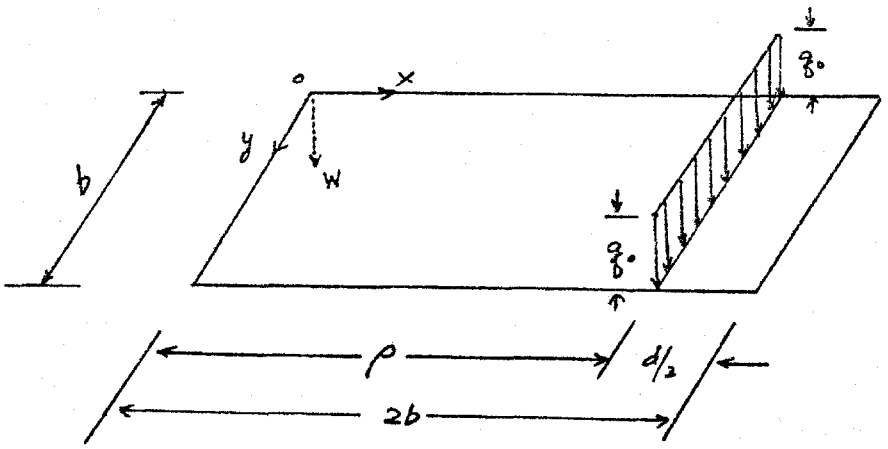

Uniform Line Load on a Plate

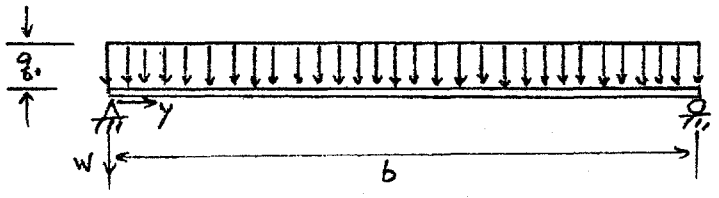

Line load in y-direction

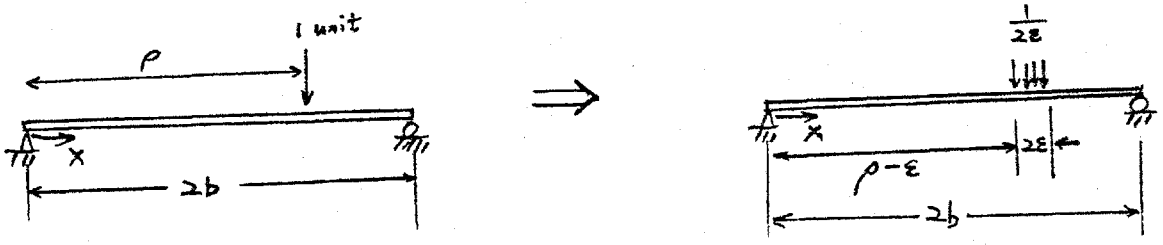

Line Load in x-direction

Fig.B : Uniformly Distributed Line Load

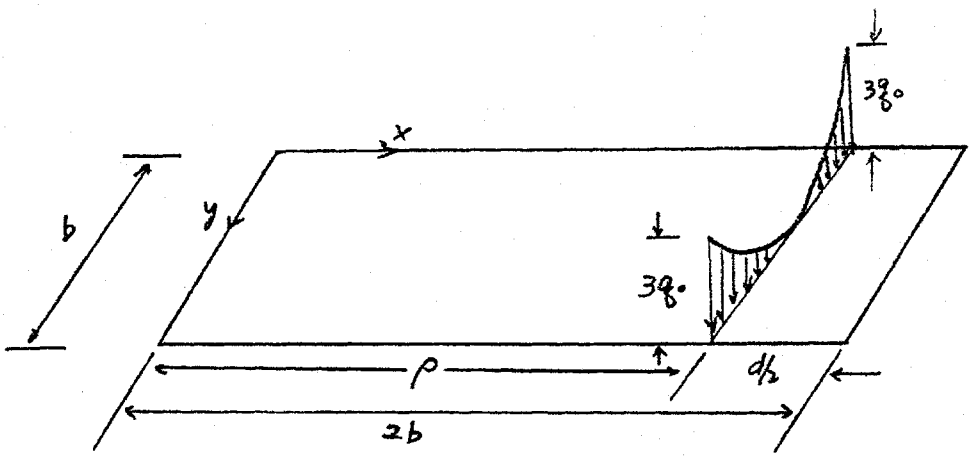

Fig. C Parabolic Line Load Acting on a Plate

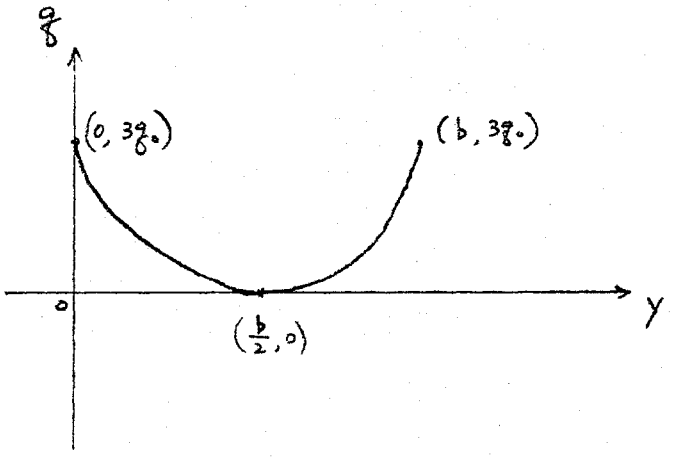

Fig. D A Parabolic Curve on y-q axes

APPENDIX IV

NOMENCLATURE

1. Matrices :

$[A]$	Static matrix
$[B]$	Deformation matrix
$[M]$	Internal end matrix
$\{P\}$	A column matrix showing values of unbalanced joint moments and unbalanced linear forces
$[S]$	Stiffness matrix
$\{X\}$	A column matrix showing values of joint rotations or translations
$\{\theta\}$	A column matrix showing values of elastic end rotations
$[\ ]^T$	A symbol used to indicate the transpose of a matrix

2. Notations

a	Length of Plate in x-direction
b	Width of Plate in y-direction; the width of chord member of square HSS
C	Compressive force in triangular pinned truss
d	Width of web member of square HSS
D	Elastic flexural rigidity of plate of unit width, $\frac{E\ I}{1-\nu^2}$
E	Elastic modulus of steel
E_t	Tangent modulus of steel

G	Shear modulus
H	Height of Vierendeel truss ; height of stiffening plate
I	Moment of inertia
J	Joint modulus ($J = M/\phi$)
K	Plate coefficient
L	lenght ; span lenght of beam ; panel lenght of Vierendeel truss
L_a L_b	Modified length of the structural member with semi-rigid connections at ends
m_p	Fully plastic moment of plate (per unit width)
M	Applied bending moment
P	Load
Q	Maximum intensity of distributed load
t	Plate thickness
x,y	Co-ordinate axes
W	Transverse deflection of thin plate
Z	$1.0/J$ or ϕ/M
Z_p	Plastic section modulus
α	The angle made between the diagonal yield line and the vertical
β	The angle made between the diagonal yield line and the horizontal
γ	Shearing deformation
Δ, δ	Deflection
ϵ	Small increment
φ	Coefficient of restraint

λ	Width ratio (d/b)
ν	Poission's ratio
ρ	A certain distance from one end beam where a concentrated load is acting
Σ	Summation
σ	Sress
σ_c	Buckling stress
σ_y	Yield stress
σ_p	Proportional limit stress
τ	Shearing strss; E/E_t
ϕ	Relative angle of rotation between two members at joint

3. Abbreviations

AISC	American Institute of Steel Conctruction
CIDECT	The International Committee for the study and Development of Tubular Structures (Comite' international pour l'etude et le de'veloppement de la Construction Tubulaire)
HSS	Hollow structural Sections
Min.	Minimum
Max.	Maximum
NBC	National Building Code
UDL	Uniformly distributed Load

APPENDIX V

LIST OF REFERENCES

(1) Mehrotra, B.L. , "Stiffening in Tubular Junctions - Some New Concepts", Journal of the structural Division, ASCE, Vol 97, No. ST9, Sept. 1971 pp. 2453 - 2457

(2) Mehrotra, B.L. , "Matrix Analysis of Welded tubular Joints", Ph.D. Thesis, McGill University, Canada, Dec. 1969

(3) Wang, C.K. , "Matrix Formulation of Slope-deflection Equations", Journal of the Structural Division, ASCE, Vol. 84, No. ST6, Proc. Paper 1819, Oct.,1958 pp. 1819-1 —— 1819-19 .

(4) Wang, C.K. , "Matrix Methods of Structural Analysis", International Textbook Company, 2nd edition, 1970 pp. 83

(5) Gere, J.M. , "Moment Distribution", D.Van Nostrand Company, Inc., Princeton, 1963 pp. 239

(6) Gere, J.M. ,ibid, pp. 241

(7) Lothers, J.E. , "Advanced Design in Structural Steel", Prentice - Hall, Inc. 1960 pp. 375

(8) Rathbun, J.C., "Elastic Properties of Riveted Connections", ASCE Vol. 101, 1936 pp. 524 - 595

(9) National Building Code of Canada, 1965

(10) Bleich, F. , "Buckling Strength of Metal Structures" McGraw - Hill Book Company, Inc., New York, 1952

(11) Hudoba, J. , "Plastic Design Capabilities of Hollow Structural Sections", M.Eng. Thesis, McMaster University, Jan. 1971

(12) Redwood, R.G. , "Behaviour of Joints Between Rectangular Hollow Structural Members", Civil Engineering and Public Works Review, Oct., 1965, pp. 1463 - 1468

(13) Jubb, J.E. and Redwood, R.G., "Design of Joints to Box Sections", The Institution of Structural Engineers, Conference on Industrialised Building and the Structural Engineer, May 17, 1966

(14) Wood, R.H. , "Plastic and Elastic Design of Slabs and Plates", Thames & Hudson, 1961

(15) Cute, D. , Camo, S. , and Rumpf, J.L. , "Welded Connections for Square and Rectangular Structural Steel Tubing", Research Report No. 292 - 10 , Drexel Institute of Technology, Philadelphia, Pa., November 1968.

(16) Drucker, D.C. and Chen, W.F. , "On the Use of Simple Discontinuous Fields to Bound Limit Loads",

(17) Drucker, D.C. , Prager, W., Greenberg, H.J. , "Extended Limit Design Theorems for Continuous Media", Q. Applied Math. 9, pp. 381 - 389, 1952

(18) Jaeger, L.G. , "Elementary Theory of Elastic Plates", Pergamon Press Ltd., 1964, Chapter 2

(19) Timoshenko, S. and Woinowsky - Krieger, S., "Theory of Plates and Shells" McGraw-Hill Book Co., 1959, Chapter 4.

(20) Preliminary Results of "Rectangular Hollow Structural Viereneel Joint Tests", Corby Research Center, U.K.

(21) Woods, R., "Analytic Geometry" 1959

(22) Duff, G., "Joint Behaviour of a Welded Beam-Column Connection in Rectangular Hollow Sections." Thesis, The College of Aeronautics, Cranfield, England, June 1963

(23) Mehrotra, B.L. and Redwood, R.G., "Load Transfer Through Connection Between Box Sections", Journal of the Engineering Institute of Canada, Aug. - Sept. , 1970

(24) Redwood, R.G. , "The Bending of Plate Loaded Through a Rigid Rectangular Inclusion", International Journal of Mechanical Sciences, Vol. 7 , 1965

(25) Reissner, E., "Analysis of Sheer-lag in Box Beams by the Principle of Minimum Potential Energy", Q. Applied Math. Oct., 1946

(26) Wilbur, J.B. and Norris, C.H., "Elementary Structural Analysis" McGraw-Hill Book Co., Inc., New York 1948

(27) Borg, S.F. , Gennaro, J.J., "Modern Structural Analysis", 1969